

Mechanisms of Cytoprotection Mediated by G-Protein Coupled Receptor GPR39

Inaugural-Dissertation

zur Erlangung des Doktorgrades
der Mathematisch-Naturwissenschaftlichen Fakultät
der Heinrich-Heine-Universität Düsseldorf

vorgelegt von

Sonja Dittmer
aus Hamburg

Düsseldorf, Oktober 2008

aus dem Institut für Neurologie
der Heinrich-Heine Universität Düsseldorf

Gedruckt mit der Genehmigung der
Mathematisch-Naturwissenschaftlichen Fakultät der
Heinrich-Heine-Universität Düsseldorf

Referent: PD Dr. Axel Methner
Koreferent: Frau Prof. Christine Rose

Tag der mündlichen Prüfung: 30.10.2008

1. INTRODUCTION	4
1.1 CELL DEATH IN HEALTH AND DISEASE	4
1.1.1 APOPTOSIS	4
1.1.2 NECROSIS	5
1.1.3 AUTOPHAGY	5
1.2 CELL DEATH STIMULI	5
1.2.1 UNFOLDED PROTEIN RESPONSE	5
1.2.2 OXIDATIVE STRESS	8
1.3 G-PROTEIN COUPLED RECEPTORS	10
1.3.1 STRUCTURE AND FUNCTION	10
1.3.2 GPCRS AS DRUG TARGETS	14
1.3.3 PROTECTIVE ACTION OF GPCRS IN THE NERVOUS SYSTEM	15
1.3.4 EFFECTS OF GPCRS IN CANCER	15
1.3.5 G-PROTEIN COUPLED RECEPTOR 39	16
2. AIM OF THIS STUDY	17
3. MATERIALS	18
3.1 CHEMICALS	18
3.2 ENZYMES	18
3.2.1 RESTRICTION ENDONUCLEASES	18
3.2.2 MISCELLANEOUS ENZYMES	18
3.3 KITS	18
3.4 ANTIBODIES	18
3.4.1 PRIMARY ANTIBODIES	18
3.4.2 SECONDARY ANTIBODIES	19
3.5 MEDIA	20
3.5.1 BACTERIAL MEDIA	20
3.5.2 CELL CULTURE MEDIA	20
3.6 BUFFERS AND SOLUTIONS	21
3.7 BACTERIA	22
3.7.1 ESCHERICHIA COLI DH5	22
3.7.2 ONE SHOT® CCDB SURVIVAL™	22
3.8 CELL LINES	22
3.8.1 NEURO-2A (N2A)	22
3.8.2 HUMAN EMBRYONIC KIDNEY CELLS (HEK 293)	22
3.8.3 HT22 CELLS	22
3.8.4 CHINESE HAMSTER OVARY CELLS (CHO)	23
3.8.5 MOUSE EMBRYONIC FIBROBLASTS (MEF)	23
3.8.6 SH-SY5Y CELLS	23
3.8.7 COS7 CELLS	23
3.9 PLASMIDS	23
3.9.1 EXPRESSION PLASMIDS	23
3.9.2 REPORTER PLASMIDS	25
3.9.3 MICRORNA (miRNA) PLASMIDS	25
3.9.4 ENTR™ PLASMIDS	26
3.10 OLIGONUKLEOTIDES	27
3.10.1 QPCR PRIMERS AND PROBES	27
3.10.2 miRNA-OLIGONUKLEOTIDES	28
3.10.2 SMALL INTERFERING RNA (siRNA)	28
3.11 INSTRUMENTS	29

4. METHODS	30
4.1 CELL CULTURE TECHNIQUES	30
4.1.1 MAINTENANCE OF CELL LINES	30
4.1.2 TRANSFECTION OF CELL LINES	30
4.1.3 CELL VIABILITY ASSAYS	31
4.2 PROTEINBIOCHEMICAL TECHNIQUES	32
4.2.1 EXTRACTION OF PROTEIN LYSATES	32
4.2.2 ESTIMATION OF PROTEIN CONCENTRATION	32
4.2.3 SDS-POLYACRYLAMID GELELECTROPHORESIS (SDS-PAGE)	32
4.2.4 IMMUNOBLOTTING (IB)	33
4.2.5 CO-IMMUNOPRECIPITATION	33
4.2.6 LUCIFERASE ASSAYS	34
4.2.7 IMMUNOCYTOCHEMISTRY	34
4.3 MOLECULAR TECHNIQUES	34
4.3.1 PRODUCTION OF CHEMICALLY COMPETENT BACTERIA	34
4.3.2 TRANSFORMATION	35
4.3.3 SMALL SCALE PLASMID DNA PREPARATION	35
4.3.4 LARGE SCALE PLASMID DNA PREPARATION	35
4.3.5 SMALL SCALE RNA PREPARATION	36
4.3.6 ESTIMATION OF DNA CONCENTRATIONS	36
4.3.7 DNA SEPARATION BY AGAROSE GELELECTROPHORESIS	36
4.3.8 ENZYMATIC RESTRICTION OF DOUBLE-STRANDED (DS)DNA	36
4.3.9 LIGATION OF DNA FRAGMENTS	37
4.3.10 POLYMERASE CHAIN REACTION (PCR)	37
4.3.11 GATEWAY™ CLONING	37
4.3.12 CDNA-REVERSE TRANSCRIPTION	39
4.3.13 QUANTITATIVE PCR (QPCR)	40
4.4 STATISTICAL ANALYSIS	41
5. RESULTS	42
5.1 GPR39 IS A MAJOR FACTOR IN HT22R PROTECTION	42
5.2 GPR39 OVEREXPRESSION INDUCES SEVERAL DOWNSTREAM TARGETS	44
5.3 GPR39 PROTECTION IS Gα13, RHOA/SRE-DEPENDENT AND REGULATED BY RGS16	45
5.3.1 GPR39 PROTECTION IS INHIBITED BY RGS16	45
5.3.2 GPR39 PROTECTION IS RHOA DEPENDENT	46
5.3.3 GPR39 MEDIATED PROTECTION CAN BE INHIBITED BY Y-27632	48
5.3.4 GPR39 INDUCED SRE-DEPENDENT TRANSCRIPTION IS NECESSARY FOR CYTOPROTECTION	48
5.4 PEDF PARTLY MEDIATES GPR39 CYTOPROTECTION	50
5.4.1 PEDF IS UPREGULATED BY GPR39	50
5.4.2 PEDF IS REGULATED DOWNSTREAM OF SRF	51
5.4.3 PEDF PARTLY MEDIATES OF THE GPR39 PROTECTIVE EFFECT	52
5.5 TNRC9 IS A NEURONAL AND EPITHELIAL TRANSCRIPTION FACTOR REGULATED BY GPR39	54
5.5.1 TNRC9 IS UPREGULATED BY GPR39	56
5.5.2 TNRC9 CONFERS PART OF THE GPR39 PROTECTIVE EFFECT	57
5.5.3 TNRC9 IS REGULATED DOWNSTREAM OF SRF	58
5.5.4 TNRC9 IS UPREGULATED BY PAR-AGONISTS	59
5.5.5 TNRC9 INCREASES PEDF	60
5.6 CITED1 IS A TRANSCRIPTIONAL COACTIVATOR REGULATED BY GPR39	61
5.6.1 GPR39 UPREGULATES CITED1	61
5.6.2 CITED1 IS UPREGULATED BY PAR-AGONISTS	62

5.6.3 GPR39 ENHANCES NUCLEAR LOCALIZATION OF CITED1	64
5.7 TNRC9 AND CITED1 INTERACT PHYSICALLY	64
5.7.1 TNRC9-CITED1 INTERACTION IS SPECIFIC	65
5.7.2 TNRC9 AND CITED1 INTERACT AT THE TNRC9-HMG-DOMAIN	66
5.8 TNRC9 AND CITED1 PROTECT SYNERGISTICALLY	67
5.9 TNRC9 AND CITED1 SYNERGISTICALLY UPREGULATE ESTROGEN RECEPTOR-MEDIATED TRANSCRIPTION	69
5.10 TNRC9 INTERACTS WITH ERα THROUGH ITS N-TERMINAL DOMAIN	70
 6. DISCUSSION	 73
 6.1 THE GPR39-MEDIATED SIGNAL TRANSDUCTION CASCADE	 73
6.2 PEDF AS ONE EFFECTOR MOLECULE DOWNSTREAM OF GPR39	74
6.3 TRANSCRIPTIONAL INTERACTION OF GPR39 DOWNSTREAM MEDIATORS	75
6.3.1 TRANSCRIPTIONAL COMPLEX CONTAINING TNRC9, CITED1 AND ERα – IMPLICATIONS IN CANCER	75
6.3.2 ESTROGEN-INDUCED NEUROPROTECTIVE PROPERTIES	76
6.4 GPR39 – A DOUBLE-EDGED SWORD	76
 7. SUMMARY	 78
 7.1 SUMMARY ENGLISH	 78
7.2 ZUSAMMENFASSUNG DEUTSCH	79
 8. APPENDIX	 80
 8.1 REFERENCES	 80
8.2 ABBREVIATIONS	91
8.3 PUBLICATIONS	93
8.4 ACKNOWLEDGMENT	94
8.5 CURRICULUM VITAE	96
8.6 ERKLÄRUNG	99

1. Introduction

Cell death in Health and Disease

Cell death is a commonly occurring and tightly regulated everyday event. It has multiple roles in embryonic development, stress-response and maintenance of genomic integrity. Cell death occurs in three major distinct patterns, apoptosis, necrosis and autophagy.

Apoptosis

Apoptosis, also known as programmed cell death, is induced by a distinct pattern of signal transduction. Three apoptotic pathways can be distinguished, namely the intrinsic pathway, the extrinsic pathway and the perforine/granzymeA-mediated pathway. Through the extrinsic pathway, the binding of a death ligand (namely tumor necrosis factor α (TNF α) and Fas-ligand (FASL)) induces the cleavage of pro-caspase 8 to caspase 8, which in turn activates caspase 3 (Cohen, 1997). Once caspase 3 is active the execution of cell death is carried out via endonuclease-mediated chromosomal degradation (Bortner, 1995), and activation of proteases.

The intrinsic pathway of apoptosis is induced by either absence of anti-apoptotic stimuli like growth factors or hormones or by cytotoxic stimuli like radiation, hypoxia, free radicals and many more. Here, changes of the membrane structure of the outer mitochondrial membrane lead to loss of membrane potential and the release of cytochrome *c* from the intermembrane space (Saelens et al., 2004). Subsequently, APAF-1 and pro-caspase 9 are activated and an apoptosome is formed (Chinnaiyan 1999), which in turn activates executor caspase 3.

More recently, a third pathway of apoptosis has been described. In this perforin/granzymeA (GrA)-mediated pathway, GrA is delivered to a target cell by cytotoxic T lymphocytes and introduced to the cell by perforin, where it activates GrA-activated DNase, which in turn enters the nucleus and induces desoxyribonucleic acid (DNA)-strand breaks (Pardo et al., 2004).

Morphologically, hallmarks of apoptosis are cell shrinkage, membrane blebbing, and finally disintegration of the cell into apoptotic bodies (reviewed in Orrenius et al., 2003). During apoptosis, dying cells expose phagocytotic proteins, such as phosphatidylserine (PS) (Li et al., 2003), on their cell surface, which are recognized by macrophages and thus lead to removal of dead cells from tissue.

Impaired apoptosis is implicated in several human diseases. In the nervous system both acute disorders like stroke and ischemia as well as chronic degenerative diseases like Alzheimer's disease (AD) and Parkinson's disease (PD) are in part subject to caspase-mediated apoptosis and can be attenuated by caspase inhibitors (reviewed in Robertson et al., 2002). On the other hand, deregulation of apoptosis leads to malignant transformation and tumor progression. A key protein in retaining genomic integrity is the tumor-suppressor p53 that induces apoptosis

when DNA-damage has occurred. p53 is expressed in mutant forms in approximately 50% of human cancer (Ryan et al., 2001). Thus, regulation and mechanisms of apoptosis are valuable targets for research and drug targeting.

Necrosis

Necrosis in contrast to apoptosis is an accidental event. Necrotic processes are induced by prolonged exposure to inflammation, toxins or hypoxia and characterized by swelling of cytoplasm and organelles and the release of lysosomal enzymes that lead to lytic processes of intracellular structures (reviewed in Orrenius et al., 2003). In human disease, necrosis mainly plays a role in inflammatory, acute conditions like stroke and ischemia, or infection.

1.1.3 Autophagy

The third major form of cell death is autophagic cell death. Autophagy is a tightly controlled event that has several physiological roles in development and homeostasis. Examples are the reallocation of nutrients from unnecessary processes in starving organisms (Yorimitso et al., 2005) or the clearance of intracellular pathogens (Gutierrez et al., 2004). It involves sequestration of cell compartments and proteins in a vacuole called autophagosome that subsequently fuses to a lysosome to form an autolysosome (Rubinsztein et al., 2005). Autophagy has been proposed to play a role in the clearance of misfolded and aggregated protein. Therefore, impaired autophagy has been shown to be involved in diseases caused by protein aggregation like AD and Huntington disease (Ravikumar et al., 2002), or motor neuron-like disease (Rubinsztein et al., 2005).

Cell Death Stimuli

The forms of cell death introduced above are triggered by a huge variety of stimuli. Two of which need to be discussed in greater detail: the unfolded protein response and the oxidative stress.

Unfolded Protein Response

The unfolded protein response (UPR) is a response to stress on the endoplasmic reticulum (ER). The ER is the cellular organelle where secretory and membrane proteins are synthesized, folded and sorted, and where glycosylation and disulfide-bond formation are catalyzed. When proteins are continuously misfolded by mutation or physiological stress, signal transduction mechanisms termed “unfolded protein response” are triggered (reviewed in Bernales et al.,

2006). *In vitro*, this effect can be activated by tunicamycin, a nucleoside antibiotic that inhibits the transfer of N-acetylglucosamine-1-phosphate to dolichyl phosphate in glycoprotein synthesis and thus inhibits formation of N-linked glycoproteins. This leads to a form of cell death with apoptotic features (Duksin et al., 1982).

Unfolded protein response collectively describes three different pathways of sensing and responding to ER-stress. Unfolded protein load is detected by trans-ER membrane proteins. These induce signaling cascades that finally either trigger cytoprotective responses or induce apoptosis depending on the amount of protein in the ER and elapsed time. The most conserved of these pathways is induced by inositol-requiring protein 1 (IRE1). As a response to misfolded proteins, IRE1 oligomerizes and activates downstream kinases and endonucleases to promote differential splicing of XBP-1 (Calfon et al., 2002), which leads to expression of transcription factors that upregulate proteins to increase the ER-folding capacity and thereby relieve ER load (Lee et al., 2003). IRE1 is also capable of promoting apoptosis by activating apoptosis signal-regulating kinase (ASK) that in turn phosphorylates c-Jun N-terminal kinase (JNK) (Urano et al., 2000). JNK is a member of the mitogen activated protein kinase (MAPK)-family that has been reported to induce apoptosis by translocation of Bax (Tsuruta et al., 2004) or through direct activation of caspase 12 (Yoneda et al., 2001).

Protein kinase activated by double-stranded ribonucleic acid (RNA) (PKR)-like endoplasmic reticulum kinase (PERK) monitors ER stress by its ER-lumen domain and after oligomerization in response to ER-stress activates its cytosolic kinase domain (Harding et al., 1999). This in turn phosphorylates and thereby inactivates eukaryotic initiation factor 2 α (eIF2 α), which disables ribosomal assembly and decreases protein translation (Harding et al., 2000a). Decreased protein synthesis immediately protects from increasing misfolded-protein load, but can endanger the cell if vital proteins cannot be replaced. Downstream of PERK, more regulatory actions are possible, including altered translation of activating transcription factor 4 (ATF-4) which leads to upregulation of chaperones to enhance ER capacity or the activation of chop/Gadd153 to regulate and promote apoptosis (Harding et al., 2000b).

The third branch of ER-stress response is regulated by ATF-6 α . When ER-stress is sensed, ATF-6 α is translocated to the golgi-apparatus, where the transmembrane domain is removed (Ye et al., 2000). The remaining fragment is then translocated to the nucleus where it upregulates downstream factors like XBP-1 and ATF-4. Thus, all three ER-stress responses can either trigger survival-signaling cascades or induce apoptosis through mechanisms not fully understood. The main UPR pathways are depicted in figure 1.1.

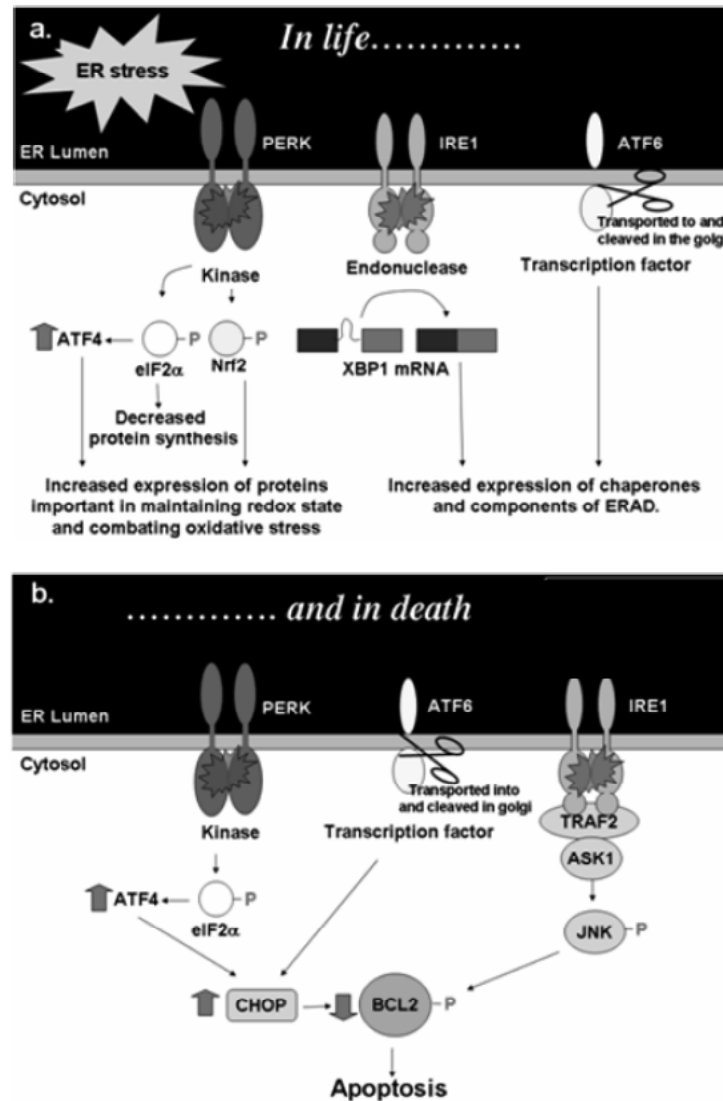


Fig. 1.1: Pathways of ER-stress response. (a) Upon ER stress, PERK and IRE1 are activated, whereas ATF6 is transported to the golgi where it is activated by cleavage. The activated pathways lead to the alleviation of ER stress and hence increased cell survival. (b) Prolonged UPR results in induction of apoptosis via PERK-dependent and possibly ATF6-dependent decrease in Bcl-2, recruitment of ASK1 and JNK activation, which phosphorylates and inactivates Bcl-2 (adapted from Herbert, 2007).

In human disease, ER stress leads to cell death in conditions linked to misfolded proteins such as some neurodegenerative diseases or alternatively to unwanted cell survival in neoplastic transformation or viral infection (reviewed in Lin et al., 2008). For example, the PERK pathway functions as an antiviral defense by mediating kinase activity similar to the double-stranded RNA-activated kinase PKR. Indeed, PERK-deficiency increases virus production of vesicular stomatitis virus, suggesting that PERK exerts a viral defense mechanism through translational blocking (Baltzis et al., 2004; Perkins et al., 2004). Herpes simplex virus encodes a protein named ICP34.5, which dephosphorylates and thereby activates eIF2α to enable enhanced translation of the virus envelope protein

(Chou et al., 1994). Therefore, intact UPR seems to be an important anti-viral mechanism to protect the organism from increased virus load.

On the other hand, cell death as a response to UPR may cause neurodegenerative disorders. In AD, abnormal protein aggregation is a common event with the key cytotoxic polypeptide being amyloid beta (A β) (Schenk et al., 1999). Expression of A β has been reported to activate caspase-12 and increase ER chaperone levels (Ferreiro et al., 2006), hinting at the involvement of the IRE1-pathway in A β -mediated neuron loss. Moreover, PERK signaling has been shown to be activated under hypoxic conditions and act cytoprotective by decreasing translation as described above. Hereby it mediates a protective mechanism not only to normal but also to neoplastic tissue, where hypoxia occurs frequently as a result of rapid proliferation. PERK activity has been found to be increased in several primary human tumors like breast and cervical cancer, melanoma and glioblastoma (Bi et al., 2005).

Taken together, unfolded protein response is a necessary mechanism to protect from accumulation of misfolded proteins or virus infection, but deregulation may have unprofitable results such as tumor progression or neuron loss.

1.2.2 Oxidative Stress

Oxidative stress is defined as an imbalance between the production and scavenging of reactive oxygen species (ROS) in a biological system. ROS include superoxide anions, hydroxyl radicals and hydrogen peroxide and are mainly by-products of respiratory chain complexes, at complex I and complex III. At complex III, the free radical semichinon ($\cdot Q^-$) is formed as an intermediate in the regeneration cycle of coenzyme Q. $\cdot Q^-$ is capable of transferring electrons to molecular oxygen and subsequently this may form a superoxide radical (Turrens et al., 1997). Furthermore, both enzymatic and spontaneous reactions can reduce O_2 to H_2O_2 that in turn can be reduced by metal cations like Fe(II) or Cu(I) to form the OH^\cdot radical (reviewed in Fridovich, 1998). Other sources of oxidative stress are exogenous sources such as ultraviolet light, radiation, toxins or cytokines.

Since ROS formation is an inevitable event, evolution has given rise to a detoxifying system. This system includes superoxide dismutases (SODs) to convert superoxide into hydrogenperoxide as well as catalases and glutathione peroxidases that convert hydrogenperoxide to water and molecular oxygen (Fridovich, 1998). Non-enzymatic compounds of the ROS defense are carotenoids, flavonoids, ascorbate and glutathione.

If the balance between ROS formation and scavenging is disturbed and ROS accumulate, these highly reactive molecules damage proteins, DNA and unsaturated lipids as present in the phospholipid bilayer of cell membranes (reviewed in Finkel & Holbrook, 2000). Oxidative stress can then result in distinct cellular responses such as senescence-like growth arrest (Chen & Ames, 1994),

apoptosis via p53 activation in a positive feedback loop (Johnson et al., 1996; Polyak et al., 1997) or other signaling processes. Furthermore, the cells may upregulate proteins involved in ROS scavenging to relieve oxidative stress including heat-shock proteins and chaperones (Allen & Tresini, 2000). Sources, defense mechanisms and possible downstream mediators are summarized in figure 1.2.

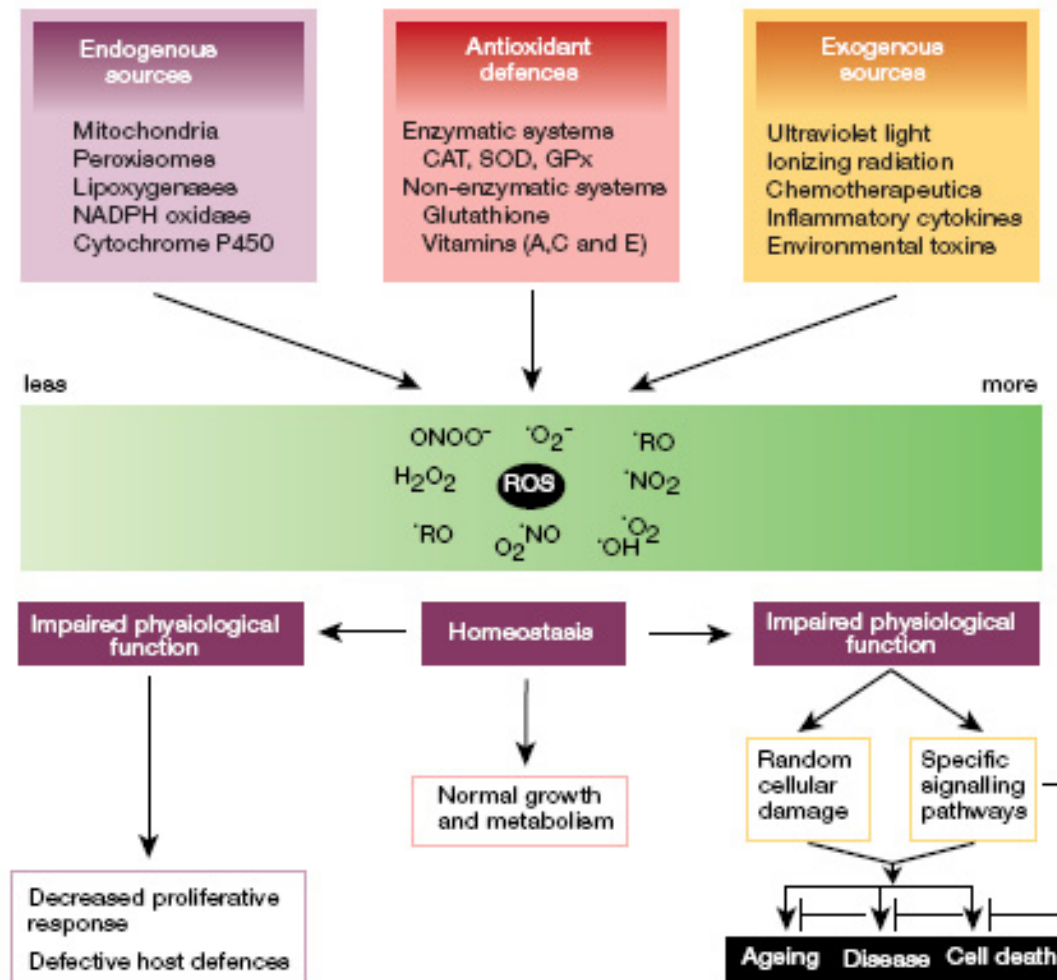


Fig. 1.2: Sources, defense mechanisms and downstream effects of oxidative stress. (Adapted from Finkel & Holbrook, 2000)

Not surprisingly, oxidative stress has been reported to be implicated in human neurodegenerative diseases and to be one of the major factors in aging. Elevated markers of oxidative stress have been found in brain tissue of AD (Butterfield et al., 2002) and PD (Dexter et al., 1989) and in cerebrospinal fluid of amyotrophic lateral sclerosis (ALS) patients (Pedersen et al., 1998). This indicates an involvement of oxidative stress in the pathology of these conditions, yet the mechanisms by which neuronal loss is mediated are not fully understood. Post-mitotic neuronal cells are particularly vulnerable to any kind of damage and neuronal cells and the brain in general are highly metabolically active and therefore may accumulate ROS in higher quantities than other organs (Behl, 1999).

The well described hippocampal cell line HT22 serves as a model for oxidative stress through oxidative glutamate toxicity that provides insight into the cellular response to oxidative stress (Davis & Maher, 1994). In oxidative glutamate toxicity high concentrations of extracellular glutamate disable the glutamate/cystine antiporter Xc⁻, which exports glutamate and at the same time imports cystine, an essential compound for the synthesis of antioxidant glutathione (Murphy et al., 1989). In the absence of glutathione ROS accumulate in the cells, which then undergo a coordinated type of cell death sharing both necrotic and apoptotic features (Tan et al., 1998).

As described above, cells experiencing oxidative stress may change their expression patterns of certain protective receptors or can be protected by activation of protective signaling pathways. For example it has been observed that the loss of protein kinase C (PKC) might contribute to the severity of oxidative damage in neurological disorders and that activation of PKC by the phorbol ester TPA can rescue these cells by increasing the activity of extracellular signal-regulated kinase (ERK) and c-Jun N-terminal kinase (Maher, 2001). Moreover, activation of group II metabotropic glutamate receptors (mGluR) can significantly decrease hippocampal neuron loss in a gerbil model of global ischemia (Bond et al., 1998). It has also been described that HT22 cells selected by chronic exposure to high concentrations of glutamate have been shown to upregulate a pattern of G-protein coupled receptors, including metabotropic glutamate receptors mGlu1 and mGlu5 (Sagara & Schubert, 1998), VPAC₁₊₂ and P2Y6, a pyrimidine-nucleotide receptor (Sahin et al., 2006) that have protective effects against oxidative stress.

G-Protein Coupled Receptors

G-protein coupled receptors (GPCRs) represent the largest group of cell surface molecules in the human proteome. The more than 800 members of this gene superfamily are encoded by more than 2% of the human genome.

Structure and Function

G-protein coupled receptors were originally defined as proteins that pass on signals from the extracellular space to intracellular compartments by inducing biochemical processes that involve the activation of heterotrimeric G-proteins. GPCRs are involved in reception of various stimuli such as amines, purines, lipids, peptides, odors, ions or even photons and regulate many physiological processes including neurotransmission, cell metabolism, secretion, visual perception and even cell proliferation or adhesion (reviewed in Pierce et al., 2002).

The large superfamily shares the common feature of seven transmembrane domains that have an α -helical structure, with an extracellular N-terminus, three extracellular loops and an intracellular C-terminal domain along with three cytosolic loops. They are classified into three major subfamilies A, B and C. Family A (rhodopsin-like receptors) is the largest subfamily, sharing 20 conserved amino acids in the transmembrane regions and a palmitoylated cysteine residue in

their C-terminal domains. Family B (secretin/glucagon-receptor family) contains approximately 25 members and shares a large N-terminal domain, a relatively short C-terminal tail and no palmitoylation site, but six well conserved cysteine residues. Family B seems to couple mainly to adenylyl-cyclase activation through G_s . Family C members (metabotropic neurotransmitters and Ca^{2+} -sensing receptors) contain a large N-terminal domain with 20 cysteine residues and no C-terminal palmitoylation site (reviewed in Liebmann, 2004).

This large amount of receptors couples to a limited number of heterotrimeric G-proteins. Heterotrimeric G-proteins consist of an α -, β - and γ -subunit, with the α -subunit harbouring a guanine-nucleotide binding site and a GTP-ase activity. G-proteins are divided into four subfamilies by sequence similarity of their α -subunits. These subfamilies also share functional similarities. $G_s\alpha$ -family members generally stimulate, whereas $G_{i/o}$ family members inhibit adenylyl cyclases. The G_q -family stimulates phospholipase C (PLC), which results in production of inositoltriphosphate (IP3) and diacylglycerol (DAG) as second messengers. The $G_{12/13}$ proteins are less well described, but have been reported to stimulate phospholipase D (PLD) and tyrosine kinases as well as guanine exchange factor Rho (RhoGEFs) (reviewed in Liebmann, 2004).

A classical example of GPCR-signaling is the formation of a complex between receptor, ligand and G-protein, which leads to an exchange of GDP for GTP on the $G\alpha$ -subunit and dissociation of the heterotrimeric G-protein into an α -subunit and a β/γ -complex. In consequence, $G\alpha$ may increase cAMP and thus activate protein kinase A (PKA), the β/γ -complex itself may activate PLC or phosphatidylinositolphosphate 3-kinase (PI 3K) (Gilman et al., 1987). These factors have a multitude of substrates and effects in cell metabolism (Fig. 1.3).

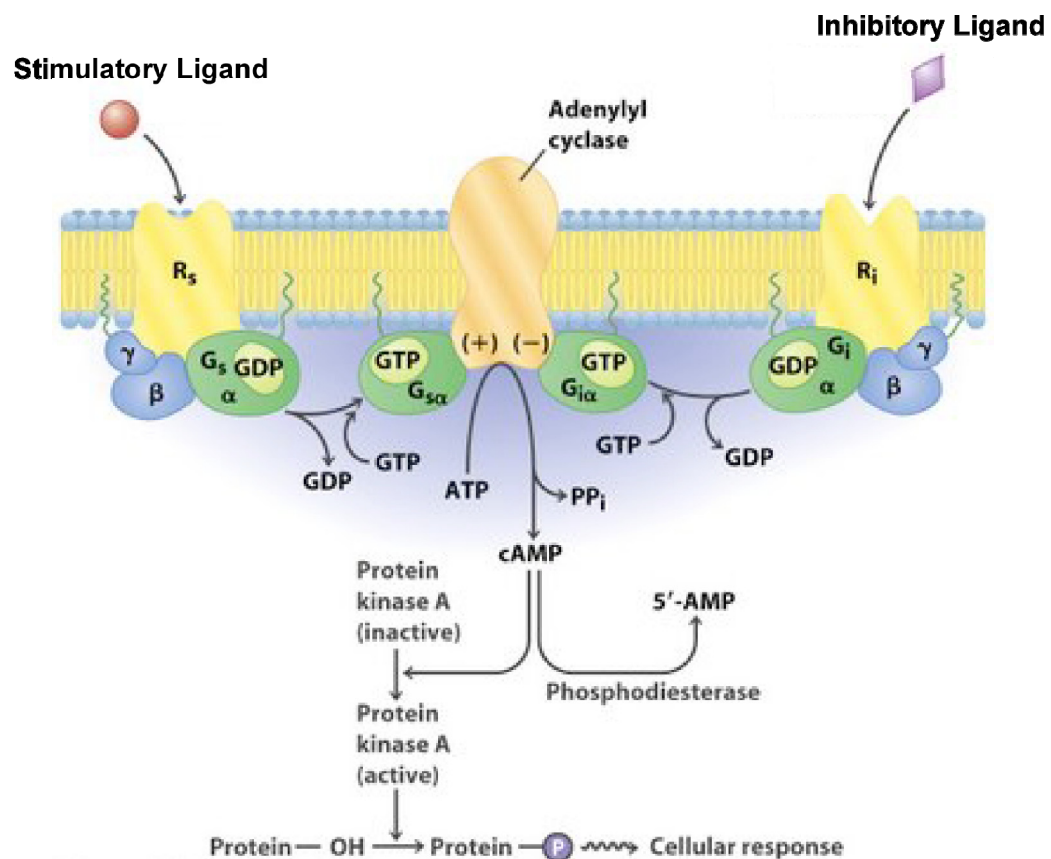


Fig. 1.3 Classical GPCR signaling cascade schematically displayed. Classical GPCR signaling involves ligand binding, exchange of GDP by GTP, dissociation of the α -subunit and the β/γ -heterodimer, activation of adenylyl cyclase and activation of PKA leading to a cellular response (adapted from Principles of Biochemistry, Robert Horton, 1996).

Receptors are meant to signal a change in the environment, such as the appearance of a smell, a changing visual signal, or a concentrational change of a certain ligand. To ensure the signaling cascade translates the signal in an appropriate magnitude, the activation of a GPCR has to be tightly regulated and sometimes dampened or inhibited almost at the moment of activation even in persistent presence of the ligand. This process is called desensitization (Ferguson et al., 2001).

Receptor desensitization occurs in different ways. One possible way is the phosphorylation of the respective receptor by its own downstream kinases PKA, PKC and G-protein coupled receptor kinases (GRKs) (Pitcher et al., 1998), which directly uncouple the G-protein from the receptor as a negative feedback mechanism or even switch coupling to a different G-protein (Lawler et al., 2001). The GRK-mediated regulation involves the specific phosphorylation of ligand-bound receptors, which promotes binding of β -arrestin and subsequently leads to steric inhibition of G-protein coupling (Zhang et al., 1997). Phosphorylation and binding of β -arrestin may then lead to trafficking of the receptor to clathrin-coated pits via direct interaction of

β -arrestin with both the phosphorylated receptor and a subunit of clathrin. This subsequently results in receptor endocytosis (Laporte et al., 1999) to an acidic endosome where receptors are either dephosphorylated and turned back to the cell membrane or degraded (Pitcher et al., 1995). Two more mechanisms of internalization have been described: caveolae-mediated internalization, which is less well described and seems to have a more positive regulating effect by shuffling receptors to different cell compartments for signaling actions (Smart et al., 1999), and the regulation by ubiquitination, which also has a regulatory role (Shenoy et al., 2001).

Another important regulatory mechanism is the regulation by regulators of G-protein signaling (RGS) proteins. The RGS protein family consists of about 25 members that share a homology domain of 130 amino acids and have a distinct selectivity for G-proteins or even for one particular receptor. Their general feature is a GTPase function, specific for heterotrimeric G-proteins that accelerates GTP hydrolysis and thus inhibits activation of downstream targets (Ross & Wilkie, 2000).

In addition to these classical features of GPCRs, crosstalk between the signal transduction cascades occurs at several levels of signaling, such as homo- or heterodimerization of GPCRs, as shown for receptor tyrosine kinases that need their homodimerization partner for ligand induced autophosphorylation (Heldin, 1995) or the κ - and δ - opioid receptors, which enhance their function by heterodimerization and alter receptor pharmacology (Jordan & Devi, 1999), as well as G-protein independent signal transduction through interaction with receptor tyrosine kinases or altered signal transduction depending on the concentration and duration of ligand presence, as shown for the thrombin receptor (Donovan et al., 1998). Considering the mass of receptors, ligands, G-proteins and downstream effectors, the diversity of GPCR-mediated signaling and the amount of cellular functions regulated are vast (hinted in Fig. 1.4). This also offers a chance to regulate multiple functions pharmacologically if the exact pathway is known.

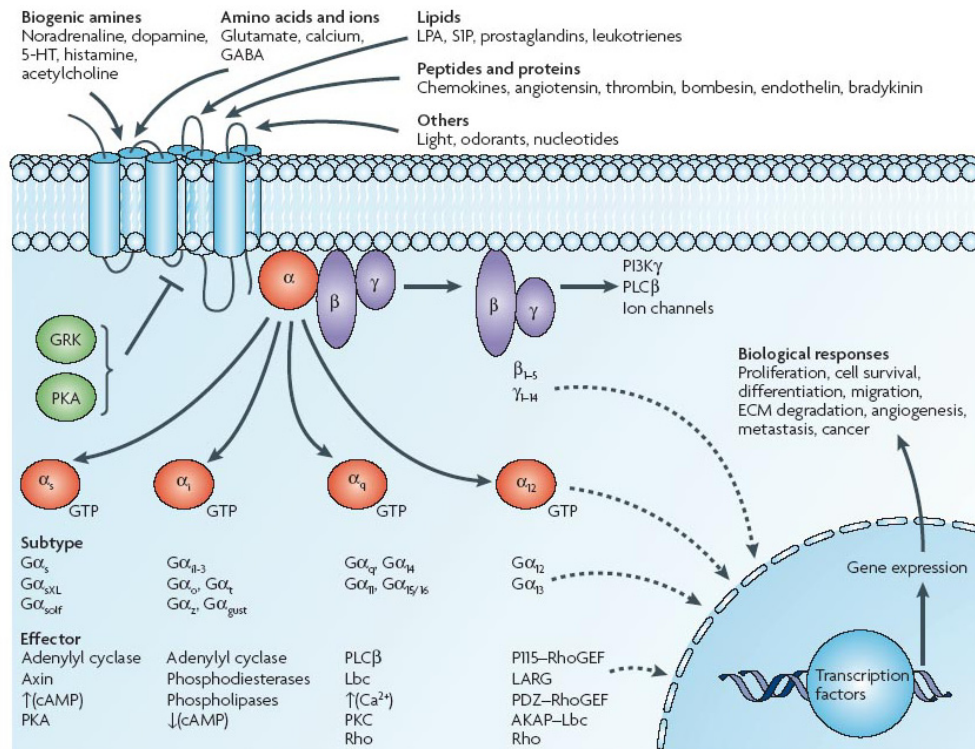


Fig. 1.4: Schematic picture of GPCR-signaling diversity. Several classes of agonists, different Gα-subtypes and a multitude of possible effectors lead to a huge amount of possible cellular responses (adapted from Dorsam & Gutkind, 2007).

GPCRs as Drug Targets

Regarding the various physiological functions, it is not surprising that GPCRs have a proven history of serving as excellent drug targets. Already, a number of pharmaceutical agents were targeting GPCRs, before structure and mechanism were even investigated. To alter receptor activity there are three different groups of ligands: agonists that increase receptor activity, antagonists that inhibit ligand binding and inverse agonists that reduce basal activity. Several hundreds of GPCR-targeting drugs have been introduced to the market in the past forty years, most of them acting as inverse agonists (reviewed in Wilson et al., 1998), the prominent examples being fexofenadine, sold as Telfast®, a histamine-receptor antagonist, and sumatriptan that causes vasoconstriction by activating the serotonin receptor (reviewed in Jakobi et al., 2006). Still more than 150 orphan GPCRs that have no known ligand or function are under investigation (Wise et al., 2004) and are subject to various de-orphanizing efforts in order to develop novel therapeutics.

Protective Action of GPCRs in the Nervous System

As a result of the multitude of physiological processes that are controlled and fine-tuned by GPCR-mediated signaling, it is not surprising that GPCRs have been described to be involved in cell survival and cytoprotection in various ways.

In the nervous system, in model mechanisms of ischemic injury, agonists of group II mGluR have been reported to significantly reduce hippocampal neuron loss after induced global ischemia in rodents (Bond et al., 1998). Dopamine-receptor 2 had a similar effect when activated by pharmacological agonists (O'Neill et al., 1998). More recently it has been reported that activation of the PAR2-receptor by central administration of a peptide agonist (SLIGRL) inhibits electrical amygdala epileptogenesis and thereby protects from epileptic brain damage (Lohmann et al., 2008). More generally, activation of group II mGluRs has been shown to protect against glutamate excitotoxicity in cortical neurons (Bruno et al., 1995) and oxidative glutamate toxicity (Sagara & Schubert, 1998). This indicates a role in neurodegenerative disease linked to oxidative stress as described above. This rather small selection of protective GPCRs indicates a broad range of therapeutic targets for human disease, as the activation of group II mGluRs may protect neurons challenged by oxidative-, glutamate- or ischemic conditions from cell death and thus relieve consequences of stroke or ischemia.

Effects of GPCRs in Cancer

Not every cytoprotective effect is of benefit to the human organism. GPCRs have repeatedly been shown to confer pro-survival and proliferation signaling in neoplastically transformed cells. The gastrointestinal peptide cholecystokinin (CCK) that activates the CCK receptor has been observed to promote $G\alpha_q$ -mediated activation of PKC and subsequently to be involved in survival and proliferation of clinically aggressive tumors of lung, colon and pancreas (Rozengurt et al., 2002). Endothelins and their respective receptors, endothelin receptor A and B (ER_A , ER_B), activate downstream targets known to be involved in cell survival and proliferation such as epidermal growth factor (EGF) and its receptor (EGFR), insulin-like growth factor and PKC. In malignant tissue, ER_A is capable of inhibiting apoptosis by obstruction of fas ligand (FASL)-mediated apoptosis or by induction of anti-apoptotic Bcl-2 and PI3K-mediated pathways. These findings have been proven for several tumor- and celltypes. Successful phase I and II clinical trials with ET_A -receptor agonists as a prostate-cancer treatment have been performed (reviewed in Nelson et al., 2003).

In addition to mere survival promoting signaling by certain GPCRs metastasis, angiogenesis, migration and invasion processes are also promoted by GPCRs. Even oncongenic viruses exploit the pro-proliferational capacities by harbouring open reading frames that encode for GPCRs (reviewed in Dorsam & Gutkind, 2007). Tumor diseases linked to oncogenic viruses are for example Burkitt lymphoma linked

to a GPCR named BILF1 encoded by the Epstein-Barr-virus genome (Paulsen et al., 2005) or Kaposi sarcoma induced by Kaposi sarcoma-associated herpes virus (KSHV) GPCRs (Sodhi et al., 2004).

G-Protein Coupled Receptor 39

GPR39 is an orphan G-protein coupled receptor with a 1660 basepair transcript, resulting in a peptide of 456 amino acids and a calculated weight of 51.5 kDa. It was classified to family A, the rhodopsin-like GPCRs and described as being constitutively active and to signal possibly through $G_{12/13}$, Rho kinase and the serum-response element (SRE) (Holst et al., 2004). It was first cloned and characterized in 1997 (McKee et al., 1997) as being closely related to the growth hormone secretagogue receptor (GHS-R) and belonging to the ghrelin receptor family. The GPR39 gene shares its 3' exon with an antisense gene called LYPD1 (Ly-6/PLAUR domain containing 1), which is highly abundant in the nervous system (Egerod et al., 2007). In 2005, GPR39 was controversially suggested to bind obestatin, a peptide derived from the ghrelin-prepropeptide and have an effect on food intake (Zhang et al., 2005). As several studies could not reproduce these findings (Lauwers et al., 2006; Yamamoto et al., 2006; Tremblay et al., 2007; Gourcerol et al., 2007), GPR39 was again considered an orphan GPCR. GPR39 has been described to be expressed throughout the gastrointestinal-tract including liver, pancreas, kidney and adipose tissue (Egerod et al., 2007). Its main distribution was also reproduced in the Japanese quail (Yamamoto et al., 2007). In adipose tissue, downregulation of GPR39 was observed in obesity-associated type 2 diabetes mellitus (Catalán et al., 2007). In an in-situ hybridization screen of mouse-brain tissue, highest levels of GPR39 messenger RNA (mRNA) in the CNS were detected in amygdala, hippocampus and auditory cortex, but not hypothalamus, which would be expected to be the site of obestatin action (Jackson et al., 2006). More recently, a stimulatory effect of zinc ions on GPR39 signaling was suggested (Holst et al., 2007; Yasuda et al., 2007).

Previous studies of our group have shown GPR39 to be upregulated in a cell line resistant to oxidative glutamate toxicity and to be protective against oxidative stress by increasing glutathione and additionally against cell death caused by tunicamycin or ceramide (Dissertation Mert Sahin, AG Methner, 2006). Mert Sahin also demonstrated GPR39 abundance in several nervous tissues, such as the spinal cord, cerebral cortex, amygdala, dentate gyrus, Purkinje- and Granular cell layer and in the retina and retinal pigment epithelium and lung. The mechanism of GPR39-mediated protection from oxidative stress however remained unclear.

2. Aim of this Study

GPR39 is an orphan GPCR found to be protective against diverse cytotoxic or pro-apoptotic conditions like oxidative glutamate toxicity, tunicamycin or ceramide stress. The aim of this study was to clarify how the orphan G-protein coupled receptor GPR39 protects from cell death.

To find out the exact mechanism, two stable monoclonal cell lines were established that differed only threefold in GPR39 overexpression. These two cell lines provided the chance for a transcriptomal comparison, which could show possible downstream mediators by giving information about increased or decreased transcripts when comparing the two cell lines. From this approach, a list of possibly interesting downstream proteins or pathways could be used to identify the signal transduction pathway, mediator and effector proteins.

A better understanding of the GPR39 signal-transduction cascade could offer ideas which conditions or diseases and their treatment could be improved by specific pharmacological alteration of GPR39 signaling.

3. Materials

Chemicals

Unless otherwise denoted, chemicals were purchased from Roche (Mannheim), Merck (Darmstadt), Roth (Karlsruhe), Sigma-Aldrich (Steinheim), Fluka Chemie GmbH (Buchs) and Invitrogen (Karlsruhe).

Enzymes

Restriction Endonucleases

All restriction enzymes were purchased from New England Biolabs (NEB, Frankfurt) and used according to manufacturers protocol along with the appropriate buffers supplied by NEB.

Miscellaneous Enzymes

T4-DNA-Ligase	NEB, Frankfurt
Reverse Transcriptase	Invitrogen, Karlsruhe
LR Clonase	Invitrogen, Karlsruhe

Kits

Nucleobond Kit PC500	Machery-Nagel, Düren
QIAprep Spin Mini Kit	Qiagen, Hilden
RNeasy Mini Kit	Qiagen, Hilden
Profound c-myc-Tag CoIP Kit	Pierce, Bonn
Profound HA-Tag CoIP Kit	Pierce, Bonn
Luciferase Assay Kit	Promega, Mannheim
Gel Extraction Kit	Qiagen, Hilden
BCA Protein Assay Kit	Interchim, Montluçon
QPCR Core Kit for SYBR Green	Eurogentech, Cologne

Antibodies

Primary Antibodies

Anti-myc-tag antibody: Monoclonal mouse antibody against the c-myc epitope, clone 4A6 (EQKLISEEDL) (Millipore, Schwalbach/Ts.). The antibody was used for immunoblotting in a 1:1000 dilution.

Anti-HA-tag antibody: Polyclonal rabbit antibody against the influenza hemagglutinin-HA-epitope (YPYDVPDYA) (Abcam, Cambridge). The antibody was used for immunoblotting in a 1:1000 dilution

Anti-FLAG®-tag antibody: Polyclonal rabbit or monoclonal mouse antibodies, that recognizes the FLAG epitope (DYKDDDDK) (Sigma-Aldich, Steinheim). Both Antibodies were used for immunoblotting in a 1:1000 dilution.

Anti-VP16-tag antibody: Polyclonal rabbit antibody against the activation domain (amino acids 413-490) of herpes simplex virus HSV-VP16. (Abcam, Cambridge). The antibody was used for immunoblotting in a 1:2000 dilution.

Anti-β-actin antibody: Monoclonal mouse antibody against β-actin, clone C4 (Millipore, Schwalbach/Ts.). The antibody was used for immunoblotting in a 1:2000 dilution and served as a loading control.

Anti-SRF antibody (G-20): Polyclonal rabbit antibody against the C-terminus of serum response factor (SRF) (Santa Cruz, Heidelberg). The antibody was used for immunoblotting in a 1:1000 dilution.

Anti-PEDF antibody: Polyclonal rabbit antibody produced against full-length pigment epithelium derived factor (PEDF) (Millipore, Schwalbach/Ts.). The antibody was used for immunoblotting in a 1:1000 dilution and for neutralization of PEDF in cell culture experiments at a concentration of 2 µg/ml.

Anti-TNRC9 antibody: Polyclonal rabbit antibody against mouse TNRC9. This antibody was a kind gift from Anirvan Ghosh, La Jolla. It was used in 1:1000 dilution for immunoblotting.

Anti-Cited1 antibody: For the detection of Cited1 using immunofluorescence, the rabbit polyclonal antibodies I51904K and J722220K were used at a dilution of 1:100; for immunocytochemistry, the mouse monoclonal antibodies H1, 2H2 and 2H6 were used at 1:1000. These antibodies were a kind gift from Toshi Shioda, Harvard University.

Secondary Antibodies

Horseradish peroxidase (HRP)-conjugated antibodies: goat-α-rabbit and goat-α-mouse IgG secondary antibodies were purchased from Serotec, Duesseldorf. Both antibodies were used at a 1:5000 dilution.

IRDye-conjugated antibodies: goat-α-rabbit and goat-α-mouse IgG secondary antibodies conjugated to near infrared conjugates IRdye 680 nm and IRdye 800 nm were purchased from Licor, Königstein. These antibodies were used in a 1:30.000 dilution.

Alexa-543 conjugated antibody: The goat- α -rabbit antibody conjugated to Alexa-543 was purchased from Molecular Probes (Karlsruhe) and used according to the manufacturers protocol.

Media

Bacterial Media

LB-Medium (Luria-Bertani Broth)

20 g of ready-made LB media powder (Invitrogen, Karlsruhe) were dissolved in 1 l of distilled water and autoclaved before use.

LB-Agarplates

32 g of LB-Agar powder (Invitrogen, Karlsruhe) were dissolved in 1 l of distilled water and autoclaved before pouring into 10 cm petri dishes.

LB-Amp

LB-Medium + 100 μ g/ml Ampicillin

LB-Kan

LB-Medium + 100 μ g/ml Kanamycine

Cell Culture Media

Media for N2A, SH-SY5Y, HEK 293, COS-7 and MEF cells (see 3.7)

The most commonly used cell culture media consisted of DMEM High Glucose (Dulbeccos modified eagles medium) (PAA, Pasching, Austria) supplemented with 10% of fetal calf serum (FCS) (Hyclone, Vienna, Austria) and 1% Penicillin/Streptomycine (Gibco, Karlsruhe). 1% Penicillin/Streptomycine equals 100 U/ml Penicillin and 100 μ g/ml Streptomycine.

HT22-Medium

Medium for HT22 cells consisted of DMEM (PAA, Pasching, Austria) supplemented with 5% of fetal calf serum (Hyclone, Vienna, Austria), 1% Penicillin/Streptomycine (Gibco, Karlsruhe), HT22R medium additionally contained 10 mM glutamate.

CHO-Medium

Medium for Chinese hamster ovary cells (CHO) consisted of DMEM/F12-Medium (Gibco, Karlsruhe) with 10% of fetal calf serum (Hyclone, Vienna, Austria), 2 mM L-glutamine (Gibco, Karlsruhe) and 1% Penicillin/Streptomycine (Gibco, Karlsruhe).

Buffers and Solutions

MTT-Solubilization Buffer, pH 4

Dimethylformamide	20% (v/v)
SDS	20% (w/v)
Acetic acid	10% (v/v)
aqua dest	

TFB 1

RbCl	100 mM
MnCl	250 mM
K ₂ CO ₃	30 mM
CaCl ₂	10 mM
Glycerol	15% (v/v)
aqua dest	

TFB 2

MOPS	10 mM
RbCl	10 mM
CaCl ₂	75 mM
Glycerol	15% (v/v)
aqua dest	

PBS (Phosphate Buffered Saline) pH 7,4

NaCl	137 mM
KCl	2.7 mM
KH ₂ PO ₄	1.4 mM
Na ₂ HPO ₄	100 mM
aqua dest	

PBS-T

0,05% (v/v) Tween20 in PBS

TBE-Buffer (10x)

Tris	900 mM
Borsäure	900 mM
EDTA	10 mM
aqua dest	

Annexin V-Binding Buffer (10x) pH 7,4

Hepes	100 mM
NaCl	1,4 M
CaCl ₂	25 mM
aqua dest	

Miscellaneous Buffers

Buffers not mentioned above were purchased from Gibco (Karlsruhe) or Invitrogen (Karlsruhe).

Bacteria

In general in this study bacteria were exclusively used for the production of large amounts of plasmid DNA or molecular cloning purposes.

Escherichia Coli DH5

This most commonly used strain of *E. coli* carries the following genotype: F' Phi80dlacZ DeltaM15 Delta(lacZYA-argF)U169 deoR recA1 endA1 hsdR17(rK-mK+)phoA supE44 lambda- thi-1.

One Shot® ccdB Survival™

The One Shot® *ccdB* Survival™ bacteria strain is resistant to the toxic effects of the *ccdB* gene (Bernard and Couturier, 1991; Salmon *et al.*, 1994) and is therefore the suitable strain to propagate vectors carrying the *ccdB* gene (i.e. Gateway™ destination vectors, Invitrogen, Karlsruhe).

Cell Lines

Neuro-2A (N2A)

The Neuro-2A cell line is a commonly used cell line derived from a murine neuroblastoma.

Human Embryonic Kidney Cells (HEK 293)

HEK 293 cells were generated by transforming cultured cells from a healthy embryonic kidney with sheared DNA from the human adenovirus 5. By this process cells were immortalized and are easy to maintain and transfect.

HT22 Cells

HT22 cells are derived from a murine hippocampus and are used as a model for oxidative glutamate toxicity. In this study, both HT22 wildtype cells, that will be referred to as HT22S and HT22R cells are used. HT22 R cells are a polyclonal

subpopulation that is resistant against glutamate toxicity. They were generated by repeatedly exposing the HT22S cells to 10 mM of glutamate and further propagating the surviving cells.

Chinese Hamster Ovary Cells (CHO)

The CHO cell line is derived from chinese hamster ovary cells and is commonly used for expression of recombinant proteins.

Mouse Embryonic Fibroblasts (MEF)

The mouse embryonic fibroblast-cell line was generated by a lab member by immortalization of primary cells from E12.5-13.5 mouse embryos.

SH-SY5Y Cells

SH-SY5Y cells are derived from a human neuroblastoma.

COS7 Cells

The COS7 cell line is derived from kidney cells of the African green monkey and immortalized by transformation with a version of the SV40 genome. It is used to transfect cells to produce recombinant proteins.

Plasmids

Expression Plasmids

In this study, several expression plasmids and constructs were used. They are listed alphabetically in table 3.1.

Gene	Species	Vector- Backbone	Features (Mutations, Deletions, Tags)	Source (if available)
Bax	mouse	pcDNA3.1	EGFP-tag	Pawel Kerner
Cited1 HA	mouse	pRC/CMV	HA-tag	Toshi Shioda
Cited2 HA	mouse	pRC/CMV	HA-tag	Toshi Shioda
Cited3 HA	mouse	pRC/CMV	HA-tag	Toshi Shioda
Cited4 HA	mouse	pRC/CMV	HA-tag	Toshi Shioda
Empty Vector		pcDNA3.1		Invitrogen
Empty Vector		pcDNA5.1		Invitrogen
Empty Vector		pEGFP-C3	EGFP-tag	Clontech
Empty Vector		pEGFP-N1	EGFP-tag	Clontech
Empty Vector		pCI-neo		Promega

ER α -VP16	mouse	pVP16	VP16 transactivation-tag	Addgene
ER β -VP16	mouse	pVP16	VP16 transactivation-tag	Addgene H.P.
GPR39	human	pcDNA5.1	wildtype	Nothacker
GPR39	mouse	pcDNA5.1	HA-tag	AG Methner
GPR39	mouse	pDESTmyc	myc-tag	this study
GPR39	mouse	pDEST-flag	flag-tag	this study
GPR39	mouse	pEGFP-C3	EGFP-tag	this study
hSRF-VP16	human	pCS2+	VP16 transactivation-tag	Ulrike Philippa
hSRF-VP16	human	pCS2+	dM (nonfunctional deletional mutant)	Ulrike Philippa
TNRC9	mouse	pCI-neo	wildtype	this study
TNRC9	mouse	pEGFP-C3	EGFP-tag	this study
PEDF	mouse	pCMV-Sport6	wildtype	Ana Luisa
RGS16	mouse	pcDNA3.1	wildtype	Pina
RhoAT9N	mouse	pcDNA3.1	T19N	UMR cDNA
Smad4-flag	mouse	pcD-D4.3FR	flag-tag	UMR cDNA
SRF delta-CT	mouse	pCS2+	d-CT (dn)	addgene
TNRC9	mouse	pbos	Full lenght, myc-tag	this study
TNRC9	mouse	pbos	Basepairs 1-501, myc-tag	Anirvan
TNRC9	mouse	pbos	Basepairs 1-711 myc- tag	Ghosh
TNRC9	mouse	pbos	Basepairs 1-869 myc- tag	Anirvan
TNRC9	mouse	pbos	Basepairs 712-1734 myc-tag	Ghosh
TNRC9	mouse	pbos	Basepairs 871-1734 myc-tag	Anirvan
TNRC9	mouse	pbos	Basepairs 1171-1734 myc-tag	Ghosh

Table 3.1: Listing of expression constructs used in this study, their vector backbones and source if available.

Reporter Plasmids

To determine the activity of certain promoters or responsive elements, several specific reporter constructs are commercially available. The constructs are listed in table 3.2.

Reporter Construct	Reporter Gene	Reporting Element or Promoter Region	Source
pCRE-Luc	Luciferase	cAMP-Response Element	Stratagene
pERE-Luc	Luciferase	Estrogen-Response Element	Addgene
pSRE-Luc	Luciferase	Serum-Response Element	Stratagene

Table 3.2: Listing of reporter constructs used, their respective reporter gene and source.

MicroRNA (miRNA) Plasmids

For the specific knockdown of gene transcripts, the corresponding sequences were cloned into the pcDNA™6.2-GW/EmGFP-miR (Invitrogen, Karlsruhe). This vector enables the expression of microRNA (miRNA) in mammalian cells under control of a DNA polymerase II promoter. The three miRNA constructs used in this study (pcDNA6.2-GPR39miRNA811, pcDNA6.2-GPR39miRNA965 and pcDNA6.2-GPR39miRNA1317) were derived from the linearized vector construct pcDNA6.2-GW/EmGFP-miR and the oligonucleotides specified in 3.12.3.

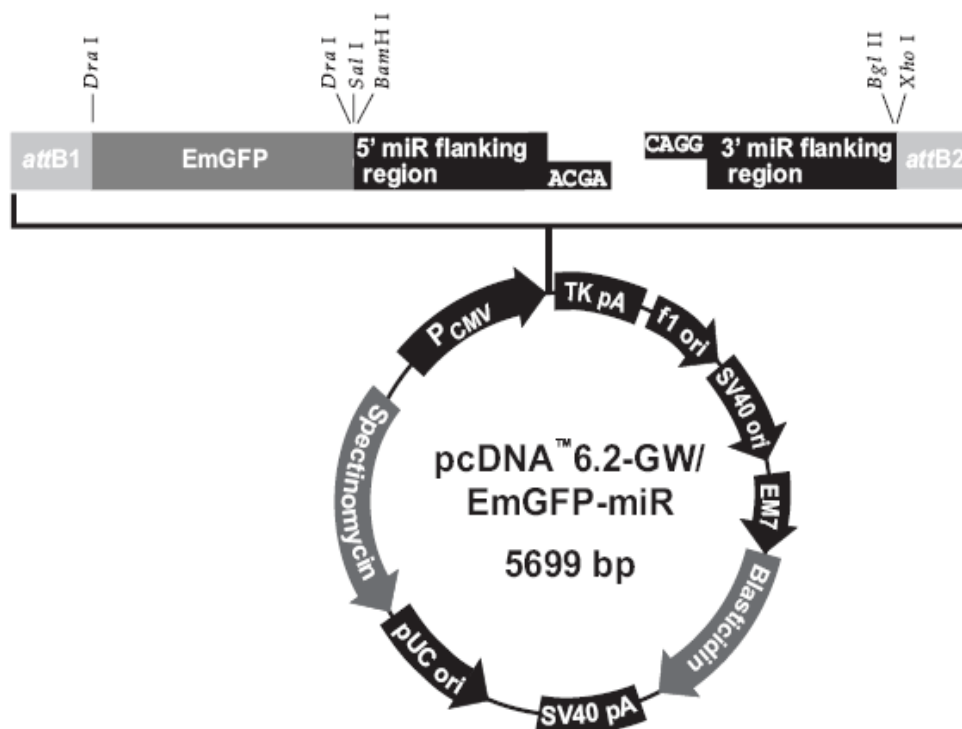


Fig. 3.1: Vector backbone map of pcDNA[™]6.2 (Invitrogen). The vector contains the Gateway®-attachement sites B1 and B2, an EmGFP sequence, blasticidin and spectinomycin resistance genes for both prokaryotic and eukaryotic hosts and two different “sticky-ends” in a linearized situation. Expression is driven by a DNA-polymerase II promoter (source: Invitrogen homepage).

ENTR[™] Plasmids

The Gateway System substitutes conventional cloning via restriction and ligation with homologous recombination. To use this system, the gene of interest is cloned into the ENTR[™] -vector of choice. The ENTR[™] vectors 1A, 2B and 3C differ in their reading frame by one base. From the ENTR[™] vector the gene can be transferred to a destination (DEST[™]) vector of choice by performing the LR-reaction (4.3.10).

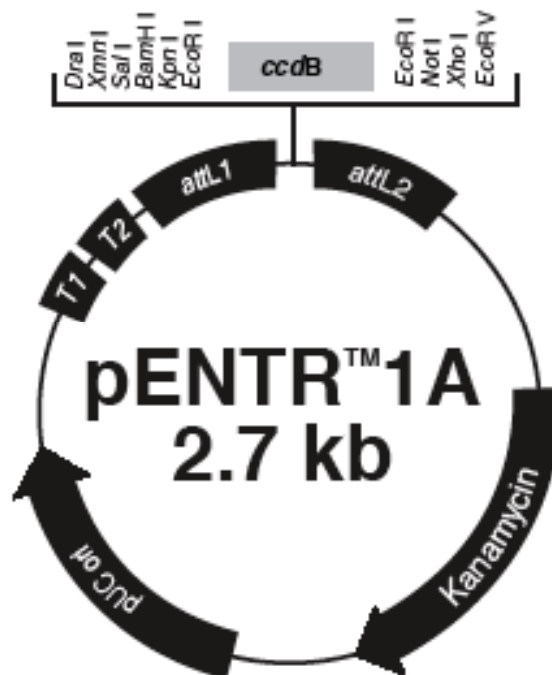


Fig. 3.2: The ENTR™ vector (Invitrogen) is an instrument for the use of the Gateway® System (Invitrogen). It contains attachment-sites (attL1 and attL2) for the recombination reaction with a destination vector. The multiple cloning site encloses the ccdB-gene, that disables growth of bacteria transformed with an empty ENTR™ vector (source: Invitrogen homepage).

Oligonukleotides

Oligonucleotides for quantitative polymerase chain reaction (PCR) or miRNA were purchased from MWG (Matrinsried). Oligonucleotides are displayed in 5'-3'-orientation.

qPCR Primers and Probes

GPR39 for

TAATACGACTCACTATAGGG

GPR39 rev

AGGGGCAAACAACAGATG

GPR39 probe (5' FAM, 3' TAMRA)

GGCGACCATCCTCCAAAATCGG

GAPDH for

TGCCAGCCTCGTCCCGTAGA

GAPDH rev

GCGCCCAATACGGCCAAAT

GAPDH probe (5' FAM, 3' TAMRA)

AAAATGGTGAAGGTCGGTGTGAAC

hTNRC9 for

ATACAGGGCCAGCCTCGTT

hTNRC9 rev

TCTGCTGAACAGAACGGATG

hTNRC9 probe (5' FAM, 3' TAMRA)

TGCTGAGTCAGCAGAAGCCCAGAC

QuantiTect Primer Assays (for SYBRgreen)

For all genes quantified with SYBR green (TNRC9, Cited1 and PEDF), QuantiTect Primer Assays (Qiagen, Hilden) were used.

miRNA-Oligonukleotides**GPR39 811 top**TGCTGTACAAAGCCAATCAGCAGTTTGT TTTGGCCACTGACTGACAAACT
GCTTTGGCTTTGTA**GPR39 811 bottom**CCTGTACAAAGCCAAGCAGTTTGT CAGTCAGTGGCCAAAACAAACTGC
TGATTGGCTTTGTAC**GPR39 965 top**TGCTGTGCAGATGGACATATTGGAGTGTT TTTGGCCACTGACTGACACTCC
AATGTCCATCTGCA**GPR39 965 bottom**CCTGTGCAGATGGACATTGGAGTGTCAGTCAGTGGCCAAAACACTCCAAT
ATGTCCATCTGCAC**GPR39 1317 top**TGCTGAAGGGCAGGAGGATCATGTATGTT TTTGGCCACTGACTGACATACA
TGACTCCTGCCCTT**GPR39 1317 bottom**CCTGAAGGGCAGGAGTCATGTATGTCAGTCAGTGGCCAAAACATACATG
ATCCTCCTGCCCTTC**Small Interfering RNA (siRNA)**

For knockdown experiments, siRNA pools and subpools from Dharmacon (Chicago, USA) were used.

Instruments

7500 Real Time PCR System	AppliedBiosystems, Darmstadt
Biofuge Strato	Heraeus, Osterode
Captair Bio PCR Hood	Erlab, Cologne
Curix 60 Developer	Agfa, Cologne
Facs Calibur	Beckton Dickinson, Heidelberg
FluoroGenios Pro	Tecan, Männedorf
GDS-Gel Imaging System	Intas, Göttingen
Heracell 150 Incubator	Kendro, Schwerte
Herasafe Sterile Hood	Kendro, Schwerte
iBlot Dry Blotting Device	Invitrogen, Karlsruhe
IX81-Flourescence Microscope	Olympus, Hamburg
Odyssey Infraredscanner	Licor, Bad Homburg
P25 Powerpack	Biometra, Göttingen
Sonoplus Sonicator	Bandelin, Hamburg
Subcell GT Powerpack	Biorad, München
Tabletop Centrifuge 5415R	Eppendorf, Hamburg
T Gradient PCR Cycler	Biometra, Göttingen
Thermomixer compact	Eppendorf, Hamburg
Xcell Sure Lock System	Invitrogen, Karlsruhe

4. Methods

Cell Culture Techniques

Maintenance of Cell Lines

All adherent cell lines were maintained in their respective media (see 3.5.2) and kept in 10 cm-dishes. At approximately 80% confluency they were washed with PBS twice and trypsinized until they were disattached from the plastic ware. Depending on the cell line they were split 1:10 or 1:5 every three to four days. To obtain frozen stocks, all cells were grown to 90% confluency, harvested by trypsination and centrifuged for 4 min at 800 rpm. The pellet was washed twice with PBS and resuspended in 90% FCS and 10% DMSO. The cells were transferred to cryotubes at a density of approximately 3×10^6 cells/ml and cooled down to -80°C before they were transferred to liquid nitrogen. Cells were thawed in a 37°C waterbath and suspended in 10 ml of pre-warmed media, centrifuged at 800 rpm for 4 min and the pellet resuspended in 10 ml of media and plated into a 10 cm culture dish.

For experiments, cells were trypsinized, suspended in fresh media and a sample was mixed with trypanblue-stain at a ration of 1:3. Cells were then counted in a Neubauer-chamber and seeded at the desired density into the desired format of a multiwell cell-culture plate.

Transfection of Cell Lines

For transfection of plasmid DNA, the transfection reagent Lipofectamine™ 2000 (Invitrogen) was used according to the manufacturers protocol. The active component is a cationic lipid that forms liposomal complexes with negatively charged DNA molecules whereby the DNA is imported into the target cell. One day before tranfection, cells were seeded at a high density so they could reach 90%-95% confluency at the time of transfection. DNA and Lipofectamine™ 2000 were diluted in OptiMem I (Invitrogen) medium in separate micro tubes, incubated at room temperature (RT) for 5 min and then combined. After vortexing, the mixture was incubated again for 20 min at RT to allow complex formation. Cells were washed with PBS and the solution containing DNA-lipid complexes was added directly to the cells. Medium containing the suitable amount of FCS but no antibiotics was added to the transfection solution. Typically, for transfection in a 6-well format, 5 µg of plasmid DNA and 10 µl of Lipofectamine™ 2000 were used per well. For different multiwell formats, the amounts of DNA and Lipofectamine™ 2000 were up- or downscaled.

For transfection of siRNA, a final concentration of 100 nM siRNA was diluted in the desired volume of OptiMem I, incubated for 5 minutes and combined with the transfection reagent DharmaFect™ 2 (Dharmacon) diluted in OptiMem I at a ratio of 1:25. The two solutions were mixed and incubated for 10 min to allow complex formation. The solution containing the complexes was diluted 1:5 in antibiotic-free complete medium and added to the cells. The transfection medium was replaced after 18-24 hrs and determination of knockdown efficiency and subsequent experiments were carried out 48 hrs post transfection.

Cell Viability Assays

Cell viability was estimated using two different methods. In the MTT-assay, mitochondrial activity of viable cells chemically reduces the tetrazolium salt 3-[4,5-dimethylthiazol-2-yl]-2, 5-diphenyltetrazolium bromide (MTT, Sigma) to blue, solid formazan that precipitates in the mitochondria. The amount of formazan is proportional to the number of viable cells as described before (Sahin et al., 2006).

For MTT-cell viability assays, cells were seeded in a 96-well microtiter plate at a density of 2000, 5000 or 8000 cells per well, respectively. The cells were kept in a cell culture incubator for 24 hrs to allow attachment and growth. Cells were then exposed to the indicated cytotoxins for the desired time. MTT solution was added to a final concentration of 1 mg/ml and incubated at 37°C for two hrs to permit the reducing reaction. Finally, the formazan precipitate was solubilized by adding one volume of solubilization buffer (see 3.6). After overnight incubation at RT in the dark to avoid light induced side effects, absorption was measured in a micro plate reader (FluoroGenios, Tecan) at a wavelength of 560 nm.

The distinct identification of cells undergoing apoptosis requires a more sensitive assay than pure cell viability staining. During apoptosis, phosphatidylserine (PS) that is located at the cytosolic side of the cell membrane translocates to the extracellular side. Annexin V binds specifically to PS and is regarded as a specific marker for early apoptosis. 7-Aminoactinomycin (7-AAD) on the other hand intercalates with DNA specifically between cytosine and guanine residues. As it is only able to enter cells with disintegrated membranes, a 7-AAD positive cell is considered either necrotic or late apoptotic. Necrotic cells are excluded in the double staining because they show a 7-AAD, but Annexin V negative pattern. To estimate the number of apoptotic cells, cells were either transfected with the constructs of interest and a green fluorescent control vector (i.e. pEGFP-C1) and exposed to a cytotoxin or apoptosis was directly induced by coexpression of an EGFP-tagged pro-apoptotic Bax. After 24 hrs, the cells were collected by brief centrifugation, resuspended in 100 µl of Annexin V binding buffer and stained with 5 µl of each Annexin V-PE and 7-AAD-PERCP. EGFP positive cells were gated at 488 nm in a FACSCalibur flow cytometer (Beckton Dickinson). The gated cells were then analyzed for 7-AAD and Annexin V staining by CellStar™ Software.

Proteinbiochemical techniques

Extraction of Protein Lysates

To extract total cell protein from adherent cell cultures, monolayers were grown to 90% confluency. Cells were washed with cold PBS twice, before adding the cell lysis buffer directly to the cell-culture dish. Lysates meant for subsequent interaction studies were lysed in MPER™ buffer (Pierce), lysates meant for immunoblot analysis of cytosolic proteins were lysed in Ripa™ (Invitrogen) buffer containing protease inhibitors (CompleteMini, Roche). After addition of the respective lysis buffer, all cells were incubated at 4°C on a shaker, before they were scraped into a micro tube. The lysates were then centrifuged at 13.000x g at 4°C for 20 minutes to pellet cell debris. The supernatant was then used for subsequent applications or shock frozen and stored at -80°C.

Estimation of Protein Concentration

To determine the amount of total protein in a cell lysate, the BCA-method was used. The basic principle of this method is the biuret reaction where copper (Cu^{2+}) is reduced to Cu^{1+} by proteins in an alkaline solution. The combination of BCA and Cu^{1+} creates a purple-coloured complex that has its absorption maximum at 562 nm. The amount of complex formed is proportional to the amount of protein in the sample.

To determine the concentration of samples, dilutions of a known BSA stock solution were made and 50 µl of each concentration as well as 50 µl of each sample in a 1:10 dilution were incubated in 1 ml of BCA-Solution for 30 min at 60°C. After cooling to room temperature, 3x 100 µl of each sample or standard dilution were added to a flat bottom transparent 96-well microtiter plate and the absorption was measured at 560 nm in a microplate reader (Tecan). Concentrations were estimated using Magellan™ Software (Tecan).

SDS-Polyacrylamid Gelelectrophoresis (SDS-Page)

The separation of a total protein lysate was carried out by SDS-gelelectrophoresis. In a denaturing, reducing environment, proteins are separated by their molecular weight. (Lämmli, 1970). For this purpose, protein samples were alloyed with the appropriate volumes of 10x Sample Reducing Agent (Invitrogen) and 4x LDS loading dye and incubated at 95°C for 5 minutes. Equal amounts of proteins were loaded to the wells of NuPage Novex 4-12% gradient gel (Invitrogen) along with a protein standard (MagicMarc XP Western Protein Standard™ or SeeBlue Plus Prestained™ Protein Standard, Invitrogen) and run at 200 V in 1x NuPage MES SDS Running Buffer

(Invitrogen) for 40 min. For separation of hydrophobic proteins, 2x urea sample buffer (UBS) and 10x Sample Reducing Agent were added to the lysates and incubated at 37°C for 10 min prior to loading the gel.

Immunoblotting (IB)

After separation by SDS-PAGE, proteins can be detected by immunoblotting. The proteins of interest are here detected by a specific antibody. To transfer the proteins from the polyacrylamide gel to a nitrocellulose membrane, the dryblotting method was used. In the iblot™ device (Invitrogen) gels were embedded between the two parts of the iblot™ stack, the bottom carrying a copper anode, and the transfer membrane, the top carrying a copper cathode. Both electrodes are supplied with an ion reservoir in a gel matrix. In this system, the transfer time is reduced to 7 min by minimizing the distance between electrodes and allowing high currents. After assembling the stacks, transfer of the proteins was performed by using program 2 of the iblot™ blotting device.

After transferring the proteins, the membranes were stained with Ponceau S solution to verify equal transfer of protein. Ponceau S was removed from the membrane by washing in PBS-T and the membrane incubated in 3% dry milk in PBS-T for 1 h to block unspecific binding sites. Thereafter, the membranes were incubated on a shaker in the specific primary antibody in the indicated dilution at 4°C overnight before washing the membrane three times in PBS-T and adding the secondary antibody for 1 h at RT. Secondary antibodies were conjugated to horseradish peroxidase that catalyzes a chemiluminescence reaction with ECL-substrate (Super Signal West Pico, Pierce). The luminescence signal can then be detected by x-ray film (Amersham). Alternatively antibodies with infrared fluorescent dyes (IRDye 680 or IRDye 800, Licor) were used. For imaging of the near infrared wavelengths, membranes were scanned in the respective channel in the Odyssey™ (Licor).a

Co-Immunoprecipitation

For protein-protein interaction studies, the HA-tag and myc-tag co-immunoprecipitation kits from Pierce were used. Two possibly interacting proteins were coexpressed, one of them carrying a myc- (EQKLISEEDL) or hemagglutinin (HA)-tag (YPYDVPDYA). After cell lysis in physiologic conditions, and verifying the presence of both proteins of interest by western blotting, 200 µg of protein were incubated on ice overnight with agarose beads crosslinked with a covalently immobilized specific α-HA or α-myc antibody. Subsequently, the mixture was transferred to a Handee™ spin column (Pierce). After removing the cell lysate by brief centrifugation, the beads were washed with cold TBS twice. To elute the protein bound to the beads, 25 µl of 2x Non-Reducing Sample Buffer™ were added to the beads and heated to 95°C and pulse centrifuged. For SDS-gel electrophoresis of the eluted proteins, 2 µl of 10x sample reducing agent were added to the samples before

loading them onto a 4-12% Bis-Tris gel (Invitrogen).

Luciferase Assays

The basic principle of the luciferase assay is the enzymatic oxidation of luciferin by the firefly luciferase. Constructs that express luciferase in dependency of the activation of a specific promoter or responsive elements are commonly used for quantitative activation studies. For luminometric measurements, cells were transfected with the indicated constructs in a 6-well cell culture dish and incubated for the desired time. Cells were then washed with PBS twice and lysed in 200 µl of Cell Culture Lysis Buffer (Promega). The lysate was harvested, transferred into a 1.5 ml micro tube and pulse centrifuged to remove cell debris. 20 µl of cell lysate were transferred to a white microtiter plate (Nunc). 80 µl of luciferin diluted in Luciferase Assay Buffer (Promega) were injected to the well directly before measurement. Luminescence was measured for 10 sec per well and normalized to the total protein amount that was subsequently measured by the BCA method.

Immunocytochemistry

For immunocytochemical imaging, cells were grown on glass cover slips and fixed for 20 min at RT in 4% paraformaldehyde. After preincubation with 3% BSA in PBS-0,2% TritonX-100 to permeabilize the cells and block unspecific binding sites, cells were stained with the denoted primary antibodies or staining reagents in the indicated dilution in a humid chamber. After the desired incubation time the coverslips were washed with PBS twice for 15 minutes. In the case of antibody staining, a fluorescently tagged secondary antibody was used subsequently. Finally, the coverslips were washed three times in PBS. In the second washing step, 100 ng/ml 4',6'-diamidino-2-phenylindole hydrochloride (DAPI) was added to stain the nuclei. Coverslips were desalted in H₂O and embedded in Vectashield™ (Biozol). Samples were visualized with an Olympus IX-81 inverse fluorescence microscope and deconvoluted by Cell[^]R software (Olympus).

Molecular techniques

Production of Chemically Competent Bacteria

E. coli DH5α bacteria were streaked on LB-plates containing the appropriate antibiotic and incubated overnight at 37°C. Single colonies were picked and inoculated overnight in 10 ml of LB medium. 1 ml of this culture was added to 100 ml of LB medium and incubated on a shaker at 37°C until an optical density at OD₆₀₀ of 0.5 was reached. The culture was allowed to cool down on ice, transferred to sterile 50 ml round-bottom tubes and centrifuged at 4000x g for 5 min at 4°C. The

supernatants were discarded and the pellets resuspended in cold TFB 1 buffer (30 ml for a 100 ml culture). The bacteria-suspension was incubated on ice for additional 90 min before centrifugation at 4000x g for 5 min at 4°C. The pellets were then resuspended in 4 ml ice-cold TFB 2 buffer and aliquots of 50 µl were prepared and stored at -80°C.

Transformation

Transformation of competent bacteria was performed using the “heat-shock“ method. The competent bacteria *E.coli* DH5α were thawed at 37°C before adding the DNA solution to it. Typically 100 ng of plasmid DNA were used, if the concentration of the solution was available. Hereafter, the mixture was incubated on ice for 20 min before heat shocking the bacteria at 42°C for 90 sec. Subsequently, 350 µl of SOC media were added and the culture was incubated in a heated shaker at 37°C for one hour, before being plated on an LB-agar plate containing the appropriate selection antibiotic. The bacteria were allowed to form single colonies overnight in a 37°C incubator.

Small Scale Plasmid DNA Preparation

For the preparation of DNA-Plasmids up to a desired amount of 20 µg, single bacteria colonies (see transformation) were picked from an agar plate, transferred to 3 ml of LB-medium containing antibiotics in a sterile round bottom tube, before incubating the culture on a shaker overnight at 37°C. Alkaline lysis was carried out using the QIAprep Spin Miniprep Kit (Qiagen). 1 ml of bacteria suspension was sedimented at 3000 rpm for 10 min in a 2 ml microtube. The pellet was resuspended in 250 µl of buffer P1 and lysed with 250 µl of buffer P2. After addition of 350 µl of buffer P3, the precipitated compounds were pelleted by centrifugation at 13.200 rpm for 10 min at 4°C. The supernatant was decanted to the QIAprep spin column and the DNA was bound to the silica membrane by a one-minute centrifugation step at 13.200 rpm, in which the silica membrane absorbs the DNA in presence of high salt concentrations in the buffer, followed by 2 washing steps. The membrane was dried by an additional centrifugation for 2 min at 13.200 rpm. Finally 40 µl of H₂O were added directly to the membrane, incubated for 5 minutes and spun at 13.200 rpm to elute the DNA.

Large Scale Plasmid DNA Preparation

On the basis of a positive bacterial clone, larger amounts of plasmid DNA were isolated from a 150 ml bacterial culture using the Nucleobond Kit PC500 (Macherey-Nagel). Harvested bacteria were again lysed by the alkaline lysis method. After equilibrating the appropriate column the cleared lysate was loaded onto the column,

where plasmid DNA was bound to the anion-exchange resin. After subsequent washing steps, the plasmid DNA was eluted in a high-salt buffer and precipitated with isopropanol. Finally, the DNA-pellets were air-dried and reconstituted in H₂O for further use.

Small Scale RNA Preparation

To obtain total RNA from cultured cells or tissue, the RNeasy Kit (Qiagen) was used. Typically, 1×10^7 cells were lysed in 350 μ l of buffer RLT and homogenized by centrifuging the sample through the QIAshredder column. Subsequently, 350 μ l of 70% ethanol were added to provide ideal binding conditions. The lysate was then loaded onto the RNeasy silica-membrane by brief centrifugation. Bound to the column, the RNA was washed twice to remove possible contaminants. Finally, the RNA was eluted in 40 μ l of RNase free water.

Estimation of DNA Concentrations

To determine the concentration of DNA preparations, the solutions were diluted 1:100 in H₂O. The extinction was measured at OD₂₆₀ for DNA after blanking the photometer and used for estimation of concentrations. To determine the concentration of double stranded DNA (dsDNA) the value of OD₂₆₀=1,0 corresponds to 50 μ g/ml for 1 cm of optical path length. Hence, the concentration (μ g/ μ l) equals to:

$$\text{OD}_{260} \times 1/\text{dilution} \times 50/1000.$$

DNA Separation by Agarose Gelelectrophoresis

Agarose gel electrophoresis is the method of choice to separate DNA or RNA molecules by size. This is achieved by moving the negatively charged nucleic acid molecules through an agarose matrix with an electric field. Smaller molecules move faster and migrate farther than larger ones. The separation of DNA in an agarose gel also allows estimation of the size of a DNA fragment. For this purpose, DNA samples including 10x sample buffer (Bluejuice™ Invitrogen) and a DNA standard marker (1 kbplus™ Ladder, Invitrogen) were loaded to the wells of an agarose-TBE-gel containing 0,15 μ g/ml of ethidium bromide. Typically, for DNA fragments of 1000 basepairs (bp) or more, 0.8%-1,0% gels, for smaller DNA fragments depending on the expected size, up to 2% of agarose were used. The separation was performed at 100 V in a horizontal chamber containing TBE buffer. DNA was visualized by UV-light at 254 nm by GDS gel imaging software (Intas). For subsequent extraction of a single band, it was cut out with a sterile scalpel and transferred to a 1.5 ml microtube.

Enzymatic Restriction of Double-Stranded (ds)DNA

For the cloning of a target gene into a plasmid vector, as well as for the subsequent verification of a vector or the linearization of circular molecules, dsDNA was cut at

specific sequence motifs by restriction endonucleases. Typically, 5 µg of DNA in aqueous solution were digested in a total volume of 30 µl containing 3 µl of the appropriate buffer, 5 U of the restriction enzyme(s) of choice and, if required, 0,3 µl of 100x BSA stock solution. The restriction reaction was incubated for 2 hrs at 37 °C.

Ligation of DNA fragments

The ligation reaction is used to fuse a DNA fragment into a linearized vector. For this purpose, complementary overhangs are generated by restriction. The DNA ligase forms a covalent phosphodiester bond between a 3' hydroxyl group of one nucleotide with the 5' phosphate end of the other. ATP is required for the ligase reaction. Typically, in a total volume of 15 µl, 10-50 ng vector DNA, 1,5 µl of 10x ligase buffer containing ATP, 1 µl of T4 ligase and the insert DNA in a molecular ration of 5:1 (insert:vector) were used. The reaction was incubated at 37°C for 90 min.

Polymerase Chain Reaction (PCR)

The polymerase chain reaction is a technique used to amplify a piece of DNA by *in vitro* enzymatic replication (Mullins & Faloona, 1987). With PCR it is possible to amplify a single or few copies of a DNA fragment or a specific sequence across several orders of magnitude, generating millions or more copies of the DNA. For the amplification of specific DNA sequences, specific oligonucleotides were synthesized to bind to the selected sequences on the template DNA. By adding a thermostable DNA-polymerase and desoxynucleotides (dNTPs), elongation was enabled. Oligonucleotides carrying recognition sites for restriction enzymes were used to obtain DNA fragments that could subsequently be ligated into a vector construct.

For the exponential amplification, a thermocycler (T Gradient, Biometra) was used to provide the appropriate temperatures for each reaction step. These were an initial denaturing step at 95°C followed by 35 cycles of denaturing (95°C, 30 s), primer hybridization (50-60°C depending on the base sequence, 30s) and polymerization (72°C, 1 min/ kb) and a single final elongation step (72°C, 7 min). The successful amplification was verified by electrophoretic separation of the DNA. Typically, one reaction contained 1 µg of template DNA, 2 µl of forward primer (50 pmol/µl), 2 µl of reverse primer (50 pmol/µl) and 45 µl of PCR SuperMix™ (Invitrogen) containing dNTPs, MgCl₂ and recombinant Taq DNA polymerase.

Gateway™ Cloning

For most constructs generated in this study, the Gateway™ Technology (Invitrogen) was used. This system is based on the site-specific recombination properties of bacteriophage lambda (Landy, 1989) and enables the conservative transfer of the gene of interest into any destination vector in a single reaction without restriction and

ligation with high efficiencies. In brief, in the EntryTM-vector, the gene of interest is flanked by specific sequences called attachment sites (*attL*), on the respective target (DESTTM)-vector, the *ccdB* gene is flanked by heterologous DNA sequences (*attR*). In the so called LR reaction, the LR ClonaseTM enzyme facilitates the recombination of the *attL* site of the entry clone with the *attR* site of the destination vector, creating an *attB* containing expression clone and an *attP* flanked *ccdB* gene by-product. For selection of positive destination clones, entry vectors carry a kanamycin resistance gene, whereas destination vectors are ampicillin resistant.

To use this technology, genes of interest were cloned by restriction (4.3.7) and ligation (4.3.8) into the entry vectors (pENTRTM 1A, 2B and 3C, Invitrogen, Karlsruhe) that differ in their reading frame by one base. To verify reading frame and integrity of the sequence, positive clones were sent for sequencing (GATC, Konstanz). From the entry clone, genes were transferred to the desired destination vector by the LR clonase reaction. For this purpose, 100-300 ng of the entry clone were mixed with 150 ng of destination vector and 4 µl of 5x LR ClonaseTM reaction buffer. The volume was adjusted to 16 µl with TE buffer and mixed. 4 µl of LR ClonaseTM enzyme were added and the reaction was incubated for 1 h at 25°C before adding 4 µg of Proteinase K and incubating at 37°C for 10 min. The products were transformed into competent *E. coli* and selected for ampicillin resistance on an LB-agar plate. Clones were verified by restriction and electrophoretic separation of the DNA fragments.

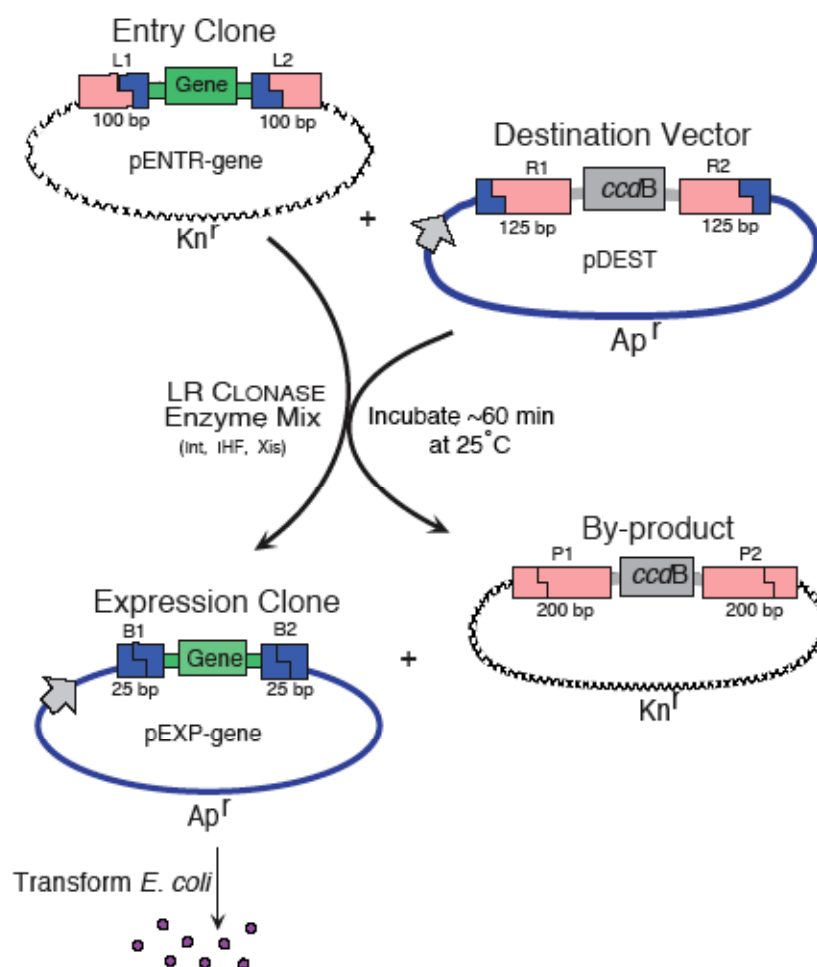


Fig. 4.1: Schematic depiction of the LR Reaction. An Entry plasmid (pENTR) containing the gene of interest flanked by recombination sites is recombined with a Destination vector (pDEST). The products are the gene of interest, transferred into the Destination construct, and a by-product containing the *ccdB* gene. (Source: Invitrogen).

cDNA-Reverse Transcription

To obtain total complementary DNA (cDNA) from an RNA sample (4.3.5), the SuperScript II Reverse Transcriptase™ (Invitrogen) was used. Reverse transcriptase is a DNA polymerase that synthesizes a complementary DNA strand from single-stranded RNA. For each 5 µg of total RNA, 1 µl of 10 mM dNTP mix and 1 µl of 0,5 µg/µl oligo(dT) primers were added and the volume was adjusted to 10 µl with RNase-free water. The samples were incubated at 65°C for 10 min before adding 4 µl

of 5x first-strand buffer as well as 2 µl of 0,1 M DTT and incubating at 42°C for 2 min. Finally, 200 U of SuperScript II RT were added and the samples were incubated at 42°C for 50 min. The reaction was heat inactivated at 70°C for 15 min for subsequent use.

Quantitative PCR (qPCR)

The quantitative or real-time PCR is the most sensitive quantification method to determine the amount of DNA in a sample as it is measured after each cycle of PCR by the use of fluorescent markers. The most common means for quantification are the use of fluorescent dyes that intercalate with double-stranded DNA, and modified DNA oligonucleotide probes that fluoresce when hybridized with a complementary DNA. Both were used in this study. The method was used to determine the amount of gene transcripts in cultured cells. Therefore, cells overexpressing certain constructs after transfection (4.1.2) or treatment with the indicated compounds were lysed, total RNA isolated (4.3.5) and reversely transcribed into cDNA (4.3.11). QPCRs were performed in a 96-well optical reaction plate (Applied Biosystems) with a total volume of 20 µl per well. Each well contained 2 µl of cDNA template and one of the following compositions depending on the primers:

Assay on demand	
2x Universal PCR Mastermix (Roche)	10 µl
Assay on demand (Applied Biosystems)	1 µl
H ₂ O	7 µl
Primer and Probe	
2x Universal PCR Mastermix (Roche)	10,5 µl
Primer forward (3 µM)	2,5 µl
Primer backward (3 µM)	2,5 µl
Probe (2,5 µM)	2,5 µl
QPCR Core Kit for SYBR Green	
10x reaction buffer	2 µl
MgCl (50 mM)	1,4 µl
dNTP Mix (5 mM)	0,8 µl
Primermix 10x	2 µl
HotGoldStar polymerase (5 U/µl)	0,1 µl
H ₂ O	11,1 µl
SYBR®Green I stock	0,6 µl

The reaction was performed in the 7500 Real Time PCR System (Applied Biosystems). The initial activation step for 10 min at 95°C was followed by 40 cycles of denaturing (95°, 15 sec) and annealing/elongation (60°C, 1min).

Relative concentrations of DNA during the exponential phase of the amplification reaction are determined by plotting fluorescence against cycle number on a logarithmic scale. The threshold for detection of fluorescence intensity above the background by the passive reference dye is manually determined. The cycle at which the fluorescence crosses the threshold is called the cycle threshold (Ct). Since the amount of DNA is duplicated in every cycle, relative amounts of DNA can be calculated. Every cycle of difference between two samples equals to a twofold increase in abundance. In this study, values are given in cycles over housekeeping gene (ΔC_t).

Statistical Analysis

Results are displayed as mean \pm standard error of means (SEM) and statistical analysis was performed (t-test or one-way analysis of variance (ANOVA)) by Graph Pad Prism Software (Graph Pad).

5. Results

GPR39 is a Major Factor in HT22R Protection

HT22R cells have been described before as a subpopulation of the HT22 cell line that is resistant against oxidative glutamate toxicity, and protected against various types of cell death stimuli (Lewerenz et al., 2006). A transcriptomal comparison between the HT22R cell line and the parental HT22S cell line resulted in a number of G-protein coupled receptors that were more abundant in the HT22R cells, with GPR39 among them. In subsequent experiments, GPR39 was shown to be protective against ER stress, oxidative glutamate toxicity and overexpression of Bax (Dissertation Mert Sahin).

To determine if GPR39 is a major factor of the HT22R resistance against oxidative glutamate toxicity, GPR39 was knocked down by a pool of four siRNAs and exposed to glutamate. The percentage of surviving cells was estimated after 24 hrs. At 30 mM glutamate, the survival rate decreased from almost 100% in control (ctrl) siRNA transfected cells to 77% in GPR39 siRNA transfected cells. At 40 mM glutamate, viability decreased from 65% (ctrl) to 45% (GPR39 siRNA) (Fig. 5.1 a, left panel). The GPR39 knockdown efficiency was determined by quantitative PCR. GPR39 siRNA transfected cells yielded a change in cycles over housekeeping gene GAPDH (Δ ct) of 1.752 cycles, which corresponds to a 3.3-fold decrease in GPR39 mRNA (Fig. 5.1 a, right panel).

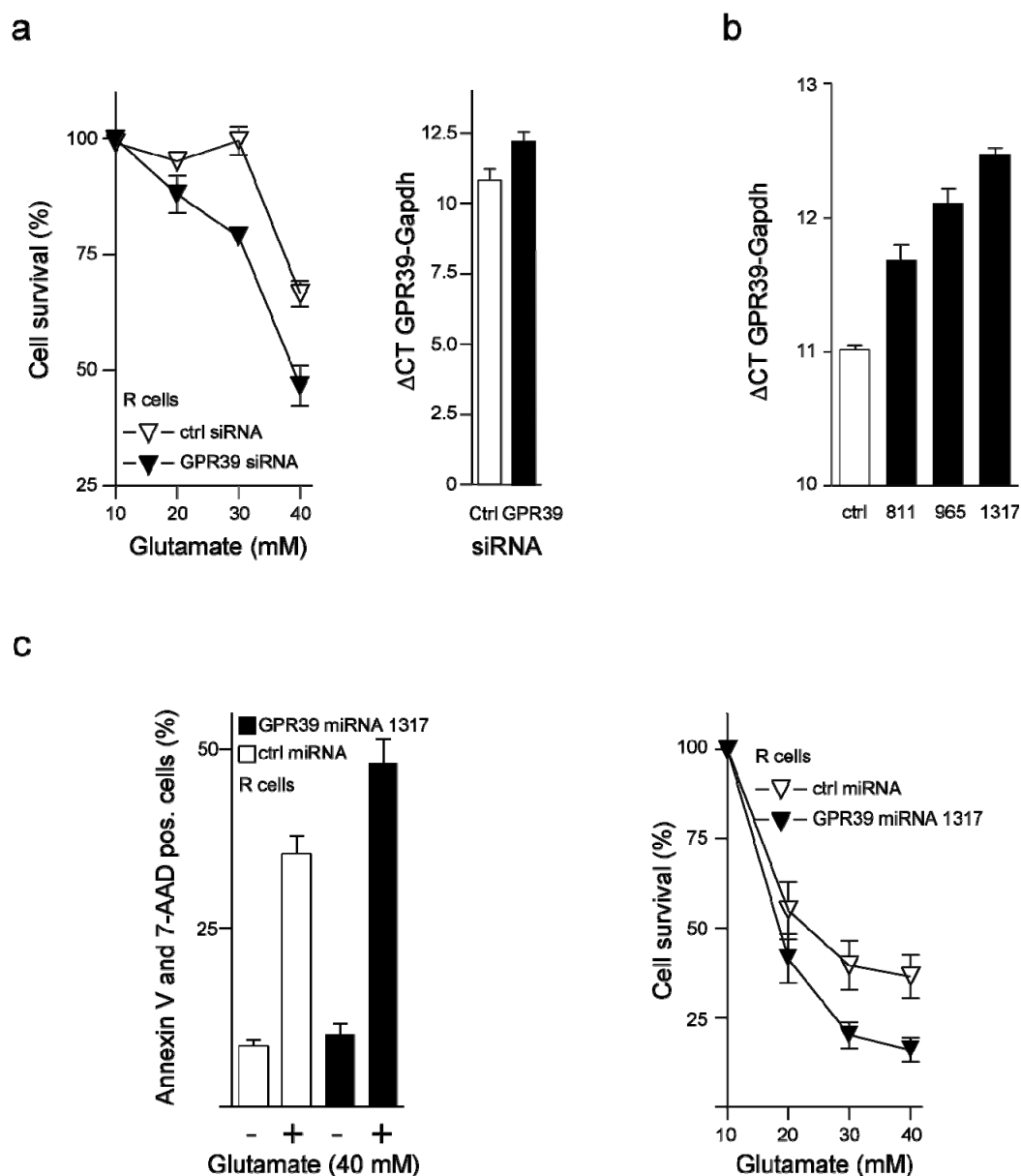


Fig. 5.1: GPR39 knockdown makes HT22R cells more susceptible to oxidative glutamate toxicity. (a) Viability of HT22R cells transfected with non-targeting siRNA (open triangle) and GPR39-siRNA (closed triangle) at different concentrations of glutamate (left panel), expression of GPR39 after transfection with non-targeting siRNA (ctrl) and GPR39-siRNA (GPR39) expressed in Δ ct over GAPDH (right panel). (b) Expression of GPR39 in HT22R cells transfected with non-targeting (ctrl) and three different GPR39-targeting (811, 965, 1317) miRNA-constructs expressed in Δ ct over GAPDH. (c) HT22R cells transfected with ctrl and GPR39-targeting miRNA treated with (+) 40mM glutamate or vehicle (-) for 24 hrs and gated for 7-AAD and Annexin V (left panel), cell survival estimation at different concentrations of glutamate (right panel). Data is represented as means of three independent experiments \pm SEM.

To confirm these results, a second method of RNA interference, miRNA was chosen. Three different GPR39 targeting oligonucleotides (3.10.2) were cloned into the miRNA vector pcDNA™6.2-EmGFP-miR, transfected in HT22R cells and GPR39 knockdown efficiency estimated by quantitative PCR. The miRNA targeting the sequence from nucleotide 1317 resulted in a change in Δ ct of 1.5 cycles, which corresponds to a 60% decrease in GPR39 mRNA abundance (Fig. 5.1 b). This construct was chosen for subsequent cell death experiments. HT22R cells transfected with the GPR39 miRNA construct or the control miRNA construct were treated with 40 mM glutamate for 24 hrs before staining with 7-AAD and Annexin V to stain apoptotic cells and analyzing by flow cytometry. Glutamate-treated cells showed an increase of 12.5% 7-AAD and Annexin V double-positive cells when transfected with GPR39 miRNA 1317 as compared to control. The viability of non-treated cells was not impaired (Fig. 5.1 c, left panel). Treating control miRNA and GPR39 miRNA 1317 transfected cells with different concentrations of glutamate and staining viable cells with MTT yielded similar results. At 30 mM and 40 mM glutamate, in GPR39 miRNA-1317 transfected cells, approximately 20% (at 30 mM ctrl: 39.7%, GPR39 miRNA-1317: 20.1%; at 40 mM ctrl: 36.5%, GPR39 miRNA: 15.9%) less viability was observed when compared to control miRNA transfected cells (Fig. 5.1 c, right panel). These results confirm, that GPR39 is indeed a major factor in the resistance of HT22R cells.

GPR39 Overexpression Induces Several Downstream Targets

To be able to identify downstream targets of GPR39, two monoclonal HEK293 cell lines overexpressing GPR39 were established, that only differed threefold in GPR39 expression. When compared for cytoprotection, Clone 1, the higher expressing clone was protected more against glutamate toxicity, ER-stress, hydrogenperoxide and Bax overexpression than the lower expressing clone 17 (Dissertation Mert Sahin). These two cell lines were used for a transcriptomal comparison by Affymetrix chip human genome U133 Plus 2.0 (Affymetrix). Total RNA was extracted from both cell lines and reversely transcribed. The chip hybridization and analysis were carried out by Dr. Stefan Golz (Bayer Healthcare AG, Wuppertal). Differentially expressed transcripts are shown in Fig. 5.2 in descending order. They can roughly be divided in enzymes (enolase (Eno2), tissue plasminogen activator (PLAT), putative serine protease (PRSS23)), extracellular matrix molecules (collagen II α 1 (COL2A1), integrin binding protein (EDIL3)) and proteins involved in signal transduction or transcription (pigment epithelium derived factor (PEDF), trinucleotide-repeat containing 9 (TNRC9), Cbp/p300-interacting transactivator, with Glu/Asp-rich carboxy-terminal domain 1 (Cited1), GPR39 itself and a regulator of g-protein signaling (RGS16)). The following work focuses on the signal-transduction

molecules.

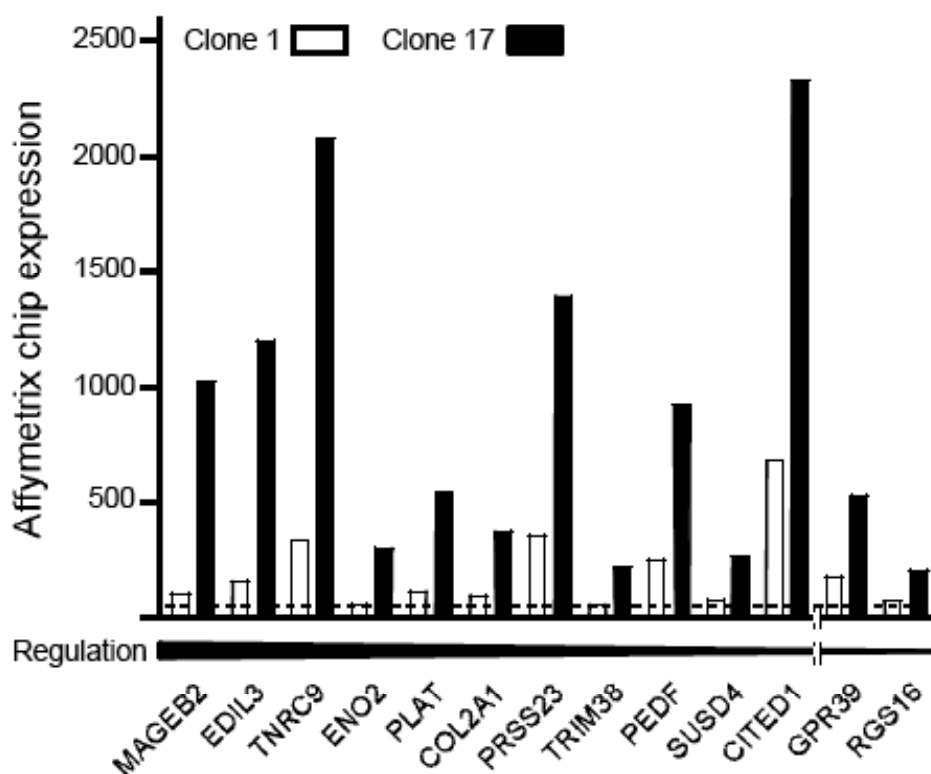


Fig. 5.2: GPR39 induces several downstream targets. Transcriptomal comparison of HEK293 clone 1 and clone 17 performed by hybridization of cDNA to Affimetrix chip human genome U133 Plus 2.0. Transcripts regulated in clone 17 and present in clone 1 are shown in descending order of regulation.

GPR39 Protection is $G\alpha_{13}$, RhoA/SRE-dependent and Regulated by RGS16

The regulator of G-protein signaling RGS16 was upregulated threefold in the GPR39 overexpressing clone 17. This protein was of particular interest, because RGS proteins have been shown to be upregulated as a compensatory effect to the upregulation of the receptor whose signaling pathway they regulate as a desensitization mechanism (Druey et al., 1996). RGS16 has been described to be a specific inhibitor of $G\alpha_{13}$ signal transduction by translocation of the RGS16- $G\alpha_{13}$ complex to detergent resistant membranes, which reduces the catalysis of nucleotide exchange of p115Rho-GEF on RhoA (Johnson et al., 2003).

GPR39 Protection is Inhibited by RGS16

To prove the hypothesis that RGS16 might be an inhibitor of GPR39 signaling, HEK293 cells were transfected with GPR39 with empty vector and GPR39 coexpressed with RGS16. These cells were then exposed to different concentrations of tunicamycin and cell viability determined by MTT method (4.1.3). Indeed, GPR39 mediated protection against tunicamycin toxicity was completely abolished by RGS16 (viability at 10 μ g/ml vector ~8.2%, GPR39 ~29.7% and GPR39+RGS16 ~5.3%) (Fig. 5.4 a).

GPR39 Protection is RhoA Dependent

The result described above (5.3.1) strongly suggested coupling of GPR39 to G α 13. Since G α 13 signaling involves a nucleotide exchange on RhoA, we further suspected the involvement of RhoA. RhoA has been described to positively regulate actin polymerization (Mack et al., 2001). Thus, mouse embryonic fibroblasts were transfected with empty vector, GPR39 and GPR39 + RGS16 and serum starved for 48 hrs to induce actin stress fibre formation, before fixing and staining the cells with rhodamine-coupled phalloidin.

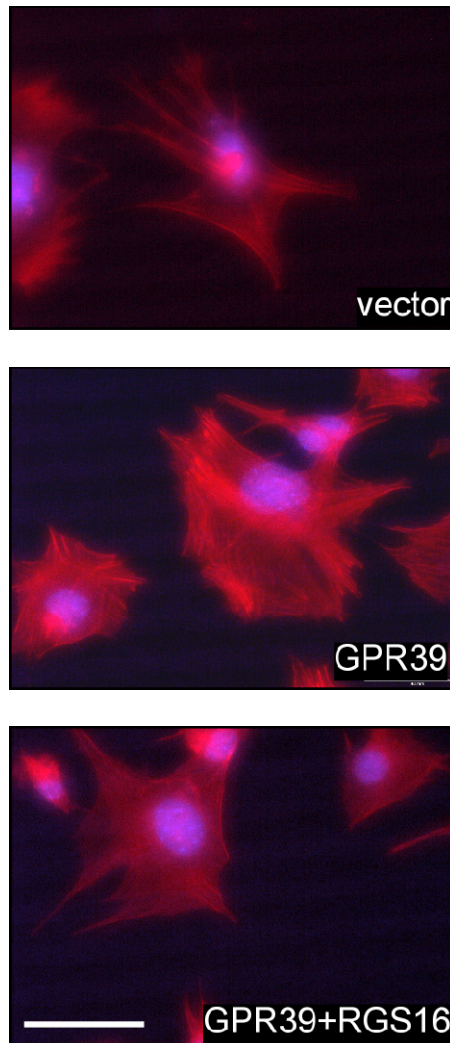


Fig. 5.3: GPR39 overexpression enhances formation of actin stress-fibers after serum-starvation. Mouse embryonic fibroblasts transfected with vector, GPR39 or GPR39+RGS16, serum starved for 48 hrs and stained with rhodamine-coupled phalloidin and DAPI. Scalebar corresponds to 10 μ m.

GPR39-transfected cells displayed prominent stress fiber formation that was not observed in vector transfected or in RGS16 coexpressing cells (Fig. 5.3). This result confirms the involvement of RhoA. In a second approach, HEK293 cell viability was estimated after treatment with different concentrations of tunicamycin in cells transfected with empty vector, GPR39 and GPR39 along with a dominant negative RhoA construct (T19N). As a result, viability at 10 μ g/ml was decreased from ~26.2% (GPR39), to 19.1% by coexpression of RhoA(T19N) (Fig. 5.4 b).

GPR39 Mediated Protection can be Inhibited by Y-27632

RhoA can signal either through ERK6 (p38 γ)-axis (Marinissen et al., 2001) or the Rho-associated kinase p160ROCK pathway (Uehata et al., 1997). Since p160ROCK has been published to foster SRE-induction in an ERK and p38 independent manner, and GPR39 has also been shown to induce SRE-dependent transcription (Holst et al., 2004), the RhoA-p160ROCK-pathway was more likely to be involved in GPR39 signaling. To strengthen this hypothesis, cytotoxicity experiments were performed, in which after transfection of GPR39, p160ROCK was inhibited by its specific inhibitor Y-27632 and HEK293 cell viability estimated after 24 hrs of tunicamycin treatment by the MTT method. At 10 μ g/ml cell viability was decreased from 15.8% (GPR39) to 4.9% (GPR39 +Y-27632) (Fig. 5.4 c). This result suggests an involvement of p160ROCK in the GPR39 protective signal-transduction pathway.

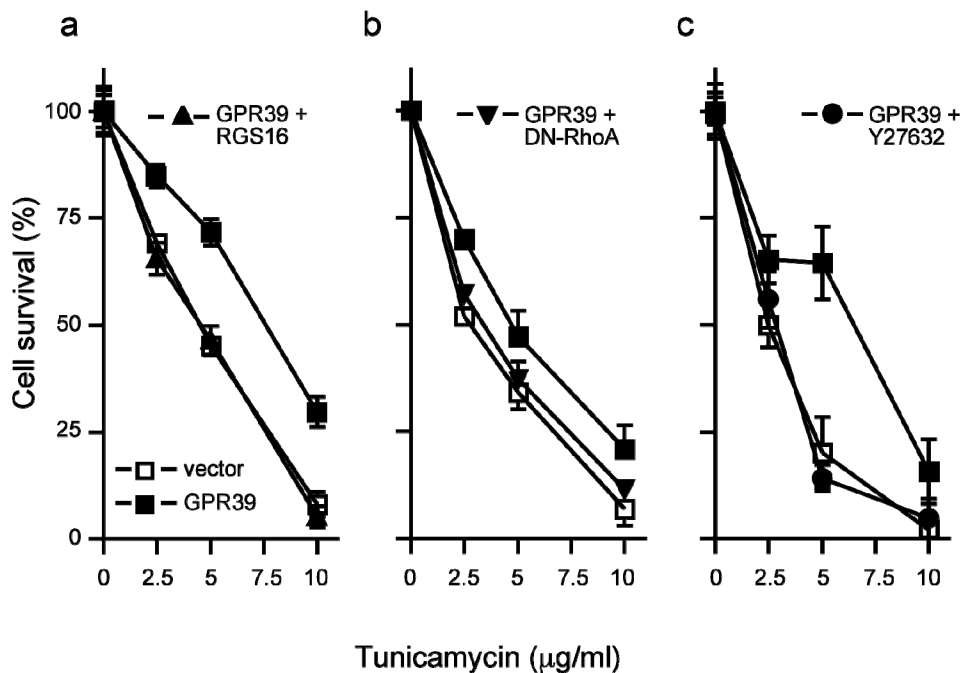


Fig. 5.4: GPR39 protection is G α 13/RhoA and negatively regulated by RGS16. Cell survival of HEK293 cells transfected with vector, GPR39 and (a) GPR39+RGS16, (b) GPR39+RhoA T19N or (c) GPR39+Y27632 after treatment with different concentrations of tunicamycin. Data is given as means of three independent experiments \pm SEM.

GPR39 induced SRE-dependent Transcription is Necessary for Cytoprotection

Holst et al. showed that GPR39 induces SRE-dependent transcription. To determine if this induction can be altered by inhibition of the pathway suggested by the results

5.3.1-5.3.3, SRE induction was measured by luciferase assay (4.2.8) 48 hrs after transfecting HEK293 cells with the SRE luciferase reporter construct (pSRE-LUC, Stratagene) and either empty vector, GPR39 alone or GPR39 co-expressed with RGS16 or RhoA(T19N) respectively. SRE-promoter induction was increased fourfold after GPR39 overexpression, which was completely abolished when RGS16 or RhoA (T19N) were co-expressed (Fig. 5.5 a). This shows that SRE-dependent transcription is acting downstream of RGS16 and RhoA. To prove the involvement of SRE in GPR39-mediated protection, first a protective effect of SRE-induction had to be shown. To this end, a dominant active construct of the serum response factor (SRF-VP16) was used in cytotoxicity assays (Schratt et al., 1993). A non-functional mutant lacking the DNA-binding domain (SRF-VP16-ΔM) served as control. HEK293 cells were transfected with the constructs indicated above, treated with tunicamycin and cell viability was determined. The dominant active SRF-VP16 increased cell viability from ~7.6% (empty vector) to ~40.9% at 10 μg/ml tunicamycin. The SRF-V16-ΔM slightly increased cell viability to ~20.6% (Fig. 5.5 b). This only shows the protective nature of the serum response factor and the SRE-induced transcription, respectively. To ascertain the role of the SRE in GPR39-mediated protection, a dominant negative (dn) SRF mutant was used in the same assay. GPR39 and the dnSRF were coexpressed and cell viability was determined as described above. Here, dnSRF completely abolished the protective effect by GPR39. The dnSRF overexpressed alone made cells even more susceptible to tunicamycin toxicity (Fig. 5.5 c).

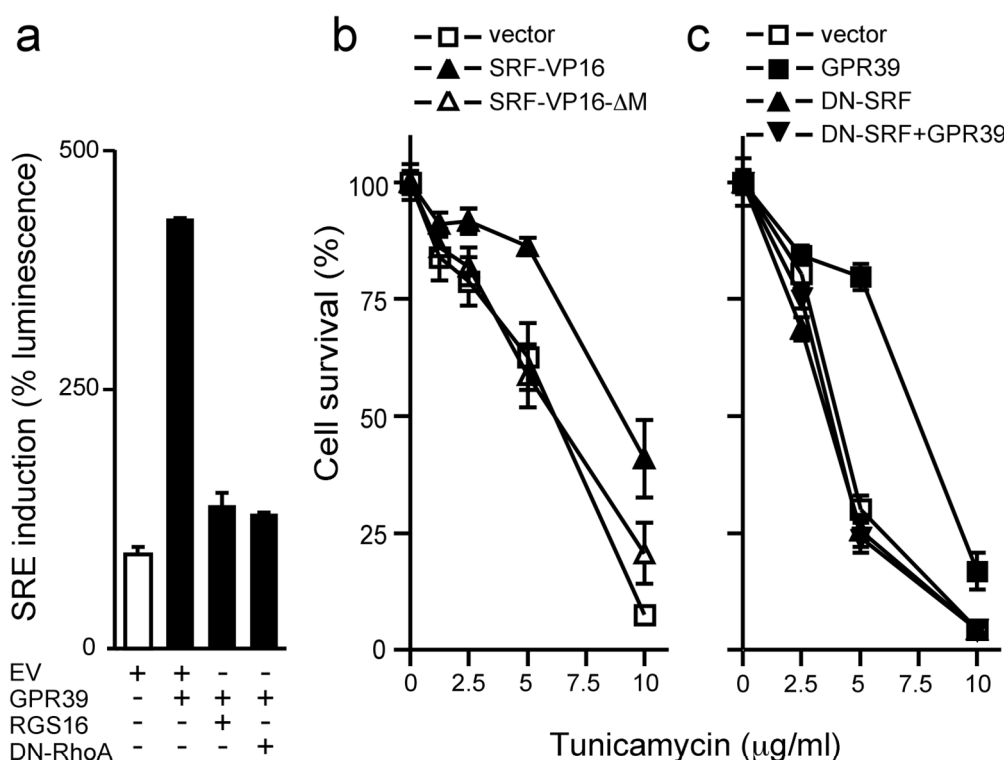


Fig. 5.5: GPR39-protection is SRE-dependent. (a) Percentage of luminescence normalized to empty vector (EV) in cells transfected with GPR39, GPR39+RGS16 and GPR39+RhoA T19N. (b) Viability of HEK293 transfected with vector, the constitutively active mutant SRF-VP16 or the non-functional mutant SRF-VP16 Δ M (c) Viability of HEK293 transfected with vector, GPR39, dominant negative SRF and GPR39+dominant negative SRF. Data is given as means of three independent experiments \pm SEM.

Taken together these results suggest that the GPR39 protective signal-transduction cascade is regulated by RGS16, and therefore mediated by G α 13, which activates RhoA via p115-rhoGEF, p160ROCK. Further downstream, the protective effect is mediated by serum-response element dependent transcription.

PEDF Partly Mediates GPR39 Cytoprotection

PEDF was also among the differentially expressed transcripts on the array described in 5.2. In the comparison of GPR39-overexpressing clones 1 and 17, PEDF was 3.7-fold upregulated in clone 17. PEDF is a protein that has been discovered and described as being secreted by cultured fetal human retinal pigment epithelium cells with neuronal differentiative activity (Tombran-Tink et al., 1991). Later studies revealed PEDF to act as a protective factor that is capable of protecting neurons in different brain regions from diverse insults like oxidative damage and glutamate excitotoxicity (reviewed in Tombran-Tink Bernstable). Therefore we considered PEDF as an interesting potential effector protein of the protective GPR39 cascade.

PEDF is Upregulated by GPR39

Since the chip array (5.2) showed an upregulation of PEDF in the GPR39 overexpressing clone 17, this upregulation was first confirmed by quantitative PCR. To this end, total RNA from clones 1 and 17 was extracted, reversely transcribed and the relative abundance determined by qPCR using the SYBRgreen method. mRNA abundance of PEDF in clone 1 and 17 differed by 1.5 Δ ct (Fig. 5.6 a). This confirmed the transcriptional upregulation observed in the array data. In a second approach, PEDF secretion was measured on the protein level. HT22 cells were transfected with GPR39 or empty vector as control and cultured in serum-free media for 48 hrs. Supernatants were collected and PEDF measurement carried out by Prof. Ana Luisa Pina (Regensburg) by ELISA. GPR39 transfected cells secreted approximately 4.5-fold more PEDF than control transfected cells (Fig. 5.6 b).

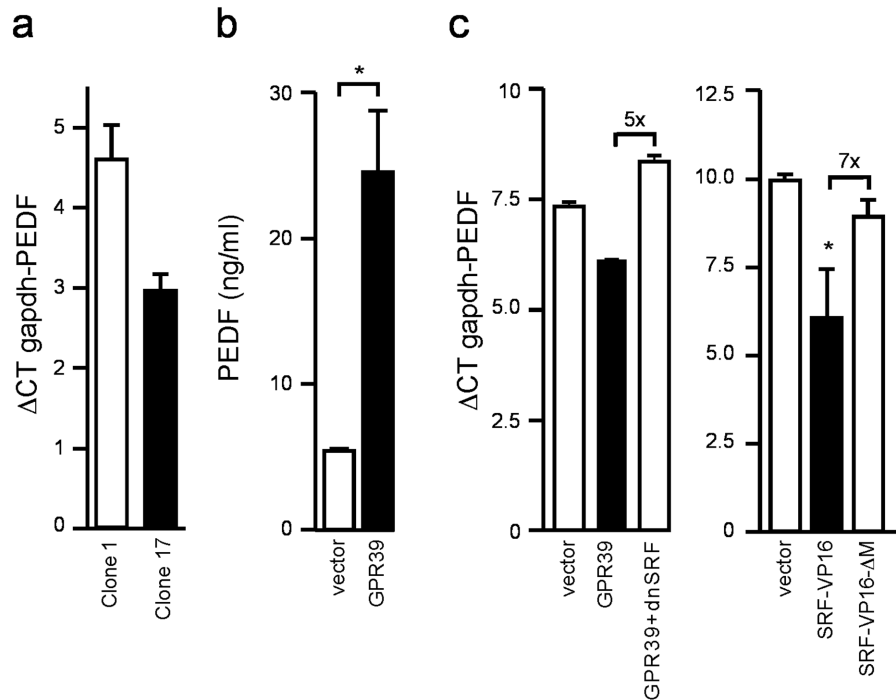


Fig. 5.6: GPR39 induces the secreted factor PEDF in an SRF-dependent way. (a) Transcriptional comparison of HEK293 clones 1 and 17 expressed in ΔCT over GAPDH. (b) Secreted PEDF from HT22 cells transfected with GPR39 measured by ELISA. (c) Expression of PEDF after transient transfection of vector, GPR39 and GPR39 plus dominant negative SRF (left panel), respectively vector, SRF-VP16 and SRF-VP16 ΔM (right panel) expressed in ΔCT over GAPDH. Asterisks indicate statistical significance as determined by t-test or one-way ANOVA.

PEDF is Regulated Downstream of SRF

To determine whether PEDF is regulated downstream of SRF, HT22 cells were transfected with GPR39, GPR39 and the dominant negative SRF construct or empty vector as control. In order to investigate if SRF alone is capable of upregulating PEDF, cells were transfected with empty vector, SRF-VP16 and SRF-VP16- ΔM . PEDF abundance was estimated by qPCR. The coexpression of GPR39 and the dominant negative SRF transcript showed that the fourfold increase mediated by GPR39 overexpression was abolished by dnSRF. GPR39 and GPR39-dnSRF transfected cells yielded a fivefold difference in PEDF abundance (Fig. 5.6 c, left panel). Cells transfected with the dominant active SRF-VP16 and the nonfunctional mutant differed in PEDF expression sevenfold (Fig. 5.6 c, right panel). These findings together suggest that the upregulation of PEDF by GPR39 is mediated through SRF and that SRF alone is sufficient to increase PEDF levels.

PEDF Partly Mediates of the GPR39 Protective Effect

To strengthen the hypothesis that PEDF is an effector protein of GPR39-mediated cytoprotection, first the protective effect of PEDF in the used cell model had to be demonstrated. HT22 cells were preincubated with 50 ng/ml or 100 ng/ml PEDF (a kind gift from Ana Luisa Pina, Regensburg) for 24 hrs before being exposed to different concentrations of tunicamycin. Cell viability was estimated by MTT 24 hrs later. To avoid high PEDF concentrations in serum containing media, these experiments were carried out in 2% serum. In this experiment, PEDF showed a concentration-dependent protective effect against ER-stress by tunicamycin. At 2.5 $\mu\text{g/ml}$ tunicamycin, cells pre-treated with 100 ng/ml PEDF were approximately 20% more viable than control cells, viability of cells pretreated with 50 ng/ml PEDF were in between (vehicle: 19%, 50 ng/ml PEDF: 32%, 100 ng/ml: 39%) (Fig. 5.7 a). In the reverse experiment, HT22 cells were seeded at a low density and treated with conditioned media from GPR39 or empty vector transfected HT22 cells. In order to remove PEDF from the conditioned media, 2 $\mu\text{g/ml}$ of either specific α -PEDF antibody (Millipore) or control antibody (rabbit polyclonal α -chicken antibody, Davids Biotechnology) were added to the media 24 hrs before exposing the cells to tunicamycin. Cell viability was measured by MTT 24 hrs later. GPR39-conditioned medium indeed had a protective effect, yet not as pronounced as GPR39 overexpression. Neutralizing PEDF with a specific antibody decreased this protective effect. At 1 $\mu\text{g/ml}$ tunicamycin, control cells were approximately 22% viable, GPR39-conditioned media treated cells in contrast were more than 55% viable. The cells treated with the PEDF-neutralized medium showed about 36% viability (Fig. 5.7 b).

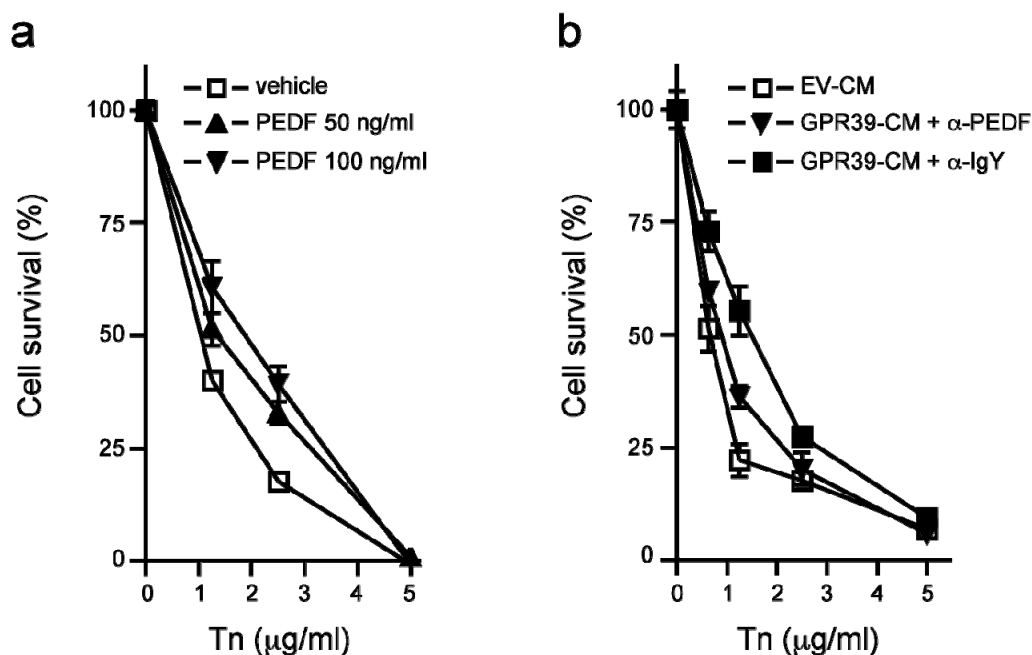


Fig. 5.7: Removing cytoprotective PEDF from GPR39-conditioned medium attenuates its protective properties. (a) Cell viability of HT22 cells pretreated with the indicated amounts of PEDF for 24 hrs and exposed to tunicamycin for 24 hrs. (b) Cell viability of HT22 cells exposed to tunicamycin in media conditioned from HT22 cells transfected with vector (EV-CM) or GPR39 (GPR39-CM) in the presence of an antibody against PEDF (+ α -PEDF) or a control antibody (+ α -IgY).

These results strengthen the hypothesis that PEDF may be at least one of the effector proteins of the GPR39 protective signal-transduction cascade summarized in Fig. 5.8.

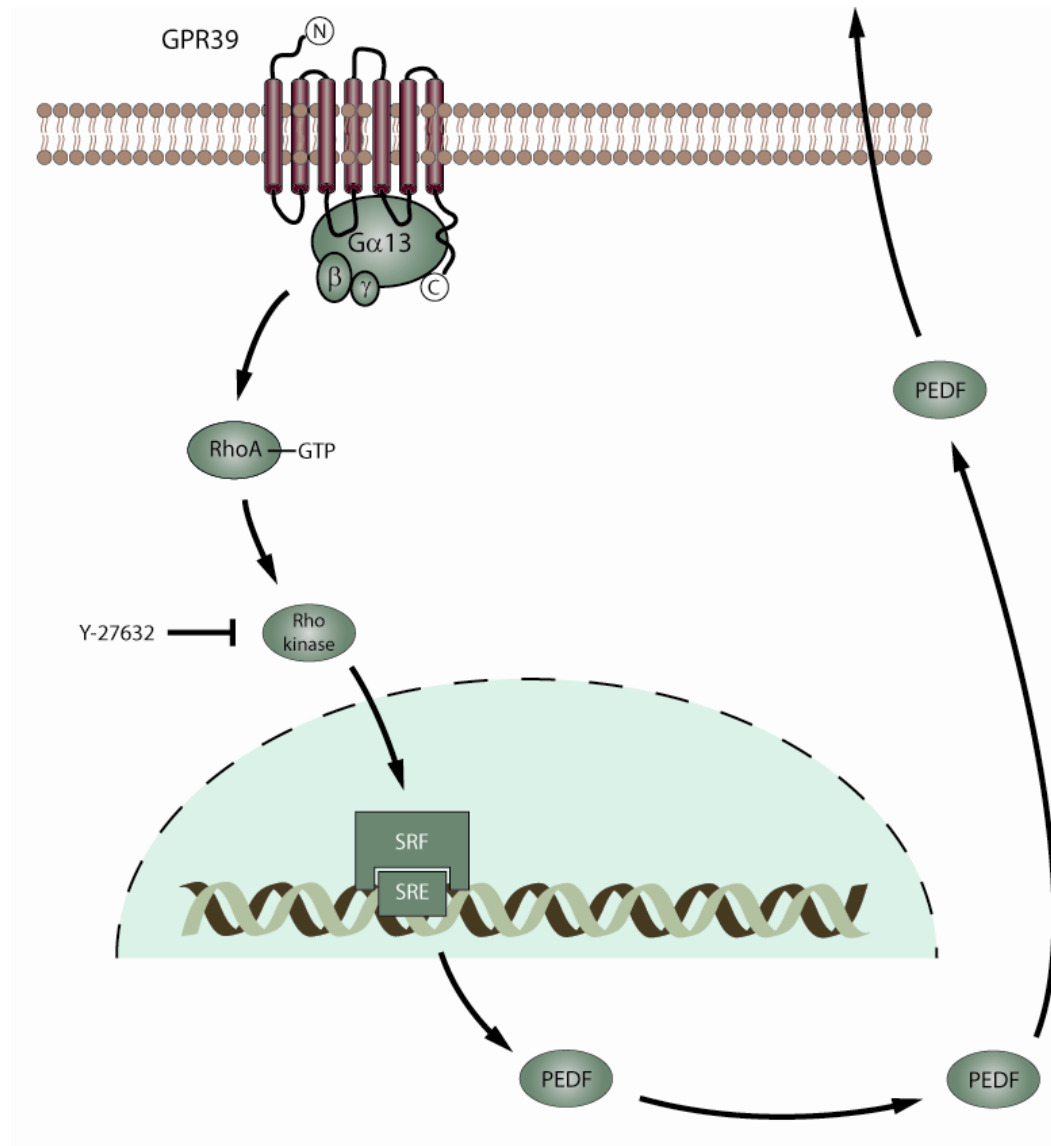


Fig. 5.8: Summary of GPR39-mediated signal transduction

TNRC9 is a Neuronal and Epithelial Transcription Factor Regulated by GPR39

On the microchip array (5.2) TNRC9 was upregulated fivefold in clone 17. TNRC9 (trinucleotide repeat containing 9) is a high mobility group (HMG) transcription factor that belongs to the conserved subfamily of tox proteins (O'Flaherty et al., 2003). It was first identified in a screen for transcripts harbouring trinucleotide repeat expansions (Margolis et al., 1997). Recently, a single-nucleotide polymorphism near the 5' end of TNRC9 was found to be strongly associated with breast cancer (Easton et al., 2007). TNRC9 contains a central HMG-domain and a C-terminal glutamine-rich tail (Fig. 5.9).

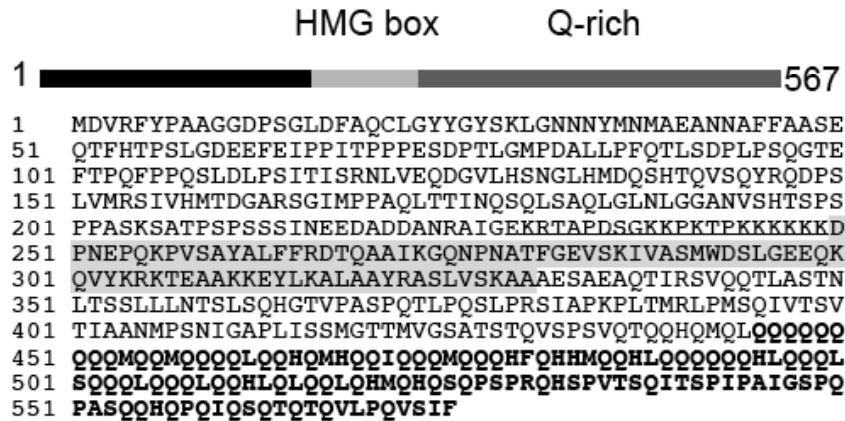


Fig. 5.9: Sequence and structure of TNRC9. Amino acid sequence of TNRC9 and schematic image of its structure with nuclear localization signal (underlined), high mobility group domain (HMG, highlighted) and glutamine rich tail (Q-rich, bold).

A whole body cDNA-panel and cDNA-samples from human primary cell lines were used for a qPCR based screen carried out by Stefan Golz (Bayer Health Care AG, Wuppertal) to find out the overall abundance of TNRC9, showing that it is mainly present in the ileum and the nervous system, namely in cerebellum, frontal and occipital lobe and in the retina (Fig. 5.10 a), as well as in epithelial human primary cell lines, namely in renal and intrahepatic biliary epithelials (Fig. 5.10 b).

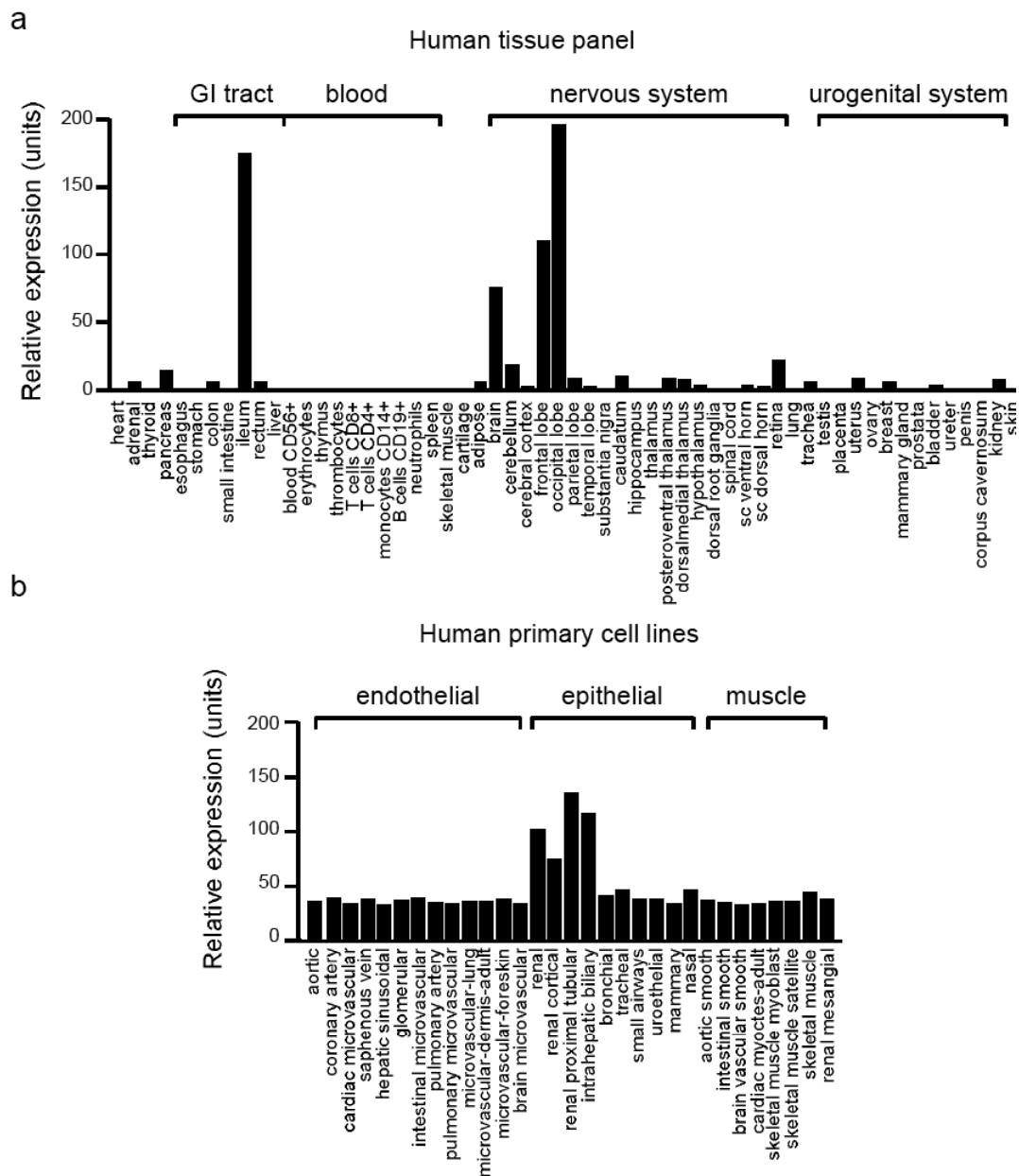


Fig. 5.10: TNRC9 is mainly expressed in the nervous system and epithelial cells. (a) Relative expression of TNRC9 mRNA in a whole body panel plotted as relative expression units, sorted by their affiliation to certain tissue systems and (b) relative expression in the indicated human primary cell lines. These measurements were performed by Dr. Stefan Golz, Bayer AG, Wuppertal.

To confirm its subcellular localization, full-length mouse TNRC9 was cloned into pEGFP-C3 (Clontech) and transiently transfected. Nuclei were counterstained with DAPI and nuclear localization could be confirmed by fluorescent microscopy (Fig. 5.11).

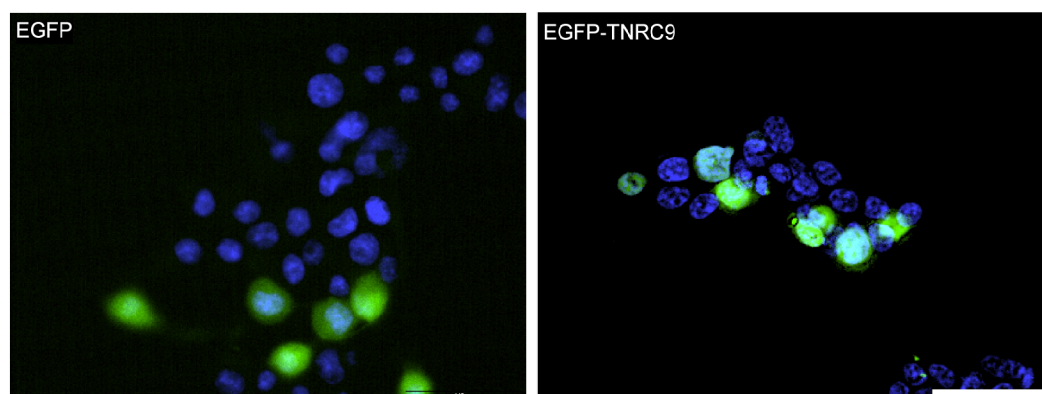


Fig. 5.11: TNRC9 is a nuclear protein. Fluorescent microscopy image showing N2a cells transfected with EGFP or TNRC-EGFP, nuclei counterstained with DAPI. Scalebar corresponds to 10 μ m.

TNRC9 is Upregulated by GPR39

TNRC9 was among the possible target genes that were upregulated in GPR39 overexpressing clone 17. This data was confirmed on the protein- and on the RNA level. N2a cells were transiently transfected with GPR39 and GPR39 plus RGS16. Cells were lysed and immunoblotted for TNRC9 with a specific antibody. The antibody detected a band at a molecular weight of approximately 63 kDa, which is the predicted size of TNRC9. This band was increased after GPR39 overexpression and decreased when coexpressing RGS16 (Fig. 5.12 a). Also, the chip data was confirmed by qPCR with GPR39 overexpressing cells showing a change in cycles over housekeeping gene of 3.4 Δ ct. This corresponds to a ~10-fold increase on the transcriptional level (Fig. 5.12 b).

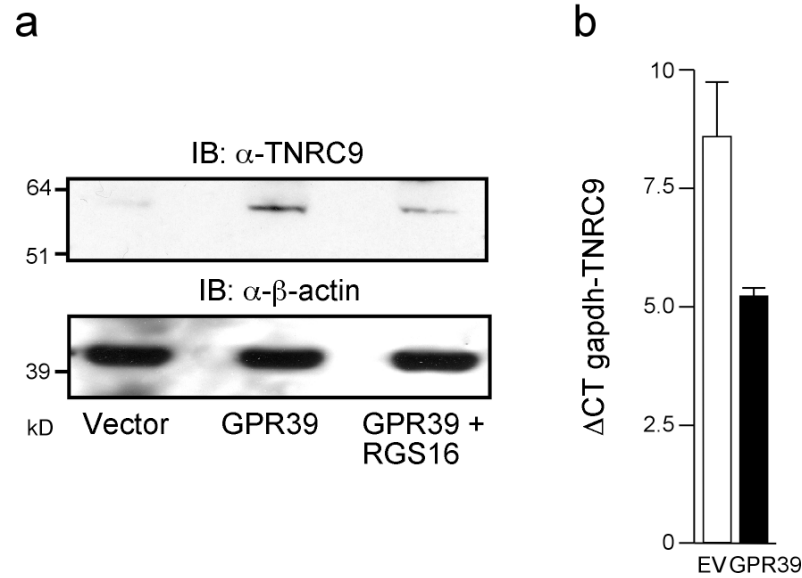


Fig. 5.12: TNRC9 is upregulated by GPR39. (a) Immunoblot against TNRC9 and loading control β -actin of N2a-cell lysates after transfection of vector, GPR39 or GPR39+RGS16. (b) Expression of TNRC9 in N2a cells transfected with vector or GPR39, data given as ΔCT over GAPDH. Bar graphs represent means of three independent experiments \pm SEM.

TNRC9 Confers Part of the GPR39 Protective Effect

To find out if TNRC9 is implicated in the GPR39 protective cascade, N2a cells were transfected with TNRC9 in pciNeo and selected in 1.5 mg/ml Genitocin (Invitrogen) for 14 days. This stable cell line was exposed to different concentrations of tunicamycin and cell viability measured by MTT. TNRC9 alone only had a small protective effect compared to the control cell line stably transfected with empty vector. This effect was only present at low tunicamycin concentrations (Fig. 5.13 a). Next, it was tested whether knockdown of TNRC9 in GPR39-overexpressing cells would decrease cell viability after tunicamycin treatment. In this approach, N2a cells were transfected with GPR39 and TNRC9-specific siRNA or non-targeting control siRNA. Indeed, cell viability was decreased by TNRC9 knockdown (at 5 μ g/ml: vector: 6.3%, GPR39: 22.5%, GPR39 + TNRC9 siRNA: 10.1%). In these experiments, the GPR39 protective effect was not very pronounced, probably due to the cytotoxic effects of siRNA transfection or to low transfection efficiencies with the siRNA in the same transfection reaction as the overexpression construct (Fig. 5.13 b). This data shows that there is some protective effect mediated by TNRC9 alone, that TNRC9 is implicated in the GPR39-mediated protection, but also, that TNRC9 alone is not as cytoprotective as GPR39.

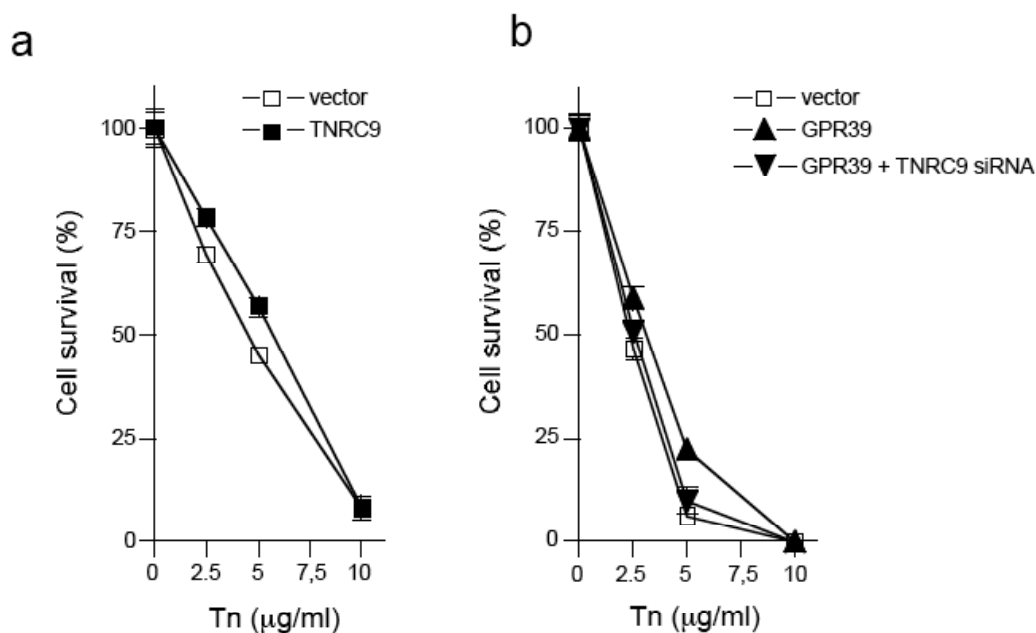


Fig. 5.13: TNRC9 has a small protective effect. (a) Viability of N2a cells overexpressing TNRC9 or vector after 24 hrs exposure to different tunicamycin concentrations. (b) Viability of N2a cells transfected with vector, GPR39 or GPR39+TNRC9 siRNA. Datapoints represent means \pm SEM of three independent experiments.

TNRC9 is Regulated Downstream of SRF

To determine where in the GPR39 signal-transduction cascade TNRC9 is acting, N2a cells were transfected with the dominant active SRF construct and its non-functional counterpart and immunoblotted with the specific TNRC9 antibody. The SRF-VP16 in comparison to the non-functional mutant exhibited a robust increase in TNRC9 protein. The loading control showed no significant difference (Fig. 5.14 a). In a second approach, TNRC9 was transfected with an SRE-Luciferase construct and SRE-activation was measured by luciferase assay 48 hrs later. TNRC9 transfected cells exhibited no increase in SRE-dependent transcription compared to empty vector transfected control, but even a slight decrease (Fig. 5.14 b). These results prove that TNRC9 is regulated downstream and not upstream of SRF and SRE-dependent transcription.

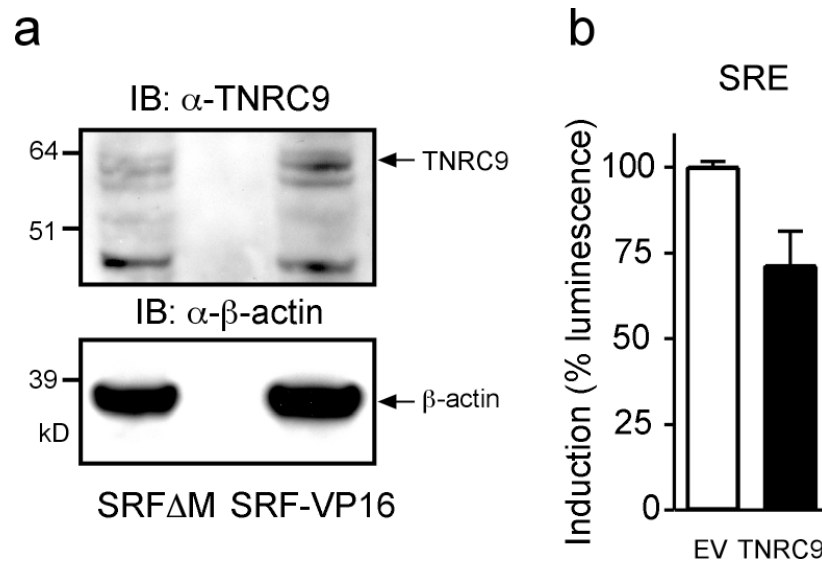


Fig. 5.14: TNRC9 is regulated downstream of SRF. (a) Immunoblot (IB) against TNRC9 and loading control β -actin of total N2a-cell lysates after transfection of SRF-VP16 and SRF-VP16 Δ M. (b) Percentage of luminescence normalized to vector (EV) in N2a cells transfected with TNRC9. Bar graphs represent means of three independent experiments \pm SEM.

TNRC9 is Upregulated by PAR-Agonists

As proteinase-activated receptors 1 and 2 (PAR) have been demonstrated to activate RhoA (reviewed in Flynn and Buret, 2004), it was tested whether activation of the RhoA pathway by PAR agonists would similarly increase TNRC9 abundance. Human-specific thrombin receptor activating peptide 14 (Trap-14, Bachem) and PAR2 agonist I (Merck) capable of activating both mouse and human PAR2 were used at different concentrations to treat human SH-SY5Y cells. TNRC9 abundance was quantified by qPCR 24 hrs later. 10 μ M Trap-14 increased TNRC9 abundance 6.5-fold (Fig. 5.15 a), treatment with 1 μ M PAR2 agonist I resulted in a 3.8-fold increase (Fig. 5.15 b). Both agents increased TNRC9 in an overall concentration-dependent manner. This data was confirmed on the protein level by treating N2a cells with 250 μ M PAR2-agonist I, and immunoblotting against TNRC9. The treated cells showed a robust increase in TNRC9 on protein level, whereas the loading control showed no difference (Fig. 5.15 c).

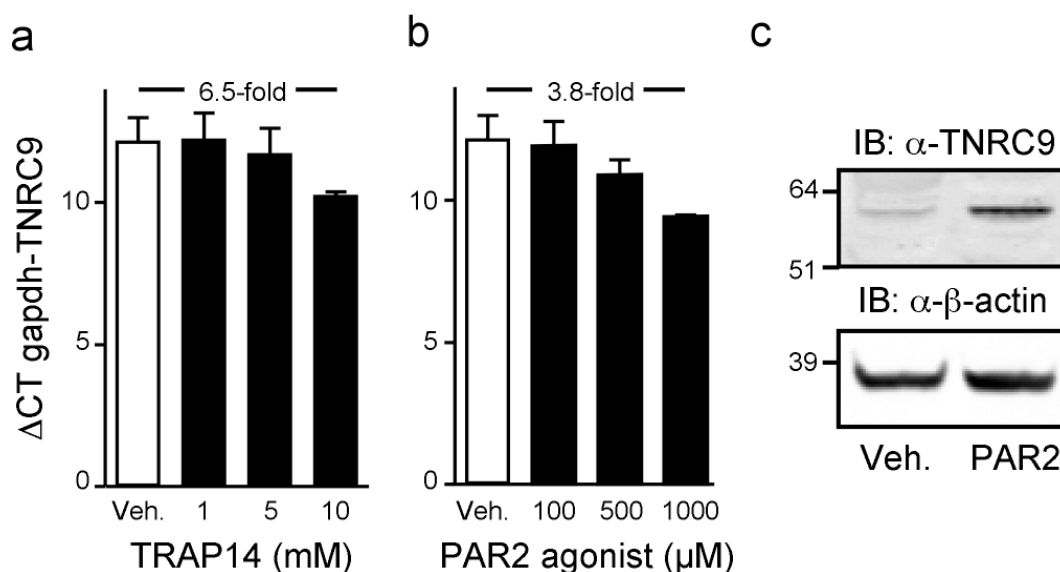


Fig. 5.15: TNRC9 is induced by PAR-activation. Expression of TNRC9 in SH-SY5Y cells treated with increasing concentrations of (a) PAR1 agonist TRAP-14 or (b) PAR2 agonist I, data given as Δ ct over GAPDH. (c) IB against TNRC9 and loading control β -actin in N2a cells treated with 250 μ M PAR2-agonist I. Bargraphs present means \pm SEM from three independent experiments.

TNRC9 Increases PEDF

Finally, it had to be determined if TNRC9 acts upstream or downstream of the GPR39-effector protein PEDF. For this purpose, HT22 cells were transfected with TNRC9, and PEDF quantified by qPCR. TNRC9 overexpressing cells exhibited a 2.8-fold increase of PEDF on transcriptional level (Fig. 5.16 a). In the same experiment, supernatants of the transfected cells were collected and PEDF measured by ELISA (this measurement was done by Ana Luisa Pina). PEDF secretion in TNRC9 transfected cells was increased approximately fourfold (Fig. 5.16 b).

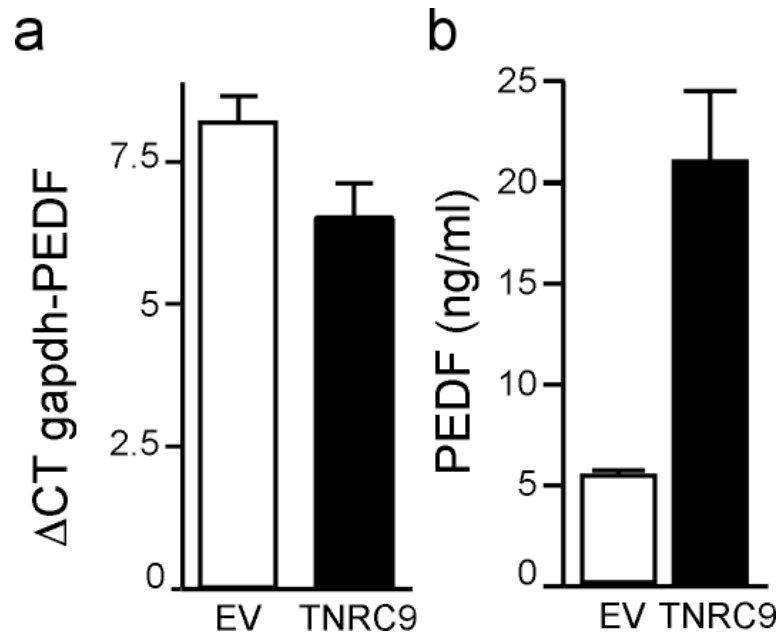


Fig. 5.16: TNRC9 upregulates PEDF. (a) Expression of PEDF in HT22 cells transfected with vector (EV) or TNRC9 expressed in Δ ct over GAPDH. (b) Secreted PEDF from HT22 cells transfected with TNRC9, measured by ELISA. This experiment was performed by Ana Luisa Pina, Regensburg. Data is presented as mean \pm SEM from three independent experiments.

Taken together, these results prove that TNRC9 is upregulated by GPR39, as well as by PAR-activation and SRF overexpression. It plays a role in GPR39-mediated cytoprotection. SRE-dependent transcription is not altered by TNRC9, but TNRC9 overexpression induces PEDF transcription and secretion. Thus, TNRC9 must act downstream of SRE, but upstream of PEDF.

Cited1 is a Transcriptional Coactivator Regulated by GPR39

Another protein upregulated in response to GPR39 overexpression in clone 17 in the chip array was Cbp/p300-interacting transactivator, with Glu/Asp-rich carboxy-terminal domain, 1 (Cited1), a transcriptional coactivator without own DNA-binding properties. It has been reported to interact with SMAD4 (Shioda et al., 1998) and estrogen receptors α (ER α) and β (ER β) (Yahata et al., 2001).

GPR39 Upregulates Cited1

To verify the chip data, Cited1 expression was evaluated by immunoblot using the same samples used in 5.5.1. On the protein level a Cited1-band at 28 kDa was undetectable in vector-transfected cells, but became clearly visible after overexpression of GPR39. In contrast to TNRC9, Cited1 expression was not reduced by coexpression of RGS16 (Fig. 5.17 a). This is possibly a result of a $G\alpha_{13}$ -independent mechanism of Cited1 regulation. Also, Cited1 transcription was determined after GPR39 overexpression by qPCR. GPR39 increased Cited1 transcript by 2.3-fold (Fig. 5.17 b).

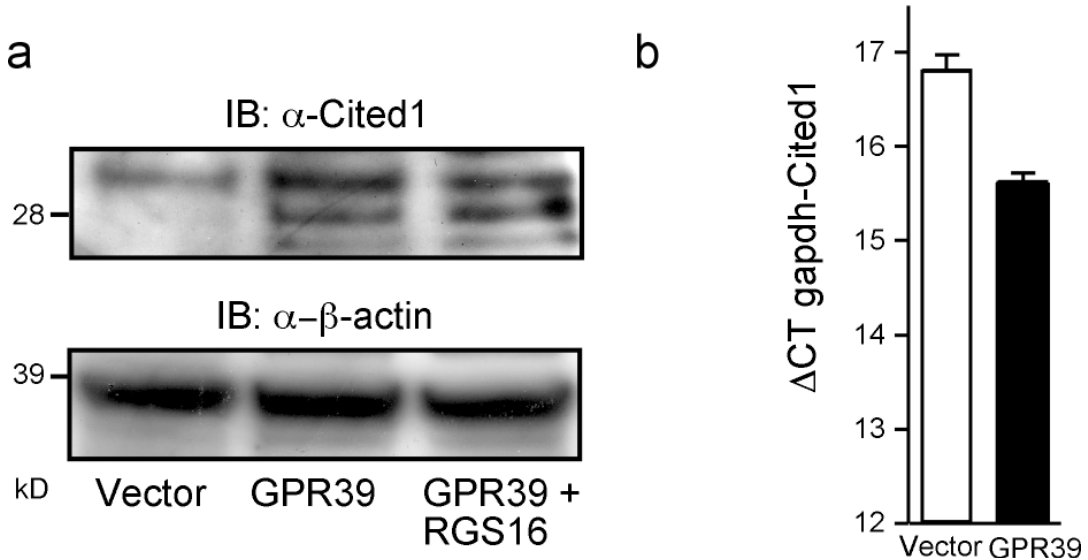


Fig. 5.17: Cited1 is induced by GPR3. (a) Immunoblot against Cited1 and β -actin as loading control in N2a cells transfected with vector, GPR39 and GPR39+RGS16. (b) Expression of Cited1 in N2a cells transfected with vector or GPR39, data given as Δct over GAPDH.

Cited1 is Upregulated by PAR-Agonists

To determine whether PAR activation would induce upregulation of Cited1, SH-SY5Y cells were treated with different amounts of PAR1-agonist TRAP-14 and PAR2-agonist I for 24 hrs. Quantitative PCR revealed a small, yet concentration-dependent effect on Cited1 transcription. 10 mM Trap-14 increased Cited1 by 1.5-fold (Fig. 5.18 a), 1 mM PAR2 agonist I had a similar effect (1.8-fold upregulation) (Fig. 5.18 b). Again, these findings were supported by immunoblot analysis that showed an increased Cited1-band after treating N2a cells with 250 μ M PAR2-agonist I, whereas the actin loading control showed no difference (Fig. 5.18 c).

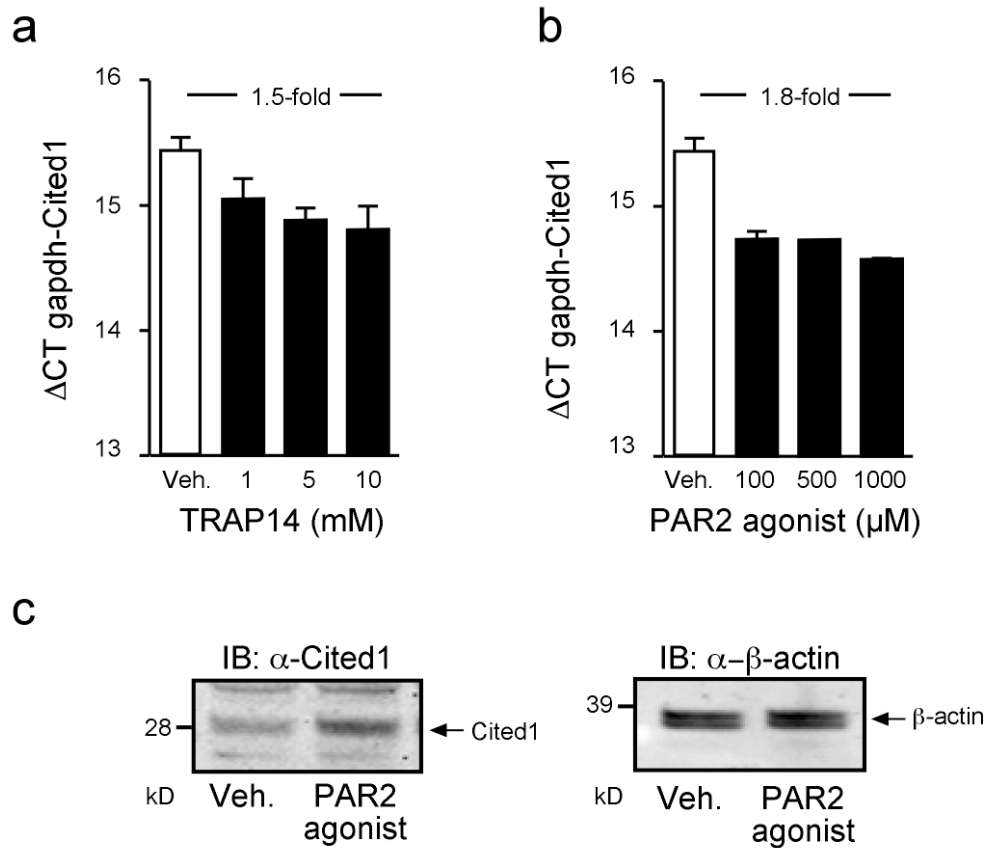


Fig. 5.18: Cited1 expression is induced by PAR-activation Expression of Cited1 in SH-SY5Y cells treated with increasing concentrations of PAR1-agonist TRAP-14 (a) or PAR2-agonist I (b), data given as Δ ct over GAPDH. (c) Immunoblot against Cited1 and loading control β -actin of N2a cells treated with 250 μ M PAR2-agonist I.

GPR39 Enhances Nuclear Localization of Cited1

Other than TNRC9, Cited1 was mainly found in the cytosol. To determine whether TNRC9 and Cited1 would co-localize after GPR39 overexpression, N2a cells were transfected with either TNRC9-EGFP and empty vector or GPR39, respectively. Cells were fixed, permeabilized and stained with a specific Cited1 antibody. Visualization was performed on a confocal microscope (Zeiss). This demonstrated that the mostly cytosolic location of Cited1 (Fig. 5.19, upper panel) shifted to an enhanced nuclear signal in the presence of GPR39 (Fig. 5.19, lower panel).

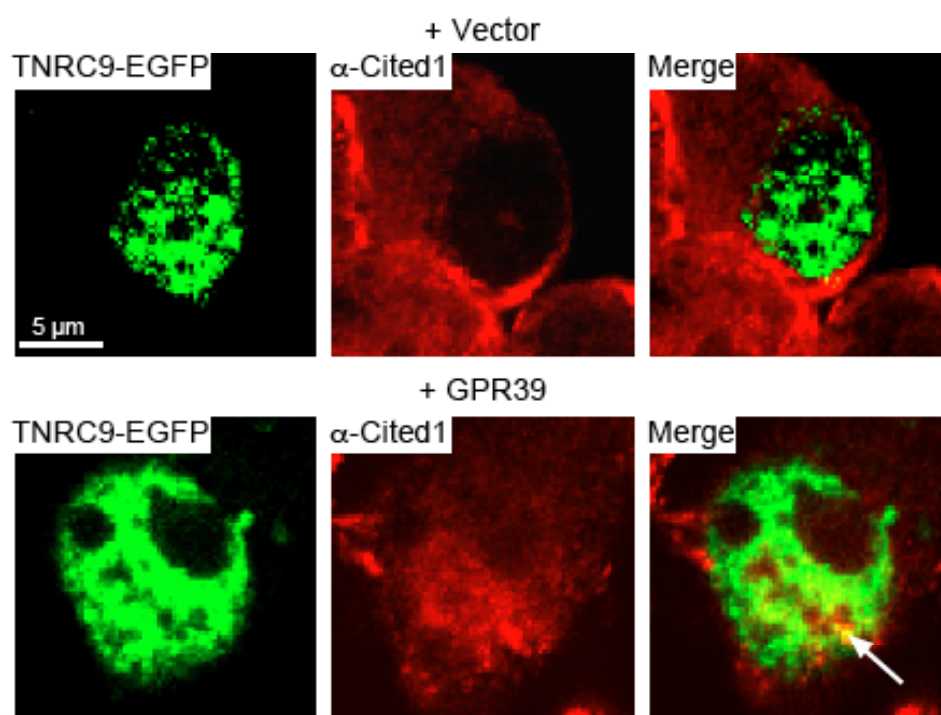


Fig. 5.19: GPR39 overexpression enhances nuclear localization of Cited1. N2a cells transfected with TNRC9-EGFP and vector (upper panel) or GPR39 (lower panel) and stained for endogenous Cited1. Cells were visualized by confocal microscopy. Arrows indicate nuclear co-localization of Cited1 and TNRC9. Scalebar corresponds to 5 μ m.

TNRC9 and Cited1 Interact Physically

Since a transcription factor and a transcriptional coactivator appeared to be upregulated in concert by both GPR39 overexpression and PAR-activation, the obvious question to ask was whether these two proteins might interact physically. Therefore, CHO cells were co-transfected with a myc-tagged TNRC9 construct and

an HA-tagged Cited1 construct. Cells were lysed and the presence of both proteins was verified by immunoblot. An HA-tagged deletional mutant of PUMA served as a control. For immunoprecipitation (IP), the lysates were incubated with agarose beads crosslinked to a specific α -myc-antibody. Antibody bound proteins were collected and eluted, separated by SDS-PAGE and blotted to nitrocellulose. By probing the membrane with the α -HA antibody, co-immunoprecipitation of HA-tagged Cited1-protein could be shown. The same procedure was performed vice versa with beads linked to α -HA-antibody and probing the immunoblot with α -myc-antibody. Either way, the co-immunoprecipitation of TNRC9 and Cited1 showed an interaction between these two proteins. HA-tagged Δ -PUMA could not be pulled down with TNRC9 (Fig. 5.20 a).

TNRC9-Cited1 Interaction is Specific

To determine the specificity of the TNRC9-Cited1 interaction, three more members of the Cited-family were co-transfected in COS7 cells with TNRC9 and co-immunoprecipitation was performed. The result showed a clear interaction of TNRC9 with Cited1 only, the other three family members Cited2, 3 and 4 could not be co-precipitated (Fig. 5.20 b).

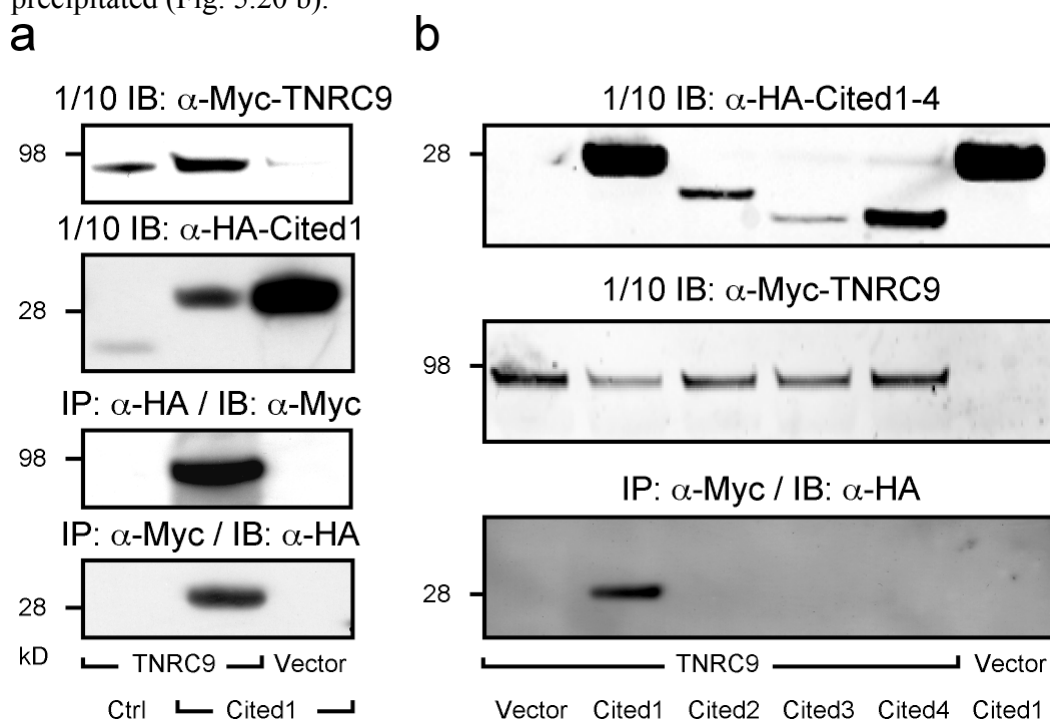
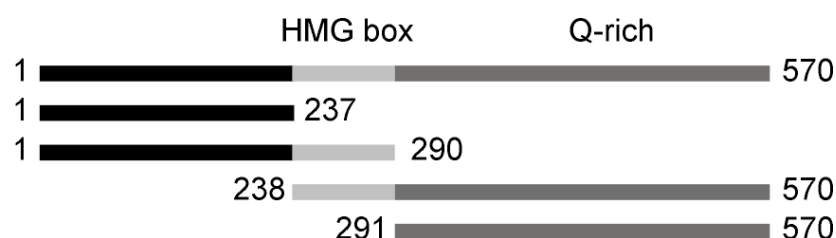


Fig. 5.20: TNRC9 specifically interacts with Cited1. (a) Co-immunoprecipitation of myc-tagged TNRC9 and HA-tagged Cited1 done in CHO cells. Pulldown was performed both ways, precipitating with myc-antibody and staining with HA-antibody and vice versa. (b) Co-immunoprecipitation of HA-tagged Cited1, 2, 3 and 4 with myc-tagged TNRC9 done in COS7 cells.

TNRC9 and Cited1 Interact at the TNRC9-HMG-Domain

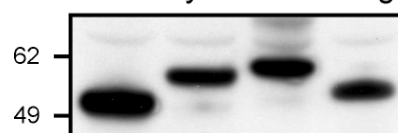
TNRC9 contains three distinct domains: the N-terminus and a glutamine-rich C-terminal tail flank a central HMG-domain. Four deletional mutants were used to define the domain of interaction: the N-terminal only, the N-terminal with the HMG-domain, the C-terminal domain with and without the HMG-domain (Fig. 5.21 a). These four mutants were co-expressed with TNRC9 in CHO cells and co-immunoprecipitation was performed, revealing an interaction only in the two constructs containing the central HMG-domain, with a stronger signal in the sample lacking the C-terminal part (Fig. 5.21 b). Taken together, these results show a specific interaction between TNRC9 and Cited1 at TNRC9s central domain.

a

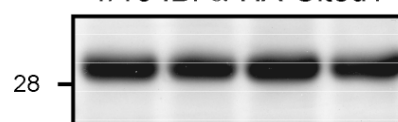


b

1/10 IB: α -Myc-TNRC9 fragments



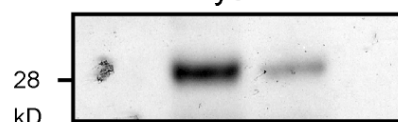
1/10 IB: α -HA-Cited1



1-237 1-290 238-570 291-570

Cited1

IP: α -Myc / IB: α -HA



1-237 1-290 238-570 291-570

Cited1

Fig. 5.21: TNRC9 interacts with Cited1 through its HMG-domain. (a) Schematic illustration of TNRC9 deletional mutants containing either the N- or C-terminus with or without the central HMG-domain. (b) Co-immunoprecipitation of HA-tagged Cited1 with myc-tagged TNRC9 deletional mutants.

TNRC9 and Cited1 Protect Synergistically

The interaction of TNRC9 and Cited1 and the fact that TNRC9 only had a small cytoprotective protective effect suggested that these two proteins might have a synergistic effect on cell survival. To find out, HEK239 and N2a cells were transiently transfected with EGFP and TNRC9 and Cited1 alone and together and treated with 5 µg/ml tunicamycin. After 24 hrs, the cells were collected and double-stained for Annexin V and 7-AAD. The percentage of apoptotic cells was then determined by flow cytometry. When compared to empty vector control, TNRC9 showed an increase in cell viability in both N2a cells and HEK294 cells. The rate of apoptotic cells was slightly decreased by TNRC9 alone (HEK: 18.2%, N2a: 16.5%), and less by Cited alone (HEK: 12.1%, N2a: 14.1%). Coexpression of both proteins resulted in almost 30% decrease in apoptosis in both cell lines, suggesting a synergistic effect (Fig. 5.22 a). The same experiment was repeated, this time directly inducing apoptosis by overexpressing pro-apoptotic Bax. In this experiment, the previous results could be confirmed, with the anti-apoptotic effect of TNRC9 and Cited1 together being as protective as the well described anti-apoptotic protein Bcl-2, that served as a positive control (Fig. 5.22 b).

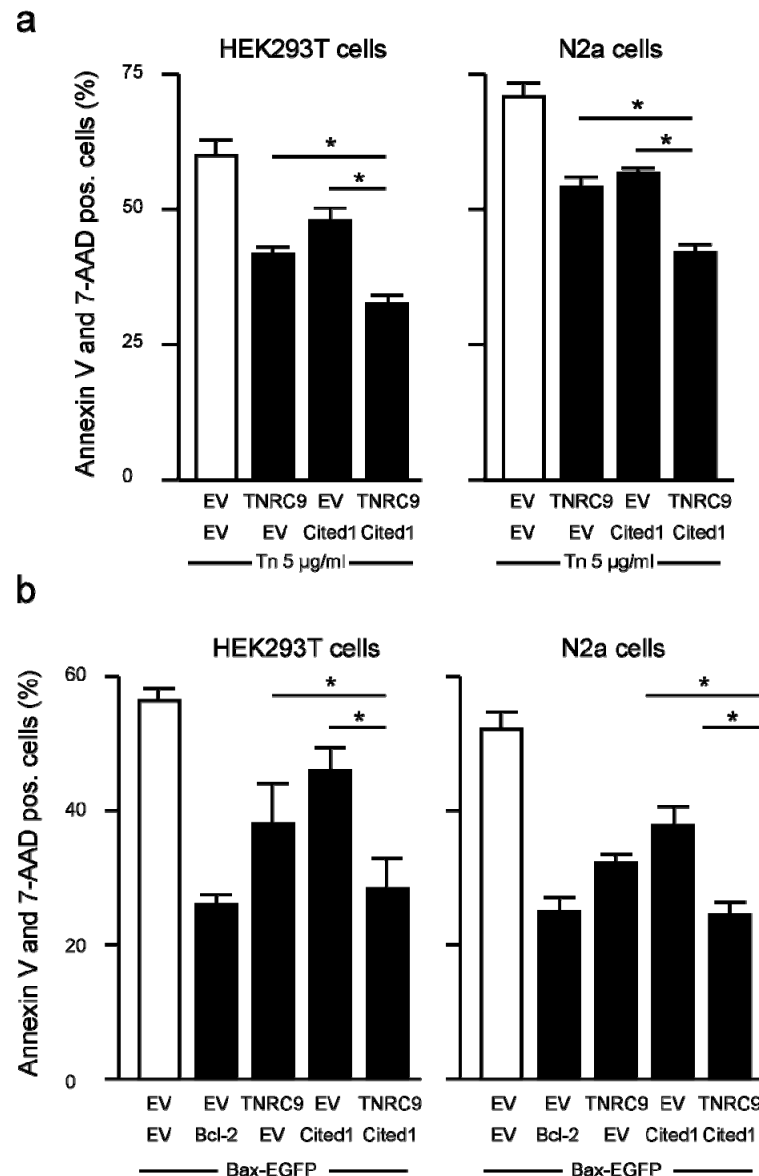


Fig. 5.22: TNRC9 and Cited1 synergistically protect. (a) HEK293 or N2a cells were transfected with EGFP and TNRC9 or Cited1 alone or both constructs and treated with 5 μ g/ml tunicamycin for 24 hrs. (b) HEK293 and N2a cells were transfected with the constructs above along with an EGFP-tagged Bax. Cells were stained with Annexin V and 7-AAD and apoptotic cells counted by gating for EGFP-positive cells that were double positive for 7-AAD and Annexin V. Data is given as mean \pm SEM from three independent experiments. Asterisks indicate $P < 0.001$ as determined by one-way analysis of variance (ANOVA) and Tukey's Multiple Comparison Test.

5.9 TNRC9 and Cited1 Synergistically Upregulate Estrogen Receptor-mediated Transcription

To find out how TNRC9 and Cited1 mediate their cytoprotective effect, activation of three different sets of genes was examined, all three being regulated by responsive elements near their transcription starts. The serum-response element (SRE) was chosen because of its activation through GPR39, although no effect of TNRC9 alone on the SRE was observed in previous experiments (4.3.6) but an effect in coexpression with Cited1 could not be excluded. However, two more responsive elements were investigated, namely the cAMP-response element (CRE), because an interaction of Cited1 and the Creb-binding protein (CBP) has been reported previously (Yahata et al., 2000) and the estrogen-response element (ERE) since Cited1 had been reported to be a selective coactivator for estrogen-dependent transcription (Yahata et al, 2001). For this purpose, three luciferase reporter constructs (pSRE-Luc, pCRE-Luc, pERE-Luc) were co-transfected with TNRC9 or Cited1 alone or together and the reporter activity was measured by luciferase assay and normalized to total protein. Neither Cited1 or TNRC9 alone, nor in combination had a significant effect on SRE-induction (Fig. 5.23 a) even though a slight increase could be observed for the sample overexpressing both TNRC9 and Cited1. For CRE, no effect at all could be detected (5.23 b). For ERE, a threefold increase was observed after overexpression of TNRC9 alone, a twofold increase after transfection of Cited1. Together, TNRC9 and Cited1 increased ERE-dependent transcription 15-fold (Fig. 5.23 c). So a significant synergistic effect was only found in ERE-dependent transcription.

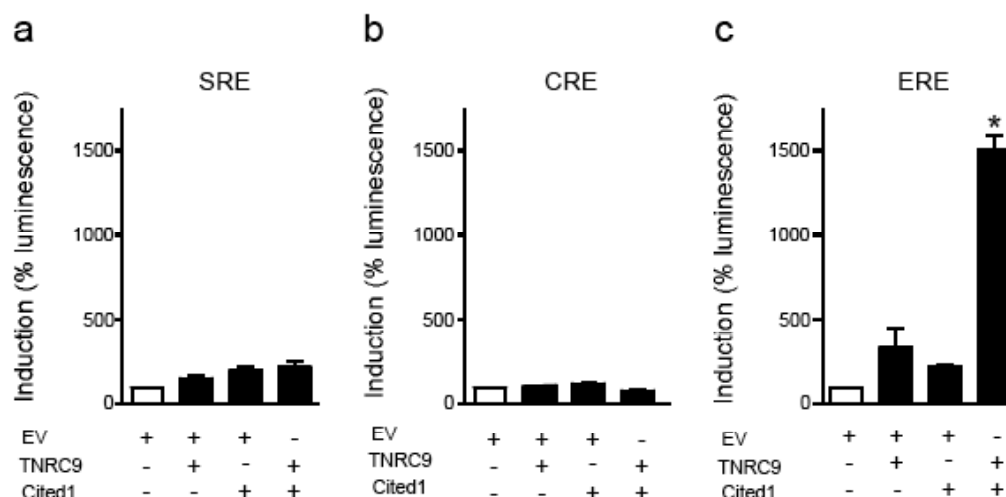


Fig. 5.23: TNRC9 and Cited1 synergistically upregulate estrogen dependent transcription. Percentage of induction of the respective reporter constructs (a) serum-response element (SRE), (b) cAMP-response element (CRE), (c) estrogen-response element (ERE), measured by luciferase assay 24 hrs after transfection of the indicated constructs and normalized to control (EV). Asterisk indicates statistical significance as determined by one-way analysis of variance (ANOVA).

TNRC9 interacts with ER α Through its N-terminal Domain

Because of the above results, we hypothesized an interaction between TNRC9 and ER α . To elucidate this question, CHO cells were transfected with both myc-tagged TNRC9 and VP16-tagged ER α and co-immunoprecipitation was performed. Indeed, it was possible to pull down ER α with TNRC9 (Fig 5.24 a). To determine the domain of interaction, myc-tagged TNRC9-deletional mutants (Fig. 5.21 a) were co-transfected with VP16-tagged ER α and co-immunoprecipitated. Precipitation was only possible in the presence of the N-terminal domain of TNRC9 alone (Fig. 5.24 b). The mutant containing both N-terminal domain and central HMG-domain was not sufficient to pull down ER α , which could indicate another protein binding to the HMG domain and sterically inhibiting an interaction with the N-terminus.

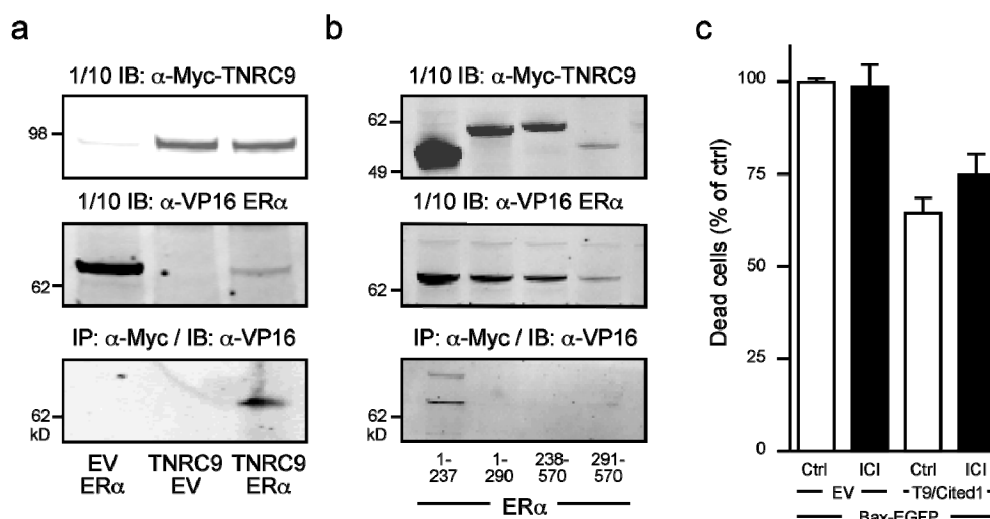


Fig. 5.24: TNRC9 interacts with ER α at its N-terminus, cytoprotection is ER-dependent. (a) Co-immunoprecipitation of VP16-tagged ER α with myc-tagged TNRC9 and (b) TNRC9 deletional mutants. (c) Percentage of apoptotic cells transfected with Bax-EGFP and empty vector (EV) or TNRC9 and Cited1, respectively in the presence of 1 μ M ICI 182,780 or vehicle (ctrl), normalized to EV.

Further it was tested, whether a specific inhibitor of ER α ICI (ICI 182,780 (Tocris, Bristol, UK)) had an effect on the cytoprotective action of the TNRC9-Cited1 transcriptional complex. ICI specifically downregulates and degrades ER α (Kansra et al., 2005). For this purpose, N2a cells were transfected with pro-apoptotic Bax and TNRC9+Cited1 in presence and absence of 1 μ M ICI 182,780. Apoptotic cells were

then counted by staining with Annexin V and 7-AAD. The presence of ICI had no effect on the apoptosis-rate in vector transfected cells, but increased the percentage of apoptotic cells in TNRC9+Cited1 transfected cells (Vehicle: 64.5% versus 1 μ M ICI: 74.8%) (Fig. 5.24 c). These findings indicate a role of ER α in the TNRC-Cited1-mediated cytoprotection and suggest the possibility of a transcriptional complex of TNRC9, Cited1 and ER α to enhance ERE-mediated transcription. Regulation and interaction of TNRC9, Cited1 and ER α are summarized in figure 5.25.

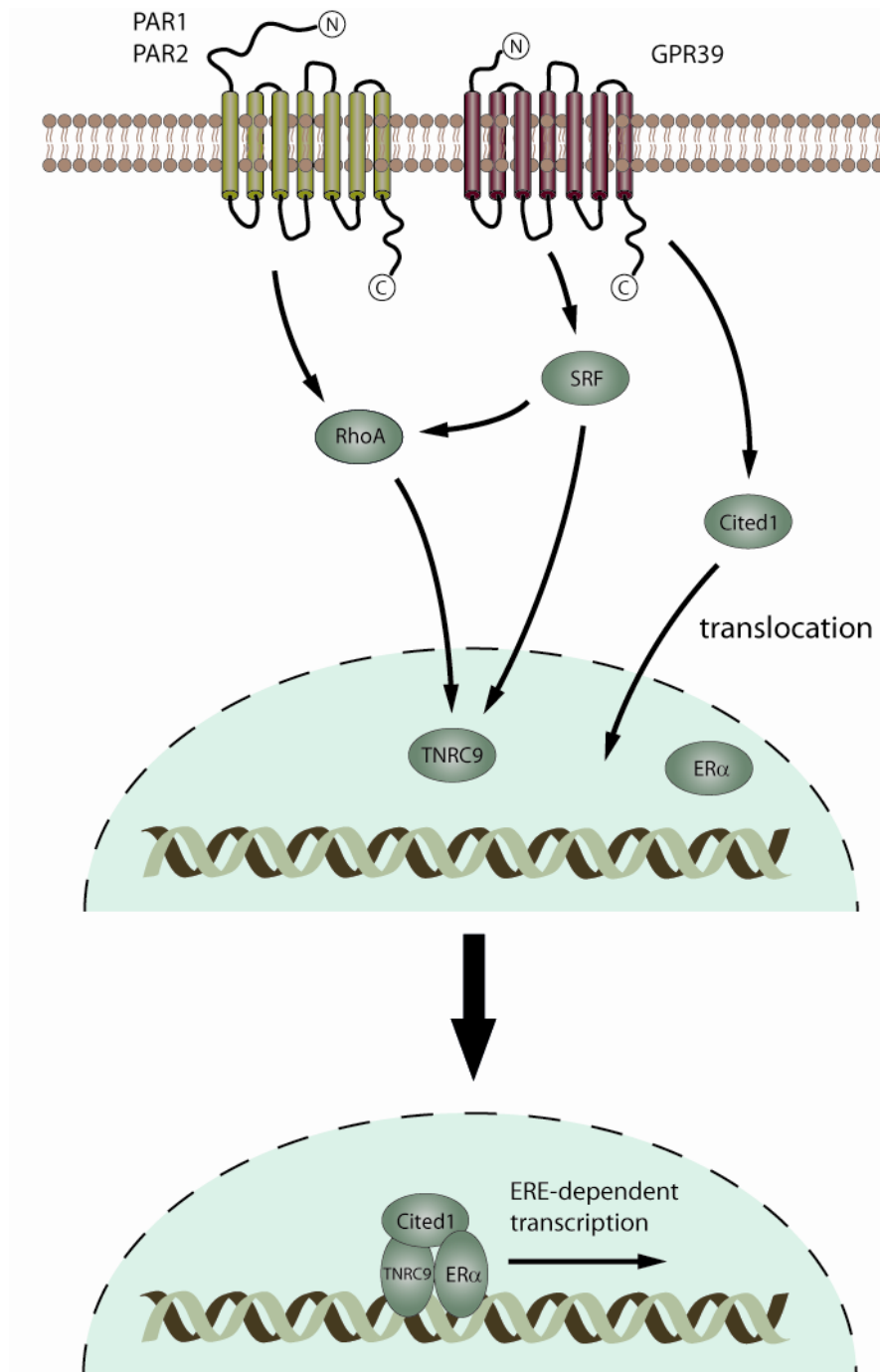


Fig. 5.25: Schematic cartoon of TNRC9 and Cited1 regulation and interaction.

6. Discussion

In summary, the results of this study suggest that GPR39 exerts its cytoprotective effect through coupling to $G\alpha_{12/13}$ and stimulating a signaling cascade by activating RhoA and Rho-kinase, subsequently inducing SRE-dependent transcription and leading to the increased secretion of the neurotrophic factor PEDF. These actions are negatively regulated by RGS16. Furthermore, GPR39 leads to the concerted upregulation of the transcription factor TNRC9 and the transcriptional co-regulator Cited1. These two proteins interact, synergistically protect from cell death and increase estrogen-dependent transcription. Moreover, TNRC9 interacts with $ER\alpha$, which suggests a transcriptional complex of Cited1, $ER\alpha$ and TNRC9.

The GPR39-mediated Signal Transduction Cascade

GPR39-induced cytoprotection is mediated through activation of the Rho-axis by $G\alpha_{13}$, activation of Rho-kinase and SRE, which leads to increased secretion of PEDF. The activation of the Rho-axis via $G\alpha_{12/13}$ is a known feature of proteinase-activated receptor 1, also known as thrombin-receptor. Therefore GPR39-signaling resembles thrombin signaling.

Thrombin activation has pleiotropic effects, causing both cell survival and apoptosis in a tissue (reviewed in Flynn and Buret, 2004) and ligand-concentration dependent manner (Donovan & Cunningham, 1998). A second GPCR pathway mediated through $G\alpha_{12/13}$ and therefore possibly resembling GPR39 signaling is the lysophosphatidic acid (LPA) activated receptor, which activates several GPCRs and is therefore difficult to investigate (reviewed in Radeff-Huang et al., 2004).

As GPR39 is an orphan receptor, effects of different ligand concentrations could not be tested. All observations in the present study support the previous report of GPR39 being a constitutively active receptor or activated by a ligand present in serum suggested by Holst et al., 2004. After publication of GPR39s de-orphanization by Zhang et al. in 2005, where a ligand named obestatin derived from the ghrelin precursor peptide was reported to activate GPR39 and have an effect on food uptake, cell death experiments were made in presence of obestatin without observing any alteration of GPR39-mediated protection (data not shown) which confirmed the observations of Lauwers et al., 2006, though recent studies still argue about the GPR39-obestatin relationship. Still, the signal transduction proposed here was not altered by obestatin. One most interesting downstream target of GPR39-mediated signaling was the suggested effector protein PEDF (5.3).

PEDF as one Effector Molecule Downstream of GPR39

Pigment epithelium derived factor PEDF was found to be a downstream effector of the GPR39 signal transduction cascade. PEDF was originally identified by Joyce Tombran-Tink as a protein secreted by human retinal pigment epithelium (Tombran-Tink et al., 1991). Additionally it has been described to be present in the CNS, where it shares high abundance with GPR39 in amygdala, retina and hippocampus, as well as in the lung (Tombran-Tink et al., 1996) and to protect from chronic glutamate mediated neuronal degeneration (Bilak et al., 1999) and oxidative stress (Tsao et al., 2006). Considering that GPR39 was found in a hippocampal cell model for chronic glutamate stress this effect of PEDF further supports the hypothesis of PEDF as an important GPR39 downstream effector. Further, PEDF has been shown to increase motor neuron survival in animal models of sciatic nerve section by 57% (Houenou et al., 1999). After these findings, PEDF has been suggested to be a potential therapeutic agent in diseases featuring motor neuron loss like ALS. Also, throughout the nervous system there has been evidence of an age-related decrease in PEDF that has been linked to neurodegenerative processes such as macular degeneration (Smith and Steinle, 2007; Yoshida, 2007; Holekamp et al., 2002). One possible explanation is the PEDF-dependent induction of anti-apoptotic signal transduction through an unknown receptor (reviewed in Tombran-Tink & Bernstable, 2003).

In most cases, the attempt to rescue neuron loss through anti-apoptotic agents also has huge disadvantages, since inhibition of apoptosis enhances the risk of neoplastic transformation and cancer development. PEDF, however is not only a potent anti-apoptotic factor, but also exerts anti-tumor activities. In cancer research, one major field of investigation is the role of angiogenesis and metastasis in cancer tissue (Folkman, 1971). Angiogenesis is the process by which novel bloodvessels are formed and enables the cancer to grow in size and metastasize. In studies focussing on the anti-angiogenic function of PEDF, it was found to be a potent inhibitor of angiogenesis, being twice as potent as angiostatin (Dawson et al., 1999). Low expression levels of PEDF have been linked to increased incidence of metastasis and poor prognosis in prostate and pancreatic cancer (Halin et al., 2004; Uehata et al., 2004) as well as neuroblastoma and glioma (Crawford et al., 2001; Guan et al., 2003). Gene transfer of PEDF or delivery of recominant PEDF have already been demonstrated to act as anti-angiogenic agents in melanoma (Abe et al., 2004; Garcia et al., 2004), glioma (Guan et al., 2003), Wilms' tumor (Abramson et al., 2003), or as a direct tumor suppressing agent by inhibition of proliferation in prostate cancer and melanoma (Doll et al., 2003; Abe et al., 2004) both *in vitro* and *in vivo*.

In summary, assuming that the GPR39-pathway could specifically be altered in a way that increases transcription and secretion of PEDF as observed, this alteration of GPCR-signaling could hypothetically serve as a promising non-tumorigenic inhibitor of apoptosis.

Transcriptional Interaction of GPR39 Downstream Mediators

Transcriptional Complex Containing TNRC9, Cited1 and ER α – Implications in Cancer

The downstream mediators of GPR39 signaling Cited1 and TNRC9 have been demonstrated to have a synergistic protective effect on cytotoxicity by ER-stress as well as by direct activation of apoptosis by Bax overexpression (5.7). A synergistic effect was also found on the activation of estrogen-dependent transcription (5.8), which could be explained by a physical interaction of TNRC9 and ER α (5.9).

TNRC9 has recently been found to harbour a single nucleotide polymorphism in its 5'-region, which was tightly linked to breast-cancer susceptibility (Easton et al., 2007; Stacey et al., 2007) and to be specifically expressed in ER-positive breast cancer subtypes. In contrast, basal-like breast cancer tissue expressed only low levels of TNRC9 (Nordgard et al., 2007). Though this provided strong evidence for the involvement of TNRC9 in breast cancer, the underlying mechanisms remained unclear.

Cited1 has been shown in this study to be a transcriptional coactivator of TNRC9 and has in the past been reported to stimulate ER-dependent transcription and interact with ER α (Yahata et al., 2001). Also, Cited1 has been suggested to regulate the expression of ErbB2 in a breast cancer mouse model (Dillon et al., 2007). In this study, the effect of Cited1 on ER-dependent transcription was found to synergistically enhance the TNRC9-mediated protective effect (5.8). These findings combined imply that the transcriptional complex of TNRC9, Cited1 and ER α might be the functional link between the expression of TNRC9 in ER-positive breast cancer and the Cited1-ER α interaction to mediate ER-dependent transcription.

Moreover, other malignant cancer diseases could be prone to estrogen modulation. The findings of this study also showed a high abundance of TNRC9 in several types of epithelial cells. Cited1 was originally termed melanocyte-specific gene 1 (MGS1) (Shioda et al., 1996) and found to be upregulated by TPA induction in human melanoma cells (Li et al., 1998; Ahmed et al., 2001) and even ER α has recently been reported to be involved in melanoma progression (reviewed in Tanemura et al., 2007). If it holds true that the suggested transcriptional complex may also be responsible for malignant melanoma, it could be possible to use estrogen antagonists, which are widely and successfully used to treat ER-positive breast cancer as a melanoma treatment. Therefore, the expression and interaction of TNRC9 should become subject to investigation in tumor research and therapy.

The involvement of the GPR39 cascade via RhoA in TNRC9 and Cited1 expression was strengthened by the fact that both, TNRC9 and Cited1, could be upregulated by

PAR 1 and 2, which have been linked to breast cancer as well (Booden et al., 2004; Matej et al., 2006). Also, Cited1 had previously been reported to be upregulated also in a melanoma-linked system by LPA (Ahmed et al., 2001). This also suggests that GPR39 itself may be involved in cancer occurrence or progression.

Estrogen-induced Neuroprotective Properties

In spite of the tumorigenic properties of estrogen-dependent transcription, estrogen has been reported to be neuroprotective in several *in vitro* and *in vivo* models via several pathways. First of all, estrogen is a monophenolic molecule. In this context, it has been shown to be capable of scavenging free radicals *in vitro* in a lipophilic environment and therefore inhibits lipid peroxidation (Sugioka et al., 1987), which is a beneficial effect for oxidative stress in general. *In vitro* studies have reported protective effects of estrogen in several cell models against a large amount of different insults, such as glutamate excitotoxicity (Singer et al., 1999), oxidative glutamate toxicity (Moosmann & Behl, 1999) and even haloperidol toxicity (Sasgara, 1998) to name only a few. The pathways involved in these actions are divers and reach from direct free radical scavenging as mentioned above to the classical genomic pathway of nuclear receptors via the estrogen response element, a distinct palindromic motif (Donaghue et al., 1999; Hall et al., 2001) that leads to upregulation of anti-apoptotic proteins (Singer et al., 1998) or growth factors such as brain-derived neurotrophic factor BDNF (Sohrabji et al., 1995) and other intracellular signal cascades.

The role of estrogen in AD has been studied particularly well. In AD, besides its role in protection against oxidative stress, estrogen is capable of protecting against A β -toxicity by activating Akt (Zhang et al., 2001), and of decreasing GSK-activation and thereby increasing non-amyloidogenic cleavage of amyloid precursor protein (APP) to the soluble form sAPP and at the same time reducing A β secretion (Goodenough et al., 2003).

Considering the diverse ways of neuroprotection conferred by estrogen, GPR39 signaling and cytoprotection could be used as a therapeutic principle in neurodegenerative disease as mentioned above (6.2), given that a ligand-induced activation could be triggered in a tissue-specific manner.

GPR39 – a Double-Edged Sword

The aspects of the GPR39 signal transduction cascade paint a multifaceted picture of GPR39s implication in various processes and diseases. Especially conflicting is the upregulation of PEDF, which is known to be an anti-tumoral protein through multiple pathways (discussed in 6.2) and the upregulation of TNRC9 and Cited1 (discussed in

6.3), which are both implicated in cancer formation or progression. The distinct mechanisms by which GPR39 could be capable of either suppressing or promoting tumor progression as well as the regulation of the GPR39 signal transduction cascade need to be addressed. Moreover, the discovery of ligands as well as the regulation through a possible agonist or reverse agonist could offer a chance of altering cell fate in one way or the other. Disease-involving apoptotic cell loss might be relieved, whereas undesired anti-apoptotic conditions could be prevented.

7. Summary

Summary English

GPR39 is a constitutively active G-protein-coupled receptor, capable of increasing serum-response element (SRE) mediated transcription, which was recently controversially suggested to bind obestatin. GPR39 is upregulated in a hippocampal cell line resistant against diverse stimulators of cell death and its overexpression protects against oxidative, endoplasmic reticulum and mitochondrial stress. GPR39 induces expression of RGS16 (inhibitor of G-protein signaling 16), which suggests coupling to G α 13 and induction of SRE-mediated transcription by the small GTPase RhoA. Coexpression of GPR39 with RGS16 or dominant-negative RhoA abolished cell protection, whereas overexpression of SRF protected. Further downstream the signaling cascade, GPR39 overexpression lead to a concerted upregulation of the high mobility group transcription factor TNRC9 (trinucleotide repeat containing 9), first identified as a polyglutamine-containing protein, and Cited1, a transcriptional coregulator, and the increased secretion of the anti-angiogenic and neuroprotective factor PEDF. TNRC9 and Cited1 synergistically protected against cell death induced by unfolded protein response and direct induction of apoptosis by overexpression of Bax. Together, TNRC9 and Cited1 increased estrogen-dependent transcription, which suggested the involvement of estrogen receptor α . Indeed, an interaction between TNRC9 and ER α could be shown. Furthermore, the protective effect of TNRC9 and Cited1 could be reduced by a specifically inhibiting ER α . GPR39-mediated signaling thus might be a novel therapeutic target for diseases like cancer, ischemia or neurodegeneration.

Zusammenfassung Deutsch

GPR39 ist ein konstitutiv aktiver G-Protein gekoppelter Rezeptor, von dem bisher nur bekannt war, dass er SRE (Serum Response Element) abhängige Transkription aktivieren kann. Wir fanden eine Hochregulation von GPR39 in einer Zelllinie, die gegen oxidative Glutamattoxizität resistent ist. Überexpression von GPR39 vermittelte Zellschutz gegen diverse Arten von zellulärem Stress. Das Zellüberleben bei Induktion von ER-Stress sowie bei indirektem und direktem oxidativem Stress wurde durch Überexpression von GPR39 gesteigert. Eine Transkriptionsanalyse zweier Zelllinien, die sich dreifach in der GPR39 Expression unterschieden zeigte eine Hochregulation von RGS16 (Regulator G-Protein gekoppelter Signalwege). Dies sprach für eine Koppelung von GPR39 an $G\alpha_{13}$ und die Beteiligung der GTPase RhoA. Tatsächlich wurde der zytoprotektive Effekt von GPR39 durch gleichzeitige Expression von RGS16 oder dominant negativem RhoA aufgehoben. Im weiteren Verlauf der Signalkaskade führt GPR39 zur vermehrten Sekretion des zytoprotektiven Proteins PEDF. Weiterhin sind an der Signalkaskade der Transkriptionsfaktor TNRC9 und der Expressions-Koaktivator Cited1 beteiligt, die ebenfalls in einer synergistischen Art und Weise vor Zelltod schützen und physikalisch interagieren. TNRC9 und Cited1 erhöhen synergistisch die östrogenabhängige Transkription. Auch konnte eine physikalische Interaktion zwischen TNRC9 und dem Östrogenrezeptor $ER\alpha$ nachgewiesen werden. Eine Inhibition des Östrogenrezeptor $ER\alpha$ verminderte den TNRC9 und Cited1 vermittelten Schutzeffekt. GPR39 ist also G-Protein gekoppelter Rezeptor, der vor Zelltod schützt. Dies kann zum einen degenerative Prozesse verhindern, aber auch die Bildung von Tumoren fördern. Könnte die GPR39-vermittelte Signalkaskade spezifisch moduliert werden, wäre es möglich, entweder degenerative Prozesse zu mindern oder Tumorkrankheiten zu bekämpfen.

8. Appendix

References

- Abe R, Shimizu T, Yamagishi S, Shibaki A, Amano S, Inagaki Y, Watanabe H, Sugawara H, Nakamura H, Takeuchi M, Imaizumi T, Shimizu H. **Overexpression of pigment epithelium-derived factor decreases angiogenesis and inhibits the growth of human malignant melanoma cells *in vivo***. *Am J Pathol*. 2004 Apr;164(4):1225-32.
- Abramson LP, Stellmach V, Doll JA, Cornwell M, Arensman RM, Crawford SE. **Wilms' tumor growth is suppressed by antiangiogenic pigment epithelium-derived factor in a xenograft model**. *J Pediatr Surg*. 2003 Mar;38(3):336-42; discussion 336-42.
- Ahmed NU, Shioda T, Coser KR, Ichihashi M, Ueda M. **Aberrant expression of MSG1 transcriptional activator in human malignant melanoma *in vivo***. *Pigment Cell Res*. 2001 Apr;14(2):140-3.
- Allen RG, Tresini M. **Oxidative stress and gene regulation**. *Free Radic Biol Med*. 2000 Feb 1;28(3):463-99.
- Baltzis D, Qu LK, Papadopoulou S, Blais JD, Bell JC, Sonenberg N, Koromilas AE. **Resistance to vesicular stomatitis virus infection requires a functional cross talk between the eukaryotic translation initiation factor 2alpha kinases PERK and PKR**. *J Virol*. 2004 Dec;78(23):12747-61.
- Bazan NG. **Neurotrophins induce neuroprotective signaling in the retinal pigment epithelial cell by activating the synthesis of the anti-inflammatory and anti-apoptotic neuroprotectin D1**. *Adv Exp Med Biol*. 2008;613:39-44. Review.
- Behl C, Moosmann B. **Antioxidant neuroprotection in Alzheimer's disease as preventive and therapeutic approach**. *Free Radic Biol Med*. 2002 Jul 15;33(2):182-91. Review.
- Behl C. **Alzheimer's disease and oxidative stress: implications for novel therapeutic approaches**. *Prog Neurobiol*. 1999 Feb;57(3):301-23. Review.
- Bernales S, Papa FR, Walter P. **Intracellular signaling by the unfolded protein response**. *Annu Rev Cell Dev Biol*. 2006;22:487-508. Review.
- Bernard P, Couturier M. **The 41 carboxy-terminal residues of the miniF plasmid CcdA protein are sufficient to antagonize the killer activity of the CcdB protein**. *Mol Gen Genet*. 1991 Apr;226(1-2):297-304.
- Bi M, Naczki C, Koritzinsky M, Fels D, Blais J, Hu N, Harding H, Novoa I, Varia M, Raleigh J, Scheuner D, Kaufman RJ, Bell J, Ron D, Wouters BG, Koumenis C. **ER stress-regulated translation increases tolerance to extreme hypoxia and promotes tumor growth**. *EMBO J*. 2005 Oct 5;24(19):3470-81.
- Bilak MM, Corse AM, Bilak SR, Lehar M, Tombran-Tink J, Kuncel RW. **Pigment epithelium-derived factor (PEDF) protects motor neurons from chronic glutamate-mediated neurodegeneration**. *J Neuropathol Exp Neurol*. 1999 Jul;58(7):719-28.

- Bond A, O'Neill MJ, Hicks CA, Monn JA, Lodge D. **Neuroprotective effects of a systemically active group II metabotropic glutamate receptor agonist LY354740 in a gerbil model of global ischaemia.** *Neuroreport*. 1998 Apr 20;9(6):1191-3.
- Booden MA, Eckert LB, Der CJ, Trejo J. **Persistent signaling by dysregulated thrombin receptor trafficking promotes breast carcinoma cell invasion.** *Mol Cell Biol*. 2004 Mar;24(5):1990-9.
- Bortner CD, Oldenburg NB, Cidlowski JA. **The role of DNA fragmentation in apoptosis.** *Trends Cell Biol*. 1995 Jan;5(1):21-6.
- Braak H, Braak E. **Demonstration of amyloid deposits and neurofibrillary changes in whole brain sections.** *Brain Pathol*. 1991 Apr;1(3):213-6.
- Bruno V, Battaglia G, Copani A, Cesp  des VM, Galindo MF, Ce  a V, S  nchez-Prieto J, Gasparini F, Kuhn R, Flor PJ, Nicoletti F. **An activity-dependent switch from facilitation to inhibition in the control of excitotoxicity by group I metabotropic glutamate receptors.** *Eur J Neurosci*. 2001 Apr;13(8):1469-78.
- Butterfield DA, Castegna A, Lauderback CM, Drake J. **Evidence that amyloid beta-peptide-induced lipid peroxidation and its sequelae in Alzheimer's disease brain contribute to neuronal death.** *Neurobiol Aging*. 2002 Sep-Oct;23(5):655-64.
- Calfon M, Zeng H, Urano F, Till JH, Hubbard SR, Harding HP, Clark SG, Ron D. **IRE1 couples endoplasmic reticulum load to secretory capacity by processing the XBP-1 mRNA.** *Nature*. 2002 Jan 3;415(6867):92-6.
- Catal  n V, G  mez-Ambrosi J, Rotellar F, Silva C, Gil MJ, Rodr  guez A, Cienfuegos JA, Salvador J, Fr  hbeck G. **The obestatin receptor (GPR39) is expressed in human adipose tissue and is down-regulated in obesity-associated type 2 diabetes mellitus.** *Clin Endocrinol (Oxf)*. 2007 Apr;66(4):598-601.
- Chen Q, Ames BN. **Senescence-like growth arrest induced by hydrogen peroxide in human diploid fibroblast F65 cells.** *Proc Natl Acad Sci U S A*. 1994 May 10;91(10):4130-4.
- Cheo DL, Titus SA, Byrd DR, Hartley JL, Temple GF, Brasch MA. **Concerted assembly and cloning of multiple DNA segments using *in vitro* site-specific recombination: functional analysis of multi-segment expression clones.** *Genome Res*. 2004 Oct;14(10B):2111-20.
- Chinnaiyan AM. **The apoptosome: heart and soul of the cell death machine.** *Neoplasia*. 1999 Apr;1(1):5-15.
- Cohen GM. **Caspases: the executioners of apoptosis.** *Biochem J*. 1997 Aug 15;326 (Pt 1):1-16.
- Crawford SE, Stellmach V, Ranalli M, Huang X, Huang L, Volpert O, De Vries GH, Abramson LP, Bouck N. **Pigment epithelium-derived factor (PEDF) in neuroblastoma: a multifunctional mediator of Schwann cell antitumor activity.** *J Cell Sci*. 2001 Dec;114(Pt 24):4421-8.
- Davis JB, Maher P. **Protein kinase C activation inhibits glutamate-induced cytotoxicity in a neuronal cell line.** *Brain Res*. 1994 Jul 25;652(1):169-73.
- Dawson DW, Volpert OV, Gillis P, Crawford SE, Xu H, Benedict W, Bouck NP. **Pigment epithelium-derived factor: a potent inhibitor of angiogenesis.** *Science*. 1999 Jul 9;285(5425):245-8.
- Dexter DT, Carter CJ, Wells FR, Javoy-Agid F, Agid Y, Lees A, Jenner P, Marsden CD. **Basal lipid peroxidation in substantia nigra is increased in Parkinson's disease.** *J Neurochem*. 1989 Feb;52(2):381-9.

Dillon RL, Brown ST, Ling C, Shioda T, Muller WJ. **An EGR2/CITED1 transcription factor complex and the 14-3-3sigma tumor suppressor are involved in regulating ErbB2 expression in a transgenic-mouse model of human breast cancer.** *Mol Cell Biol.* 2007 Dec;27(24):8648-57.

Donaghue C, Westley BR, May FE. **Selective promoter usage of the human estrogen receptor-alpha gene and its regulation by estrogen.** *Mol Endocrinol.* 1999 Nov;13(11):1934-50.

Donovan FM, Cunningham DD. **Signaling pathways involved in thrombin-induced cell protection.** *J Biol Chem.* 1998 May 22;273(21):12746-52.

Dorsam RT, Gutkind JS. **G-protein-coupled receptors and cancer.** *Nat Rev Cancer.* 2007 Feb;7(2):79-94.

Druey KM, Blumer KJ, Kang VH, Kehrl JH. **Inhibition of G-protein-mediated MAP kinase activation by a new mammalian gene family.** *Nature.* 1996 Feb 22;379(6567):742-6.

Duksin D, Mahoney WC. **Relationship of the structure and biological activity of the natural homologues of tunicamycin.** *J Biol Chem.* 1982 Mar 25;257(6):3105-9

Easton DF, Pooley KA, Dunning AM, Pharoah PD, Thompson D, Ballinger DG, Struewing JP, Morrison J, Field H, Luben R, Wareham N, Ahmed S, Healey CS, Bowman R; SEARCH collaborators, Meyer KB, Haiman CA, Kolonel LK, Henderson BE, Le Marchand L, Brennan P, Sangrajrang S, Gaborieau V, Odefrey F, Shen CY, Wu PE, Wang HC, Eccles D, Evans DG, Peto J, Fletcher O, Johnson N, Seal S, Stratton MR, Rahman N, Chenevix-Trench G, Bojesen SE, Nordestgaard BG, Axelsson CK, Garcia-Closas M, Brinton L, Chanock S, Lissowska J, Peplonska B, Nevanlinna H, Fagerholm R, Eerola H, Kang D, Yoo KY, Noh DY, Ahn SH, Hunter DJ, Hankinson SE, Cox DG, Hall P, Wedren S, Liu J, Low YL, Bogdanova N, Schürmann P, Dörk T, Tollenaar RA, Jacobi CE, Devilee P, Klijn JG, Sigurdson AJ, Doody MM, Alexander BH, Zhang J, Cox A, Brock IW, MacPherson G, Reed MW, Couch FJ, Goode EL, Olson JE, Meijers-Heijboer H, van den Ouweland A, Uitterlinden A, Rivadeneira F, Milne RL, Ribas G, Gonzalez-Neira A, Benitez J, Hopper JL, McCredie M, Southey M, Giles GG, Schroen C, Justenhoven C, Brauch H, Hamann U, Ko YD, Spurdle AB, Beesley J, Chen X; kConFab; AOCs Management Group, Mannermaa A, Kosma VM, Kataja V, Hartikainen J, Day NE, Cox DR, Ponder BA. **Genome-wide association study identifies novel breast cancer susceptibility loci.** *Nature.* 2007 Jun 28;447(7148):1087-93.

Egerod KL, Holst B, Petersen PS, Hansen JB, Mulder J, Hökfelt T, Schwartz TW. **GPR39 splice variants versus antisense gene LYPD1: expression and regulation in gastrointestinal tract, endocrine pancreas, liver, and white adipose tissue.** *Mol Endocrinol.* 2007 Jul;21(7):1685-98.

Ferguson SS. **Evolving concepts in G protein-coupled receptor endocytosis: the role in receptor desensitization and signaling.** *Pharmacol Rev.* 2001 Mar;53(1):1-24.

Finkel T, Holbrook NJ. **Oxidants, oxidative stress and the biology of ageing.** *Nature.* 2000 Nov 9;408(6809):239-47. Review.

Flynn AN, Buret AG. **Proteinase-activated receptor 1 (PAR-1) and cell apoptosis.** *Apoptosis.* 2004 Nov;9(6):729-37. Review.

Folkman J. **Tumor angiogenesis: therapeutic implications.** *N Engl J Med.* 1971 Nov 18;285(21):1182-6. Review.

Fridovich I. **Oxygen toxicity: a radical explanation.** *J Exp Biol.* 1998 Apr;201(Pt 8):1203-9.

Garcia M, Fernandez-Garcia NI, Rivas V, Carretero M, Escamez MJ, Gonzalez-Martin A, Medrano EE, Volpert O, Jorcano JL, Jimenez B, Larcher F, Del Rio M. **Inhibition of xenografted human melanoma growth and prevention of metastasis development by dual antiangiogenic/antitumor activities of pigment epithelium-derived factor.** Cancer Res. 2004 Aug 15;64(16):5632-42.

Gilman. **G proteins: transducers of receptor-generated signals.** Annu Rev Biochem. 1987;56:615-49. Review.

Goodenough S, Schäfer M, Behl C. **Estrogen-induced cell signaling in a cellular model of Alzheimer's disease.** J Steroid Biochem Mol Biol. 2003 Feb;84(2-3):301-5.

Gourcerol G, Taché Y. **Obestatin—a ghrelin-associated peptide that does not hold its promise to suppress food intake and motility.** Neurogastroenterol Motil. 2007 Mar;19(3):161-5. Review.

Guan M, Yam HF, Su B, Chan KP, Pang CP, Liu WW, Zhang WZ, Lu Y. **Loss of pigment epithelium derived factor expression in glioma progression.** J Clin Pathol. 2003 Apr;56(4):277-82.

Gutierrez MG, Master SS, Singh SB, Taylor GA, Colombo MI, Deretic V. **Autophagy is a defense mechanism inhibiting BCG and Mycobacterium tuberculosis survival in infected macrophages.** Cell. 2004 Dec 17;119(6):753-66.

Halin S, Wikström P, Rudolfsson SH, Stattin P, Doll JA, Crawford SE, Bergh A. **Decreased pigment epithelium-derived factor is associated with metastatic phenotype in human and rat prostate tumors.** Cancer Res. 2004 Aug 15;64(16):5664-71.

Hall JM, Couse JF, Korach KS. **The multifaceted mechanisms of estradiol and estrogen receptor signaling.** J Biol Chem. 2001 Oct 5;276(40):36869-72.

Harding HP, Novoa I, Zhang Y, Zeng H, Wek R, Schapira M, Ron D. **Regulated translation initiation controls stress-induced gene expression in mammalian cells.** Mol Cell. 2000 Nov;6(5):1099-108.

Harding HP, Zhang Y, Ron D. **Protein translation and folding are coupled by an endoplasmic-reticulum-resident kinase.** Nature. 1999 Jan 21;397(6716):271-4. Erratum in: Nature 1999 Mar 4;398(6722):90.

Hartley JL, Temple GF, Brasch MA. **DNA cloning using *in vitro* site-specific recombination.** Genome Res. 2000 Nov ;10(11):1788-95.

Heldin CH. **Dimerization of cell surface receptors in signal transduction.** Cell. 1995 Jan 27;80(2):213-23. Review.

Herbert TP. **PERK in the life and death of the pancreatic beta-cell.** Biochem Soc Trans. 2007 Nov;35(Pt 5):1205-7. Review.

Hill CS, Wynne J, Treisman R. **The Rho family GTPases RhoA, Rac1, and CDC42Hs regulate transcriptional activation by SRF.** Cell. 1995 Jun 30;81(7):1159-70.

Holekamp NM, Bouck N, Volpert O. **Pigment epithelium-derived factor is deficient in the vitreous of patients with choroidal neovascularization due to age-related macular degeneration.** Am J Ophthalmol. 2002 Aug;134(2):220-7.

Holst B, Holliday ND, Bach A, Elling CE, Cox HM, Schwartz TW. **Common structural basis for constitutive activity of the ghrelin receptor family.** J Biol Chem. 2004 Dec 17;279(51):53806-17. Epub 2004 Sep 21.

Holst B, Egerod KL, Schild E, Vickers SP, Cheetham S, Gerlach LO, Storjohann L, Stidsen CE, Jones R, Beck-Sickinger AG, Schwartz TW. **GPR39 signaling is stimulated by zinc ions but not by obestatin.** *Endocrinology*. 2007 Jan;148(1):13-20. Epub 2006 Sep 7.

Houenou LJ, D'Costa AP, Li L, Turgeon VL, Enyadike C, Alberdi E, Becerra SP. **Pigment epithelium-derived factor promotes the survival and differentiation of developing spinal motor neurons.** *Comp Neurol*. 1999 Sep 27;412(3):506-14.

Horton R, Moran LA, Ochs R, Rawn DJ, Scrimgeour KG. **Principles of Biochemistry.** 4th Edition, Prentice Hall (1996), ISBN 0134391675.

Huijts PE, Vreeswijk MP, Kroeze-Jansema KH, Jacobi CE, Seynaeve C, Krol-Warmerdam EM, Wijers-Koster PM, Blom JC, Pooley KA, Klijn JG, Tollenaar RA, Devilee P, van Asperen CJ. **Clinical correlates of low-risk variants in FGFR2, TNRC9, MAP3K1, LSP1 and 8q24 in a Dutch cohort of incident breast cancer cases.** *Breast Cancer Res*. 2007;9(6):R78.

Jackson VR, Nothacker HP, Civelli O. **GPR39 receptor expression in the mouse brain.** *Neuroreport*. 2006 May 29;17(8):813-6.

Johansen FE, Prywes R. **Identification of transcriptional activation and inhibitory domains in serum response factor (SRF) by using GAL4-SRF constructs.** *Mol Cell Biol*. 1993 Aug;13(8):4640-7

Johnson EN, Seasholtz TM, Waheed AA, Kreutz B, Suzuki N, Kozasa T, Jones TL, Brown JH, Druey KM. **RGS16 inhibits signaling through the G alpha 13-Rho axis.** *Nat Cell Biol*. 2003 Dec;5(12):1095-103.

Johnson TM, Yu ZX, Ferrans VJ, Lowenstein RA, Finkel T. **Reactive oxygen species are downstream mediators of p53-dependent apoptosis.** *Proc Natl Acad Sci U S A*. 1996 Oct 15;93(21):11848-52.

Joost P, Methner A. **Phylogenetic analysis of 277 human G-protein-coupled receptors as a tool for the prediction of orphan receptor ligands.** *Genome Biol*. 2002 Oct 17;3(11):RESEARCH0063

Jordan BA, Devi LA. **G-protein-coupled receptor heterodimerization modulates receptor function.** *Nature*. 1999 Jun 17;399(6737):697-700.

Kaneko M, Nomura Y. **ER signaling in unfolded protein response.** *Life Sci*. 2003 Dec 5;74(2-3):199-205.

Kansra S, Yamagata S, Sneade L, Foster L, Ben-Jonathan N. **Differential effects of estrogen receptor antagonists on pituitary lactotroph proliferation and prolactin release.** *Mol Cell Endocrinol*. 2005 Jul 15;239(1-2):27-36.

Laporte SA, Oakley RH, Zhang J, Holt JA, Ferguson SS, Caron MG, Barak LS. **The beta2-adrenergic receptor/betaarrestin complex recruits the clathrin adaptor AP-2 during endocytosis.** *Proc Natl Acad Sci U S A*. 1999 Mar 30;96(7):3712-7.

Lauwers E, Landuyt B, Arckens L, Schoofs L, Luyten W. **Obestatin does not activate orphan G protein-coupled receptor GPR39.** *Biochem Biophys Res Commun*. 2006 Dec 8;351(1):21-5. Epub 2006 Oct 19.

Lawler OA, Miggin SM, Kinsella BT. **Protein kinase A-mediated phosphorylation of serine 357 of the mouse prostacyclin receptor regulates its coupling to G(s)-, to G(i)-, and to G(q)-coupled effector signaling.** *J Biol Chem*. 2001 Sep 7;276(36):33596-607. Epub 2001 Jul 6.

- Lee AH, Iwakoshi NN, Glimcher LH. **XBP-1 regulates a subset of endoplasmic reticulum resident chaperone genes in the unfolded protein response.** Mol Cell Biol. 2003 Nov;23(21):7448-59.
- Lee RC, Feinbaum RL, Ambros V. **The C. elegans heterochronic gene lin-4 encodes small RNAs with antisense complementarity to lin-14.** Cell. 1993 Dec 3;75(5):843-54.
- Lewerenz J, Klein M, Methner A. **Cooperative action of glutamate transporters and cystine/glutamate antiporter system Xc- protects from oxidative glutamate toxicity.** J Neurochem. 2006 Aug;98(3):916-25.
- Li MO, Sarkisian MR, Mehal WZ, Rakic P, Flavell RA. **Phosphatidylserine receptor is required for clearance of apoptotic cells.** Science. 2003 Nov 28;302(5650):1560-3.
- Liebmann. **G protein-coupled receptors and their signaling pathways: classical therapeutical targets susceptible to novel therapeutic concepts.** Curr Pharm Des. 2004;10(16):1937-58. Review.
- Lin JH, Walter P, Yen TS. **Endoplasmic reticulum stress in disease pathogenesis.** Annu Rev Pathol. 2008;3:399-425
- Lohman RJ, O'Brien TJ, Cocks TM. **Protease-activated receptor-2 regulates trypsin expression in the brain and protects against seizures and epileptogenesis.** Neurobiol Dis. 2008 Apr;30(1):84-93.
- Mack CP, Somlyo AV, Hautmann M, Somlyo AP, Owens GK. **Smooth muscle differentiation marker gene expression is regulated by RhoA-mediated actin polymerization.** J Biol Chem. 2001 Jan 5;276(1):341-7.
- Maher P. **How protein kinase C activation protects nerve cells from oxidative stress-induced cell death.** J Neurosci. 2001 May;21(9):2929-38.
- Margolis RL, Abraham MR, Gatchell SB, Li SH, Kidwai AS, Breschel TS, Stine OC, Callahan C, McInnis MG, Ross CA. **cDNAs with long CAG trinucleotide repeats from human brain.** Hum Genet. 1997 Jul;100(1):114-22.
- Marinissen MJ, Chiariello M, Gutkind JS. **Regulation of gene expression by the small GTPase Rho through the ERK6 (p38 gamma) MAP kinase pathway.** Genes Dev. 2001 Mar 1;15(5):535-53.
- Matej R, Mandáková P, Netíková I, Poucková P, Olejář T. **Proteinase-activated receptor-2 expression in breast cancer and the role of trypsin on growth and metabolism of breast cancer cell line MDA MB-231.** Physiol Res. 2007;56(4):475-84.
- Mullis KB, Faloona FA. **Specific synthesis of DNA *in vitro* via a polymerase-catalyzed chain reaction.** Methods Enzymol. 1987;155:335-50.
- Murphy TH, Miyamoto M, Sastre A, Schnaar RL, Coyle JT. **Glutamate toxicity in a neuronal cell line involves inhibition of cystine transport leading to oxidative stress.** Neuron. 1989 Jun;2(6):1547-58.
- Nelson J, Bagnato A, Battistini B, Nisen P. **The endothelin axis: emerging role in cancer.** Nat Rev Cancer. 2003 Feb;3(2):110-6. Review.
- Nordgard SH, Johansen FE, Alnaes GI, Naume B, Børresen-Dale AL, Kristensen VN. **Genes harbouring susceptibility SNPs are differentially expressed in the breast cancer subtypes.** Breast Cancer Res. 2007;9(6):113.
- O'Flaherty E, Kaye J. **TOX defines a conserved subfamily of HMG-box proteins.** BMC Genomics. 2003 Apr 2;4(1):13.

- O'Neill MJ, Hicks CA, Ward MA, Cardwell GP, Reymann JM, Allain H, Bentué-Ferrer. **Dopamine D2 receptor agonists protect against ischaemia-induced hippocampal neurodegeneration in global cerebral ischaemia.** *Eur J Pharmacol.* 1998 Jul 3;352(1):37-46
- Orrenius S, Zhivotovsky B, Nicotera P. **Regulation of cell death: the calcium-apoptosis link.** *Nat Rev Mol Cell Biol.* 2003 Jul;4(7):552-65.
- Pardo J, Bosque A, Brehm R, Wallich R, Naval J, Müllbacher A, Anel A, Simon MM. **Apoptotic pathways are selectively activated by granzyme A and/or granzyme B in CTL-mediated target cell lysis.** *J Cell Biol.* 2004 Nov 8;167(3):457-68.
- Paulsen SJ, Rosenkilde MM, Eugen-Olsen J, Kledal TN. **Epstein-Barr virus-encoded BILF1 is a constitutively active G protein-coupled receptor.** *J Virol.* 2005 Jan;79(1):536-46.
- Pedersen WA, Fu W, Keller JN, Markesbery WR, Appel S, Smith RG, Kasarskis E, Mattson MP. **Protein modification by the lipid peroxidation product 4-hydroxynonenal in the spinal cords of amyotrophic lateral sclerosis patients.** *Ann Neurol.* 1998 Nov;44(5):819-24
- Perkins DJ, Barber GN. **Defects in translational regulation mediated by the alpha subunit of eukaryotic initiation factor 2 inhibit antiviral activity and facilitate the malignant transformation of human fibroblasts.** *Mol Cell Biol.* 2004 Mar;24(5):2025-40.
- Pierce KL, Premont RT, Lefkowitz. **Seven-transmembrane receptors.** *Nat Rev Mol Cell Biol.* 2002 Sep;3(9):639-50. Review.
- Pitcher JA, Freedman NJ, Lefkowitz RJ. **G protein-coupled receptor kinases.** *Annu Rev Biochem.* 1998;67:653-92.
- Pitcher JA, Payne ES, Csontos C, DePaoli-Roach AA, Lefkowitz RJ. **The G-protein-coupled receptor phosphatase: a protein phosphatase type 2A with a distinct subcellular distribution and substrate specificity.** *Proc Natl Acad Sci U S A.* 1995 Aug 29;92(18):8343-7.
- Polyak K, Xia Y, Zweier JL, Kinzler KW, Vogelstein B. **A model for p53-induced apoptosis.** *Nature.* 1997 Sep 8;389(6648):300-5.
- Radeff-Huang J, Seasholtz TM, Matteo RG, Brown JH. **G protein mediated signaling pathways in lysophospholipid induced cell proliferation and survival.** *J Cell Biochem.* 2004 Aug 1;92(5):949-66.
- Ravikumar B, Duden R, Rubinshtein DC. **Aggregate-prone proteins with polyglutamine and polyalanine expansions are degraded by autophagy.** *Hum Mol Genet.* 2002 May 1;11(9):1107-17.
- Robertson JD, Fadeel B, Zhivotovsky B, Orrenius S. **'Centennial' Nobel Conference on apoptosis and human disease.** *Cell Death Differ.* 2002 Apr;9(4):468-75.
- Ross EM, Wilkie TM. **GTPase-activating proteins for heterotrimeric G proteins: regulators of G protein signaling (RGS) and RGS-like proteins.** *Annu Rev Biochem.* 2000;69:795-827.
- Rozengurt E, Guha S, Sinnett-Smith J. **Gastrointestinal peptide signaling in health and disease.** *Eur J Surg Suppl.* 2002;(587):23-38. Review.
- Rubinshtein DC, DiFiglia M, Heintz N, Nixon RA, Qin ZH, Ravikumar B, Stefanis L, Tolkovsky A. **Autophagy and its possible roles in nervous system diseases, damage and repair.** *Autophagy.* 2005 Apr;1(1):11-22. Epub 2005 Apr 30.

Rubinsztein DC, Ravikumar B, Acevedo-Arozena A, Imarisio S, O'Kane CJ, Brown SD. **Dyneins, autophagy, aggregation and neurodegeneration.** *Autophagy*. 2005 Oct-Dec;1(3):177-8. Review.

Ryan KM, Phillips AC, Vousden KH. **Regulation and function of the p53 tumor suppressor protein.** *Curr Opin Cell Biol*. 2001 Jun;13(3):332-7.

Saelens X, Festjens N, Vande Walle L, van Gurp M, van Loo G, Vandenabeele P. **Toxic proteins released from mitochondria in cell death.** *Oncogene* 2004 Apr 12;23(16):2861-74.

Sagara Y, Schubert D. **The activation of metabotropic glutamate receptors protects nerve cells from oxidative stress.** *J Neurosci*. 1998 Sep 1;18(17):6662-71.

Sagara Y. **Induction of reactive oxygen species in neurons by haloperidol.** *J Neurochem*. 1998 Sep;71(3):1002-12.

Sahin M, Saxena A, Joost P, Lewerenz J, Methner A. **Induction of Bcl-2 by functional regulation of G-protein coupled receptors protects from oxidative glutamate toxicity by increasing glutathione.** *Free Radic Res*. 2006 Nov;40(11):1113-23.

Salmon MA, Van Melderden L, Bernard P, Couturier M. **The antidote and autoregulatory functions of the F plasmid CcdA protein: a genetic and biochemical survey.** *Mol Gen Genet*. 1994 Sep 1;244(5):530-8.

Schenk D, Barbour R, Dunn W, Gordon G, Grajeda H, Guido T, Hu K, Huang J, Johnson-Wood K, Khan K, Kholodenko D, Lee M, Liao Z, Lieberburg I, Motter R, Mutter L, Soriano F, Shopp G, Vasquez N, Vandever C, Walker S, Wogulis M, Yednock T, Games D, Seubert P. **Immunization with amyloid-beta attenuates Alzheimer-disease-like pathology in the PDAPP mouse.** *Nature*. 1999 Jul 8;400(6740):173-7.

Schratt G, Philippar U, Hockemeyer D, Schwarz H, Alberti S, Nordheim A. **SRF regulates Bcl-2 expression and promotes cell survival during murine embryonic development.** *EMBO J*. 2004 Apr 21;23(8):1834-44.

Shaw G, Morse S, Ararat M, Graham FL. **Preferential transformation of human neuronal cells by human adenoviruses and the origin of HEK 293 cells.** *FASEB J*. 2002 Jun;16(8):869-71.

Shenoy SK, McDonald PH, Kohout TA, Lefkowitz RJ. **Regulation of receptor fate by ubiquitination of activated beta 2-adrenergic receptor and beta-arrestin.** *Science*. 2001 Nov 9;294(5545):1307-13.

Shioda T, Fenner MH, Isselbacher KJ. **MSG1, a novel melanocyte-specific gene, encodes a nuclear protein and is associated with pigmentation.** *Proc Natl Acad Sci U S A*. 1996 Oct 29;93(22):12298-303.

Shioda T, Lechleider RJ, Dunwoodie SL, Li H, Yahata T, de Caestecker MP, Fenner MH, Roberts AB, Isselbacher KJ. **Transcriptional activating activity of Smad4: roles of SMAD hetero-oligomerization and enhancement by an associating transactivator.** *Proc Natl Acad Sci U S A*. 1998 Aug 18;95(17):9785-90.

Singer CA, Figueroa-Masot XA, Batchelor RH, Dorsa DM. **The mitogen-activated protein kinase pathway mediates estrogen neuroprotection after glutamate toxicity in primary cortical neurons.** *J Neurosci*. 1999 Apr 1;19(7):2455-63.

Singer CA, Rogers KL, Dorsa DM. **Modulation of Bcl-2 expression: a potential component of estrogen protection in NT2 neurons.** *Neuroreport*. 1998 Aug 3;9(11):2565-8.

Smart EJ, Graf GA, McNiven MA, Sessa WC, Engelman JA, Scherer PE, Okamoto T, Lisanti MP. **Caveolins, liquid-ordered domains, and signal transduction.** Mol Cell Biol. 1999 Nov;19(11):7289-304. Review.

Smith CP, Steinle JJ. **Changes in growth factor expression in normal aging of the rat retina.** Exp Eye Res. 2007 Dec;85(6):817-24.

Sodhi A, Montaner S, Gutkind JS. **Does dysregulated expression of a deregulated viral GPCR trigger Kaposi's sarcomagenesis?** FASEB J. 2004 Mar;18(3):422-7.

Sohrabji F, Miranda RC, Toran-Allerand CD. **Identification of a putative estrogen response element in the gene encoding brain-derived neurotrophic factor.** Proc Natl Acad Sci U S A. 1995 Nov 21;92(24):11110-4.

Stacey SN, Manolescu A, Sulem P, Rafnar T, Gudmundsson J, Gudjonsson SA, Masson G, Jakobsdottir M, Thorlacius S, Helgason A, Aben KK, Strobbe LJ, Albers-Akkers MT, Swinkels DW, Henderson BE, Kolonel LN, Le Marchand L, Millastre E, Andres R, Godino J, Garcia-Prats MD, Polo E, Tres A, Mouy M, Saemundsdottir J, Backman VM, Gudmundsson L, Kristjansson K, Bergthorsson JT, Kostic J, Frigge ML, Geller F, Gudbjartsson D, Sigurdsson H, Jonsdottir T, Hrafnkelsson J, Johannsson J, Sveinsson T, Myrdal G, Grimsson HN, Jonsson T, von Holst S, Werelius B, Margolin S, Lindblom A, Mayordomo JI, Haiman CA, Kiemeny LA, Johannsson OT, Gulcher JR, Thorsteinsdottir U, Kong A, Stefansson K. **Common variants on chromosomes 2q35 and 16q12 confer susceptibility to estrogen receptor-positive breast cancer.** Nat Genet. 2007 Jul;39(7):865-9.

Sugioka K, Shimosegawa Y, Nakano M. **Estrogens as natural antioxidants of membrane phospholipid peroxidation.** FEBS Lett. 1987 Jan 1;210(1):37-9.

Tan S, Wood M, Maher P. **Oxidative stress induces a form of programmed cell death with characteristics of both apoptosis and necrosis in neuronal cells.** J Neurochem. 1998 Jul;71(1):95-105.

Tanemura A, van Hoesel AQ, Mori T, Yu T, Hoon DS. **The role of estrogen receptor in melanoma.** Expert Opin Ther Targets. 2007 Dec;11(12):1639-48. Review.

Taub JS, Guo R, Leeb-Lundberg LM, Madden JF, Daaka Y. **Bradykinin receptor subtype 1 expression and function in prostate cancer.** Cancer Res. 2003 May 1;63(9):

Tombran-Tink J, Barnstable CJ. **PEDF: a multifaceted neurotrophic factor.** Nat Rev Neurosci. 2003 Aug;4(8):628-36. Review.

Tombran-Tink J, Chader GG, Johnson LV. **PEDF: a pigment epithelium-derived factor with potent neuronal differentiative activity.** Exp Eye Res. 1991 Sep;53(3):411-4.

Tombran-Tink J, Chader GG, Johnson LV. **PEDF: a pigment epithelium-derived factor with potent neuronal differentiative activity.** Exp Eye Res. 1991 Sep;53(3):411-4.

Tombran-Tink J, Mazuruk K, Rodriguez IR, Chung D, Linker T, Englander E, Chader GJ. **Organization, evolutionary conservation, expression and unusual Alu density of the human gene for pigment epithelium-derived factor, a unique neurotrophic serpin.** Mol Vis. 1996 Nov 4;2:11

Tremblay F, Perreault M, Klamann LD, Tobin JF, Smith E, Gimeno RE. **Normal food intake and body weight in mice lacking the G protein-coupled receptor GPR39.** Endocrinology. 2007 Feb;148(2):501-6.

Tsao YP, Ho TC, Chen SL, Cheng HC. **Pigment epithelium-derived factor inhibits oxidative stress-induced cell death by activation of extracellular signal-regulated kinases in cultured retinal pigment epithelial cells.** Life Sci. 2006 Jul 4;79(6):545-50.

Tsuruta F, Sunayama J, Mori Y, Hattori S, Shimizu S, Tsujimoto Y, Yoshioka K, Masuyama N, Gotoh Y. **JNK promotes Bax translocation to mitochondria through phosphorylation of 14-3-3 proteins.** EMBO J. 2004 Apr 21;23(8):1889-99. Epub 2004 Apr 8.

Turrens JF. **Superoxide production by the mitochondrial respiratory chain.** Biosci Rep. 1997 Feb;17(1):3-8.

Uehara H, Miyamoto M, Kato K, Ebihara Y, Kaneko H, Hashimoto H, Murakami Y, Hase R, Takahashi R, Mega S, Shichinohe T, Kawarada Y, Itoh T, Okushiba S, Kondo S, Katoh H. **Expression of pigment epithelium-derived factor decreases liver metastasis and correlates with favorable prognosis for patients with ductal pancreatic adenocarcinoma.** Cancer Res. 2004 May 15;64(10):3533-7.

Uehata M, Ishizaki T, Satoh H, Ono T, Kawahara T, Morishita T, Tamakawa H, Yamagami K, Inui J, Maekawa M, Narumiya S. **Calcium sensitization of smooth muscle mediated by a Rho-associated protein kinase in hypertension.** Nature. 1997 Oct 30;389(6654):990-4.

Urano F, Wang X, Bertolotti A, Zhang Y, Chung P, Harding HP, Ron D. **Coupling of stress in the ER to activation of JNK protein kinases by transmembrane protein kinase IRE1.** Science. 2000 Jan 28;287(5453):664-6.

Wadkins RM, Jovin TM. **Actinomycin D and 7-aminoactinomycin D binding to single-stranded DNA.** Biochemistry. 1991 Oct 1;30(39):9469-78.

Wilson S, Bergsma DJ, Chambers JK, Muir AI, Fantom KG, Ellis C, Murdock PR, Herrity NC, Stadel JM. **Orphan G-protein-coupled receptors: the next generation of drug targets?** Br J Pharmacol. 1998 Dec;125(7):1387-92. Review.

Wise A, Jupe SC, Rees S. **The identification of ligands at orphan G-protein coupled receptors.** Annu Rev Pharmacol Toxicol. 2004;44:43-66. Review.

Yahata T, de Caestecker MP, Lechleider RJ, Andriole S, Roberts AB, Isselbacher KJ, Shioda T. **The MSG1 non-DNA-binding transactivator binds to the p300/CBP coactivators, enhancing their functional link to the Smad transcription factors.** J Biol Chem. 2000 Mar 24;275(12):8825-34.

Yahata T, Shao W, Endoh H, Hur J, Coser KR, Sun H, Ueda Y, Kato S, Isselbacher KJ, Brown M, Shioda T. **Selective coactivation of estrogen-dependent transcription by CITED1 CBP/p300-binding protein.** Genes Dev. 2001 Oct 1;15(19):2598-612.

Yamamoto D, Ikeshita N, Daito R, Herningtyas EH, Toda K, Takahashi K, Iida K, Takahashi Y, Kaji H, Chihara K, Okimura Y. **Neither intravenous nor intracerebroventricular administration of obestatin affects the secretion of GH, PRL, TSH and ACTH in rats.** Regul Pept. 2007 Feb 1;138(2-3):141-4. Epub 2006 Oct 19.

Yamamoto I, Sakaguchi Y, Numao M, Tsukada A, Tsushima N, Tanaka M. **Primary structure and tissue distribution of GPR39 messenger ribonucleic acid in Japanese quail, Coturnix japonica.** Poult Sci. 2007 Nov;86(11):2472-6

Yasuda S, Miyazaki T, Munechika K, Yamashita M, Ikeda Y, Kamizono A. **Isolation of Zn²⁺ as an endogenous agonist of GPR39 from fetal bovine serum.** J Recept Signal Transduct Res. 2007;27(4):235-46.

Ye J, Rawson RB, Komuro R, Chen X, Davé UP, Prywes R, Brown MS, Goldstein JL. **ER stress induces cleavage of membrane-bound ATF6 by the same proteases that process SREBPs.** Mol Cell. 2000 Dec;6(6):1355-64.

Yoneda T, Imaizumi K, Oono K, Yui D, Gomi F, Katayama T, Tohyama M. **Activation of caspase-12, an endoplasmic reticulum (ER) resident caspase, through tumor necrosis factor receptor-associated factor 2-dependent mechanism in response to the ER stress.** J Biol Chem. 2001 Apr 27;276(17):13935-40. Epub 2001 Jan 29.

Yorimitsu T, Klionsky DJ. **Autophagy: molecular machinery for self-eating.** Cell Death Differ. 2005 Nov;12 Suppl 2:1542-52.

Yoshida T. **Molecular mechanism of choroidal neovascularization in age-related macular degeneration.** Nippon Ganka Gakkai Zasshi. 2007 Nov;111(11):881-91. Review.

Zhang J, Ferguson SS, Barak LS, Aber MJ, Giros B, Lefkowitz RJ, Caron MG. **Molecular mechanisms of G protein-coupled receptor signaling: role of G protein-coupled receptor kinases and arrestins in receptor desensitization and resensitization.** Receptors Channels. 1997;5(3-4):193-9. Review.

Zhang JV, Ren PG, Avsian-Kretchmer O, Luo CW, Rauch R, Klein C, Hsueh AJ. **Obestatin, a peptide encoded by the ghrelin gene, opposes ghrelin's effects on food intake.** Science. 2005 Nov 11;310(5750):996-9

Zur Hausen H. **Induction of specific chromosomal aberrations by adenovirus type 12 in human embryonic kidney cells.** J Virol. 1967 Dec;1(6):1174-85.

Abbreviations

7-AAD	7-Aminoactinomycin
AD	Alzheimers Disease
ALS	Amyotrophic Lateral Sclerosis
Bp	Basepairs
cAMP	Cyclic Adenosin Monophosphate
cDNA	Complementary DNA
CRE	cAMP Response Element
Ctrl	control
DAG	Diacylglycerol
Dapi	4'6-diamidino-2-phenylindole.
Dn	Dominant Negative
dNTP	Desoxy Nucleotide Tri-Phosphate
DNA	Desoxyribonucleic Acid
DTT	Dithiothreitol
Ds	Double-stranded
EGF	Epidermal Growth Factor
EGFP	Enhanced Green Fluorescent Protein
ER	Endoplasmic Reticulum
ERE	Estrogen Response Element
EV	Empty Vector
FAM	6-carboxyfluorescein
FCS	Fetal Calf Serum
GDP	Guanosine Diphosphate
GEF	Guanosine Exchange Factor
GPCR	G-protein Coupled Receptor
GRK	GPCR-Kinase
GTP	Guanosine Triphosphate
HMG	High Mobility Group
hrs	hours
IB	Immunoblot
ICI	Estrogen Antagonist ICI 182780
IP	Immunoprecipitation
IR	Infrared
IRE	Inositol Requiring Protein
JNK	c-jun N-terminal Kinase
kb	Kilobases
kDa	Kilodalton
mGluR	Metabotropic Glutamate Receptor

min	Minutes
miRNA	Micro RNA
mRNA	Messenger RNA
NLS	Nuclear Localization Signal
OD	Optical Density
PAR	Proteinase Activated Receptor
PBS	Phosphate Buffered Saline
PCR	Polymerase Chain Reaction
PD	Parkinsons Disease
PK	Protein Kinase
PKR	Protein Kinase activated by dsRNA
PERK	PKR-like ER-Kinase
PL	Phospho Lipase
PS	Phosphatidylserin
qPCR	Quantitative PCR
RGS	Regulator of G-protein Signaling
RNA	Ribonucleic Acid
ROS	Reactive Oxygen Species
rpm	rounds per minutes
RT	Room Temperature
SEM	Standard Error of Mean
siRNA	Small Interfering RNA
SRE	Serum Response Element
SRF	Serum Response Factor
TAMRA	Tetramethyl-6-Carboxyrhodamine
UPR	Unfolded Protein Response
V	Volt

Publications

Dittmer S, Sahin M, Pantlen A, Saxena A, Toutzaris D, Pina AL, Geerts A, Golz S, Methner A.

The constitutively active orphan G-protein-coupled receptor GPR39 protects from cell death by increasing secretion of pigment epithelium-derived growth factor.

J Biol Chem. 2008 Mar 14;283(11):7074-81.

Dittmer S, Saxena A, Toutzaris D, Yuan SH, Shioda T, Summer H, Geerts A, Golz S, Methner A.

TNRC9 is a Cited1 and estrogen receptor ER α interacting protein that induces estrogen-dependent transcription and protects from cell death.

In communication at Oncogene

Acknowledgment

Honestly, I do not know where to start. In the last three years I experienced a huge amount of friendship and support from people who hardly knew me.

First, I want to thank my group for their support and expertise and PD Dr. Axel Methner for the project and supervision. I want to thank Prof. Christine Rose for surveying my thesis.

I want to thank my collaboration partners Dr. Stefan Golz from Bayer Health Care, Ana Luisa Pina from Regensburg, Anirvan Ghosh and Shauna Yuan from San Diego and Toshi Shioda from Harvard for the contribution to my work. I thank my former colleagues from Mainz, especially Albi, Christian and Birgit for continuous support and the Graduateprogram “GRK 1033“ for support and my GRK colleagues for discussions and the good time. Here I want to mention Silke, Janine, Ilaria, Tobi and especially Holger.

Most of all, I want to thank my family for everything: the best Daddy in the world. We miss you everyday. My brave Mom who is keeping her and my head up, my Bro for buying me steaks, my Sis for reading and correcting my thesis and having an open ear for my scientific troubles. You are the best family in the world.

For the past three years living here in Düsseldorf would have been hell without Suse and Jörg Hohmann, my makeshift family who had my back through these years. I owe you so much thanks for taking best care of Amigo, for helping me with all the stuff I cant ask my Dad for, for giving me a warm dinner on the worst days, for towing my car, picking me and the horse up in the forest at 9 pm and for everytime you said “Go and see your family”. You are two of the best friends one can ask for. I want to thank the ponyclub for listening and having beers when necessary, especially Nicky for short-notice horsesitting.

I want to thank my hockeyteam the “Crash Eagles Kaarst Women” and our coach Stefan Urban for distraction, especially Denise and Jenny for great evenings, great trainings on friday night, great matches, great trips, shopping aid, food and for being there for me through the last three years. I want to thank Jenni and Nadine for nice discussions over lunch, for acupuncture at -5° C, open ears, feeding the horses over Christmas and everything else. For the wellbeing of Amigo I also thank Rolf Mischke and Dr. Markus Specker.

And then there are my best friends in the worl - Hauke, thank you for keeping me focused on the important things and keeping me motivated, for the best scientific discussions since 1999 and for keeping the faith, and last but definitely not least: Silke, thanks for holding my hand through the past 10 years, for understanding, looking back and looking forth. I thank you for being my best friends in spite of

distance, your own troubles and all other disturbances. You two are the best friends a girl can have, I am blessed with you.

8.5 Curriculum Vitae

Personal Details

Last name	Dittmer
First name	Sonja Carolyn
Date of birth	29.11.1980
Place of birth	Hamburg, Germany
Nationality	German

Education

1990-1999	Main-Taunus Gymnasium, Hofheim/Ts.
-----------	------------------------------------

Scientific Education

1999-2004	Degree in biology, Johannes-Gutenberg University, Mainz Thesis title: „Protein Aggregation in Amyotrophic Lateral Sklerosis“
01.01.2005-31.05.2005	Research position, Institute of Pathobiochemistry, University Mainz
01.08.2005-31.07.2008	PhD position, Department of Neurology, Heinrich-Heine University, Duesseldorf Thesis title: „Downstream Mediators of the Orphan G-protein-coupled Receptor GPR39“

Scholarships

- 03.2004-10.2004 Scholarship of Medical Faculty, University Mainz
- 01.2005-05.2006 Scholarship of the “German Society for Alzheimer Research”
- 08.2005-07.2007 Scholarship of the “German Society for Ageing Research”

Memberships in Scientific Organisations

- Member of NWG, Neurowissenschaftliche Gesellschaft

- Member of DFG GRK 1033 “Molekulare Ziele von Alterungsprozessen und Ansatzpunkte der Altersprävention”

Presentations on Scientific Conventions

- 4th annual meeting of GRK1033, 22.-23.11.2007, Schloß Mickeln, Düsseldorf: Talk “Action and Interaction of GPR39 Downstream Mediators” Sonja Dittmer, Mert Sahin, Ambrish Saxena, Diamandis Toutzaris, Anna Pantlen, Toshi Shioda, Anirvan Ghosh, Andreas Geerts, Stefan Golz, Axel Methner
- Neuroscience 2007, 37th annual meeting of the Society for Neuroscience, 3.-7.11.2007 in San Diego: Posterpresentation “Trinucleotide Repeat Containing 9 interacts with Cited1 to Mediate the Cytoprotective Action of G-protein-coupled Receptor GPR39”
- 3rd annual meeting of GRK1033, 21.-22.11.2006, Bonn-Bad Godesberg: Talk “Downstream Mediators of the Orphan G-protein-coupled Receptor GPR39”

Publications

- Sonja Dittmer, Mert Sahin, Anna Pantlen, Ambrish Saxena, Diamandis Toutzaris, Ana-Luisa Pina, Andreas Geerts, Stefan Golz, Axel Methner: **The constitutively active orphan G-protein coupled receptor GPR39 protects from cell death by increasing secretion of pigment-epithelial derived growth factor PEDF.** *J. Biol. Chem.* 2008 Jan 7

Method Workshops

- Organotypic Slice Cultures (NWG-Method courses, Charité Berlin)

Other Skills

Languages	German (native), English (fluent), French and Latin (basic)
Computing Skills	Microsoft Office, Photoshop, Macromedia Freehand, Soft- and Hardware Installations
Sports	Horseriding, Ski and Snowboarding, Hockey in 2 nd Womens League

-Sonja Dittmer-

8.6 Erklärung

Hiermit versichere ich ausdrücklich, dass ich die Arbeit selbständig und ohne fremde Hilfe angefertigt habe. Andere als die von mir angegebenen Quellen habe ich nicht verwendet.

Ferner versichere ich, dass ich die Dissertation bisher nicht einem Fachvertreter an einer anderen Hochschule zur Überprüfung vorgelegt oder mich anderweitig um Zulassung zur Promotion beworben habe.

- Sonja Dittmer -

Düsseldorf, 29.7.2008